SYNTHESIS AND APPLICATION OF POTASSIUM FLUORIDE/EGGSHELL-IRON (II, III) OXIDE CATALYST FOR SINGLE STAGE TRANSESTERIFICATION OF NEEM OIL

By

ADEWALE SULAIMAN OLADIPO

DEPARTMENT OF CHEMICAL ENGINEERING

AHMADU BELLO UNIVERSITY, ZARIA

NIGERIA.

DECEMBER, 2016

SYNTHESIS AND APPLICATION OF POTASSIUM FLUORIDE/EGGSHELL-IRON (II, III) OXIDE CATALYST FOR SINGLE STAGE TRANSESTERIFICATION OF NEEM OIL

By

Adewale Sulaiman OLADIPO, **B.ENG. (CHEMICAL) (ABU, ZARIA) 2011.**
P13EGCE8004

A DISSERTATION SUBMITTED TO THE SCHOOL OF POSTGRADUATE STUDIES, AHMADU BELLO UNIVERSITY, ZARIA

IN PARTIAL FULFILLMENT OF THE REQUIREMENTS FOR THE AWARD

OF A

MASTER OF SCIENCE (M.Sc) DEGREE IN CHEMICAL ENGINEERING

DEPARTMENT OF CHEMICAL ENGINEERING,
FACULTY OF ENGINEERING
AHMADU BELLO UNIVERSITY, ZARIA
NIGERIA.

DECEMBER, 2016

Declaration

I hereby declare that the work in this dissertation entitled "SYNTHESIS AND APPLICATION OF POTASSIUM FLUORIDE/EGGSHELL-IRON (II, III) OXIDE CATALYST FOR SINGLE STAGE TRANSESTERIFICATION OF NEEM OIL" has been carried out by me in the Department of Chemical Engineering. The information derived from the literature has been duly acknowledged in the text and a list of references provided. No part of this dissertation was previously presented for another degree or diploma at this or any other institution.

OLADIPO Sulaiman Adewale

Name of Student	Signature	Date

Certification

This dissertation entitled "SYNTHESIS AND APPLICATION OF POTASSIUM FLUORIDE/EGGSHELL-IRON (II, III) OXIDE CATALYST FOR SINGLE STAGE TRANSESTERIFICATION OF NEEM OIL" by Adewale Sulaiman OLADIPO meets the regulations governing the award of the degree of Masters of Science (M.Sc) in Chemical Engineering of the Ahmadu Bello University, Zaria, and is approved for its contribution to knowledge and literary presentation.

OLADIPO Sulaiman Adewale

_____	_____	_____
Name of Student	Signature	Date

Dr. O.A. Ajayi

_____	_____	_____
Chairman, Supervisory Committee	Signature	Date

Dr. Nurudeen Yusuf

_____	_____	_____
Member, Supervisory Committee	Signature	Date

Dr. S.M. Waziri

_____	_____	_____
Head of Department	Signature	Date

Professor Kabir Bala

_____	_____	_____
Dean, School of Postgraduate Studies	Signature	Date

Acknowledgements

All praises and thanks be to Allah, who has sent down upon His Servant the Book (the Quran), and has not placed therein any crookedness (18:1). I'm really grateful to the Almighty (Allah SWT) for his guidance throughout my life and the successful completion of this research work; with Him all things are possible and easy.

My sincere appreciation goes to my supervisors; Dr. O.A. Ajayi and Dr. Nurudeen Yusuf for their constant support, patience, guidance and mentorship over the course of this research work. Their doors were always open for me, and each time I ran out of ideas, their sagacious contributions always put me back on track. Therefore, I am very grateful and wish them the very best in life. My special appreciation also goes to my teacher and friend; Dr. Abdulazeez .Y. Atta for his unraveled mentorship over the years.

I would like to state that if the Chemical Engineering Department, A.B.U. Zaria grants citizenship; then I am a proud citizen. I have been trained from undergraduate through this postgraduate studies in the same department. I am truly grateful to all the staff who have in one way or the other imparted the requisite knowledge needed for me to succeed in life as a professional Chemical Engineer.

Special thanks go to Mr.Silas and his co-workers at the Multi-user Laboratory domiciled at Chemistry Department, A.B.U, Zaria for their assistance. I wish to also extend my vote of thanks to Mr.David Obada, Mr. Soloman Bawa, Mallam Musa and Mallam Shamshudeen for their invaluable assistance.

I am indebted to my friends for their consistent encouragement, concern and input; Mr. Shola O., Mr. Gambo Y., Miss. Ruqayah A., Miss. Kitike, Dr. Fatima A. Miss. Kafila O, Miss. Hauwa J, Mr. Gbenga O., Mr. Mathew A., Mr. Sani L., Mr. Musa Q., Mr. Moyo O., Miss. Aisha Z., Miss. Hadiza I., Miss. Tope A., Mr. Michael O., Mr. Modibbo S., Mr. Ibrahim G., Mr. Abdulfatai B., Mr.Abdullahi B., Mr. Isiaq A., etc. I thank you all.

Finally, my profound gratitude to my parents is beyond measure. All through my life, they have always sacrificed to ensure that I had the best in everything. They constantly prayed for me, believed in me and encouraged me to pursue my dreams. May God give them a healthy long life to reap the reward of their labour on me. My sincere appreciation also goes to my uncle and his family; Mr. Tunji Adeleye, may God reward you. May Allah reward all my siblings and brother-in-laws for their continuous support, amen.

Dedication

This dissertation is dedicated to my mother Alhaja I.F. Salami Oladipo and my entire family for their support and encouragement towards my endeavours.

Abstract

Single stage alkali-catalyzed transesterification of vegetable oils having free fatty acid (FFA) content above 0.5% promotes saponification which lowers the biodiesel yield by deactivating the catalyst. A strong solid base KF/Eggshell catalyst, which is capable of circumventing saponification while producing biodiesel in a single stage from neem oil having FFA content of 4.2% was synthesized. The catalyst was synthesized by a thermal treatment of chicken eggshell at 900^{o}C, followed by a wet impregnation of potassium fluoride (KF). The catalyst synthesis process factors such as; eggshell calcination time, potassium fluoride (KF) dosage, catalyst calcination temperature and time were optimized using a response surface methodology (RSM). The optimal synthesis conditions were found to be 2 h eggshell calcination time, KF dosage of 29 wt. %, catalyst calcination temperature of 600^{o}C for 2 h. The KF/Eggshell catalyst was characterized. BET analysis revealed that, the catalyst is mesoporous with a pore width of 3.24nm, pore volume of 0.045 cm^3/g and specific surface area of 128 m^2/g. The SEM micrograph showed that, the crystallites of the catalyst are systemically arranged; as such, present its high specific surface area to the reacting species. Also, the XRD diffractogram showed presence of a highly basic $KCaF_3$ crystal in the catalyst. Process factors of a transesterification reaction utilizing the KF/Eggshell catalyst such as; catalyst dosage, oil-methanol ratio, reaction temperature and time were also optimized. Biodiesel yield of 95% was obtained at the optimal process conditions of 6 wt. % catalyst dosage, 15:1 methanol-oil ratio, 2h reaction time and 60^{0}C reaction temperature. The analyzed physicochemical properties of the produced biodiesel meet the ASTM D6751 commercial standard for diesel engine. The chemical constituents of the produced biodiesel were analysed using GCMS and FTIR, the results revealed that saponification reaction was successfully circumvented. A magnetic form of the catalyst, KF/Eggshell-Fe_3O_4 was synthesized by a co-precipitation method for the purpose of enhancing its reusability. The magnetic KF/Eggshell-Fe_3O_4 catalyst produced 92% yield of the biodiesel after the fifth run, whereas the non-magnetic KF/Eggshell catalyst produced 79% yield for the same run. This significant difference confirmed that, the acquired magnetic property of the catalyst improved its recovery and reusability.

Table of Contents

Page

List of Figures

Figure **Page**

List of Tables

Table **Page**

Abbreviations

FFAs	Free Fatty Acids
FAMEs	Fatty Acid Methyl Esters
CCD	Central Composite Design
CCDOE	Central Composite Design of Experiment
DOE	Design of Experiment
RSM	Response Surface Methodology
FTIR	Fourier Transform Infrared Spectroscopy
GCMS	Gas Chromatography-Mass Spectroscopy
SEM	Scanning Electron Microscopy
EDS	Energy Dispersive Spectroscopy
XRF	X-ray Fluorescence Spectroscopy
XRD	X-ray Powder Diffraction Spectroscopy
BET	Brunauer-Emmett-Teller
TPD	Temperature Programmed Desorption
IEA	International Energy Agency
TGs	Triglycerides
MeOH	Methanol
KF	Potassium Fluoride

CHAPTER ONE

INTRODUCTION

1.1 Preamble

Energy is central to sustenance of livelihoods; the discovery of fossil energy resources in the last centuries contributed immensely to industrial revolution and human development, creating huge wealth. However, its non-renewability and emission of hazardous greenhouse gases, the search for a renewable and environmentally benign alternative has become an imperative quest. Biodiesel is generally defined as the monoalkyl esters of long-chain fatty acids, and has attracted considerable amount of research interests as a renewable substitute to fossil diesel. Countries like United States of America, Brazil, Indonesia, Malaysia, France and Germany are stepping up their use of biodiesel (Wen *et al.,* 2010). Biodiesel has comparable physical and chemical characteristics with the petrol-diesel and several advantages such as non-toxicity, high lubricity, ultra-low greenhouse gases emissions, biodegradability and presence of oxygen in its structure which produces efficient and complete combustion (Helwani *et al.,* 2009). Biodiesel is conventionally produced via transesterification of vegetable oils and animal fats with methanol in presence of homogeneous alkali (Encinar *et al.,* 2002), acid (Rashid *et al.,* 2008), and enzyme catalysts (Ali and Kaur, 2011). Homogeneous catalyzed transesterification yields catalyst-contaminated biodiesel and glycerol, and generate huge quantity of effluents during product purification stage (Reddy *et al.,* 2006). Heterogeneous catalysts could provide a viable solution to the product purification problems associated with homogeneous catalysts. Alkali-earth metal oxides (CaO, MgO, SrO and BaO), d-group metal oxides (ZrO, TiO and ZnO) and zeolite have been reported to successfully catalyze various vegetable oils producing biodiesel yields according to the specific surface area and basic strength of the catalysts (Masoud *et al.,* 2009; Suppes *et*

al., 2001). Alkali-earth metal carbonates have been reported to be found in chicken eggshells (Stadelman, 2000). CaO is the most promising and frequently applied metal oxide catalyst for biodiesel production, due to its cheap price, relatively high basic strength and less environmental impacts (Chouhan and Sarma, 2011). Chicken eggshells are renewable resources containing $CaCO_3$ in varying amounts. Calcination of these eggshells at temperatures above 700^{o}C could produce CaO-catalyst for biodiesel production (Wei *et al.*, 2009). USDA (2013), reported that Nigeria ranks as the largest chicken egg producer in Africa (South Africa is the next largest at 540,000 MT of eggs) with a progressive trend from 500,000 metric tons egg production in 2005 to 650,000 metric tons in 2013. This production rate ensures adequate and continuous availability of eggshell wastes from which CaO can be synthesized when treated, as untreated waste eggshells are usually disposed in landfill and its degradation often leads to pollution. Quite a number of reports have recorded great deal of effort invested in the application of eggshells as value-added products. It was adopted as a low-cost adsorbent for removal of ionic pollutant from aqueous solution (Tsai *et al.*, 2008). Pure metal oxide like CaO usually possesses a less catalytic activity in comparison with mixed metal oxides (Wachs, 2005; Ali and Kaur, 2011 and Centi *et al.*, 2001) and large number of mixed oxides such as KF/CaO–Fe_3O_4 (Hu *et al.*, 2011), KF/ZnO (Xie and Huang, 2006) and KF/Ca–Mg–Al (Gao *et al.*, 2010) have been reported for transesterification reactions. Basic heterogeneous catalysts perform more actively, react faster and are less corrosive in comparison with acidic heterogeneous catalyst (Helwani *et al.*, 2009), but they are unfavourable for feedstocks with high FFAs and high moisture content leading to saponification and hydration respectively (Wei *et al.*, 2009; Gao *et al.*, 2010). To mitigate the problem of saponification during base catalyzed transesterification, two-step method is most commonly used (Wei *et al.*, 2009).

The first step is the FFA esterification reaction, commonly carried out using homogenous acid catalyst (Wei *et al.,* 2009). The second step is transesterification reaction mostly using base catalysts (Wei *et al.,* 2009). However, the two-step method increases system complexity and the cost of production (Wei *et al.,* 2009). Thus, synthesis of a heterogeneous catalyst from adequately available spent eggshells modified with potassium fluoride (KF) for a single stage transesterification process can be cost-effective for biodiesel production from vegetable oils having high FFA content.

1.2 Statement of Research Problem

Direct transesterification of vegetable oils having free fatty acid (FFA) content greater than 0.5% using a base catalyst promotes saponification as a side reaction which lowers the biodiesel yield by deactivating the catalyst.

1.3 Research Justification

i. Dry eggshell wastes are abundantly available and contain 85 – 98% $CaCO_3$ which serves as a good precursor for CaO.

ii. Non-edible vegetable oils, recommended for biofuel production are abundantly available but generally have FFA content greater than 0.5%.

iii. The complexity of biodiesel production from oil with high FFA content in stages can be eliminated or minimized by using a simple single stage process.

iv. Utilization of waste eggshells for catalysis, reusability quality of the catalyst, usage of fairly cheap non-edible oil and the elimination of additional cost of esterification stages can potentially make the biodiesel production process cost-efficient.

1.4 Aim and Objectives

The aim of this research is synthesis and application of an efficient solid base KF/Eggshell catalyst from waste material for a single stage transesterification of neem oil having FFA content of 4.2%.

The specific objectives are;

i. Synthesis and characterization of the KF/Eggshell catalyst and its magnetized form; KF/Eggshell-Fe_3O_4.
ii. Optimization of catalyst synthesis and transesterification processes using central composite design (CCD)
iii. Characterization of the catalysts synthesized under optimal synthesis conditions
iv. Characterization of the biodiesel produced under optimal transesterification conditions
v. Comparative tests between synthesized catalyst and commercial KF/CaO catalyst
vi. Reusability studies of the KF/Eggshell catalysts and its magnetized form; KF/Eggshell-Fe_3O_4 in a transesterification process.

1.5 Research Scope

i. The tolerance of the catalyst to FFA will be tested within $0.5 \geq FFA \leq 4.2\%$ range.
ii. Optimization of the catalyst and transesterification process conditions such as (eggshell calcination time, dosage of potassium fluoride, oil-methanol ratio, reaction time etc.)
iii. Characterization of the catalyst and biodiesel produced at optimal conditions will be limited to SEM, EDX, FTIR, XRF, XRD, BET, GCMS and physicochemical analyses such as (viscosity, flash point, acid, iodine and saponification value etc.)

CHAPTER TWO

LITERATURE REVIEW

2.1 Biodiesel

Biodiesel refers to all kinds of alternative fuels derived from vegetable oils or animal fats. The prefix bio refers to renewable and biological nature, in contrast to the traditional diesel derived from petroleum; while the diesel fuel refers to its use on diesel engines. Biodiesel is produced from the conversion of triglycerides in the oils such as those from palm oil, soybean, rapeseed, sunflower and castor oil to produce methyl or ethyl esters. In this process the three chains of fatty acids of each triglyceride molecule reacts with an alcohol in the presence of a catalyst to obtain ethyl or methyl esters (Carlos *et al.,* 2016). The American Society for Testing and Materials Standard (ASTM) describes the biodiesel as monoalkyl esters of long chain fatty acids produced from vegetable oil, animal fat or waste cooking oils in a chemical reaction known as transesterification. Biodiesel has the same properties of diesel used as fuel for cars, trucks, etc. (Carlos *et al.,* 2016). Biodiesel may be mixed in any proportion with the diesel from the oil refinery. It is not necessary to make any modifications to the engines in order to use this fuel (Carlos *et al.,* 2016). The use of pure biodiesel can be designated as B100 or blended with fuel diesel, designated as BXX, where XX represents the percentage of biodiesel in the blend. The most common ratio is B20 which represents a 20% biodiesel and 80% diesel (Arbeláez and Rivera, 2007). Biodiesel has the advantages of being a renewable and biodegradable biofuel; it produces less harmful emissions to the environment than those that produced from fossil fuels. Specifically the Palm biodiesel pure or mixed with diesel fuel reduces the emissions of CO_2, nitrogen oxides (NOx) and particulate material (Carlos *et al.,* 2016).

2.2 Biodiesel Feedstock

Generally, biodiesel can be produced from any vegetable oil or animal fat. However, the quality of the biodiesel produced is dependent on some physicochemical properties of the oil. Also biodiesel production depends on the quantity of oil produced. (Borsato *et al.,* 2012). Oils with high concentrations of polyunsaturated fatty acids (e.g linoleic and linolenic acid) are undesirable for biodiesel production as they decrease their oxidation stability. In addition, these oils induce a higher carbon deposit than oils with high content of monounsaturated or saturated fatty acids such as palm oil (Borsato *et al.,* 2012). Among the vegetable oils used in biodiesel production includes; palm oil, soybean oil, rapeseed, sunflower, jatropha and waste cooking oil. More than 350 oil-bearing crops have been identified as potential sources for producing biodiesel. However, only palm, jatropha, rapeseed, soybean, sunflower, cottonseed, safflower, and peanut oils are considered as viable feedstocks for commercial production (Al-zuhair, 2007).

2.2.1 Edible and non-edible feedstocks

Depending on availability, different edible oils are utilized as feedstocks for biodiesel production by different countries. Palm oil and coconut oil are commonly used in Malaysia and Indonesia. Soybean oil is majorly used in U.S. (Demirbas, 2003). In order to reduce production costs and to avoid the food-for-fuel conflict, inedible oils are used as the major sources for biodiesel production. Compared to edible oils, inedible oils are affordable and readily available. They could be obtained from Jatropha curcas, Hevca brasiliensis (rubber seed tree), Azadirachta indica (neem) and Simmondsia chinensis (jojoba) etc. (Sani *et al.,* 2016). It has been reported that biodiesel produced from palm and Jatropha have physical properties in the right balance; conferring it with adequate oxidation stability and cold performance (Sarin *et al.,* 2007).

Most of the strict requirements set by the American and European biodiesel standards for biodiesel have been achieved (Berchmans and Hirata, 2008).

2.2.1.1 Neem oil

The neem tree Azadirachta indica A. Juss. (Meliaceae), is a tropical evergreen tree related to mahogany. Native to eastern India and Burma, it is extensively grown in Southeast Asia and Western Africa. The neem seed contains 30–37% oil. It is light orange to dark brown in color, is bitter to the taste, and has a rather strong odour that is said to combine the odours of peanut and garlic. It is comprised mainly of triglycerides and large amounts of triterpenoid compounds, which are responsible for the bitter taste (Sardar *et al.*, 2011). Neem oil has the highest potential and production among the available wild oils (Tanwar *et al.,* 2013). Only 20-25 % of the total potential of the oils is being produced and utilized (mainly in soap industry and pharmaceutical based industries). Remaining 75-80% oil potential is available in surplus, which is not even being harnessed today and can be a good option for production of biodiesel. Neem seed consists of two seed-coats. The external seed-coat contains moisture content of about 2 % which is responsible for the inbuilt high FFA right from the beginning i.e. just after oil extraction. Further, Neem oil undergoes fast oxidation and thus results in a rapid increase in its acid value (Tanwar *et al.,* 2013).

Table 2.1: Typical fatty acid composition of neem oil

Types of fatty acids	Chemical formular	Percentage (Wt. %)
Palmitic acid	C16:0	17.79
Stearic acid	C18:0	15.25
Oleic acid	C18:1	46.73
Linoleic acid	C18:3	1.71
Eicosadienoic acid	C20:2	17.15

Source: (Tanwar *et al.,* 2013)

2.3 Biodiesel Quality and Properties

Due to differences in the feedstock and technologies or manufacturing process of biodiesel, the quality of the fuel varies. In order to harmonize these variances, standards have been set by various authorities for minimum allowable product quality. The first ASTM standard (ASTM D6751) was adopted in 2002 (ASTM, 2002). In Europe, EN 14214 biodiesel standard (based on former DIN 51606) was finalized in October 2003 (Hannu, 2009).

Table 2.2: Biodiesel standard specification for fuel quality

	ASTM D6571 Standards		EN 14214 Standards		Analysis	
	Limits		Limits		Test Methods	
Properties	Min	Max	Min	Max	ASTM	EN
Density, 15°C (g/cm^3)	0.86	0.90	report	report	D1298	EN ISO 3675
Kinematic viscosity, 40°C (mm^2/s)	1.9	6.0	2.0	5.0	D445	EN ISO 3104
Flashpoint (°C)	100	-	120	-	D93	EN ISO 3679
Cetane number	47	-	51	-	D613	EN ISO 5165
Acid value (mg KOH/g)	0.0	0.5	0.0	0.5	D664	EN 14104
Ester content (% mass)	report	report	96.5	-	N/A	EN 14103
Cloud point (°C)	report	report	report	report	D2500	N/A
Pour point (°C)	report	report	-	0.0	N/A	EN ISO 3016
Iodine value (g I_2/100 g)	-	report	-	130	N/A	EN 14111
Sulphur content (% mass)	0.0	0.05	0.0	0.01	D5453	EN 20846
Total glycerine (% mass)	0.0	0.24	0.0	0.25	D6584	EN 14105
Water and sediment (% mass)	0.0	0.05	0.0	0.05	D2709	EN ISO 12937

Source: (Charter, 2008)

2.4 Biodiesel Chemical Content Characterization

The synthesis of biodiesel can be confirmed by FT-IR, NMR (1H and 13C) spectroscopy and GC/MS analyses. Various fuel physicochemical properties of biodiesel have been discussed in section 2.6, which are determinable using ASTM. The fatty acid methyl esters (FAMEs) can be identified with GC/MS studies using the retention time and the fragmentation pattern. Gas chromatography (also known as gas-liquid partition chromatography or vapor-phase chromatography) is a form of chromatography that utilizes differences in retention time to help identify a mixture of compounds by separating each according to its retention time (GCMS, 2016). Compounds with a lower molecular weight will elute out earlier than compounds with higher molecular weights due to differences in boiling points. Smaller structures have lower boiling points and will thus elute faster than those with higher boiling points. It then follows that the compounds with the lower boiling points will have shorter retention times (GCMS, 2016). Factors other than the boiling points of compounds will also affect separation. Other factors that determine the separation are: the polarity and physical size of the molecules (for example branching), the column type (i.e. polar or nonpolar), and the number of theoretical plates (GCMS, 2016). The polarity of compounds should be considered because polar compounds will have a longer elution time on a polar column (i.e. the stationary phase) while a nonpolar compound will elute in shorter times (GCMS, 2016). To this end, a "mobile-phase" is chosen that will not interact with the sample, usually a relatively inert gas such as helium, argon, or nitrogen. This mobile-phase gas is then laced with sample which passed through a tube lined with a "stationary-phase" substance, often consisting of a waxy nonpolar liquid or polymer (though differing stationary phases can be used depending on the situation); depending on the amount of intermolecular attraction between the stationary phase and each component of the sample, differing constituents

will elute through the column at different times (GCMS, 2016). The more a specific component of the sample is attracted to the stationary phase, the longer it will take to elute through the entire column (thus, for a nonpolar stationary phase, more polar compounds will exit the column first. The detector used in this experiment is a Mass Spectrometer, which ionizes samples at the end of the column to produce molecular ions (possibly fragmenting the molecule in the process), and then measuring the mass-to-charge ratio of the molecular [fragment] ions. The combination of these two methods, also known as GC/MS, allows for the detection of many compounds with good separation and at outstanding sensitivities (as low as a few picograms per second retention (GCMS, 2016). The commonly identified FAMEs were, methyl 9-hexadecenoate (C16:1), 14-methyl pentadecanoate (C16:0), methyl 9,12-octadecadienoate (C18:2), methyl 9-octadecenoate (C18:1), methyl octadecanoate (C18:0), methyl 11-eicosenoate (C20:1), methyl eicosanoate (C20:0), methyl 13-docosenoate (C22:1), methyl docosanoate (C22:0), methyl 15-tetracosenoate (24:1) and methyl tetracosanoate (C24:0) (Ali *et al.*, 2011). The peak height and area are used for evaluating the yield and conversion of samples identified provided an internal standard has been used to calibrate the machines.

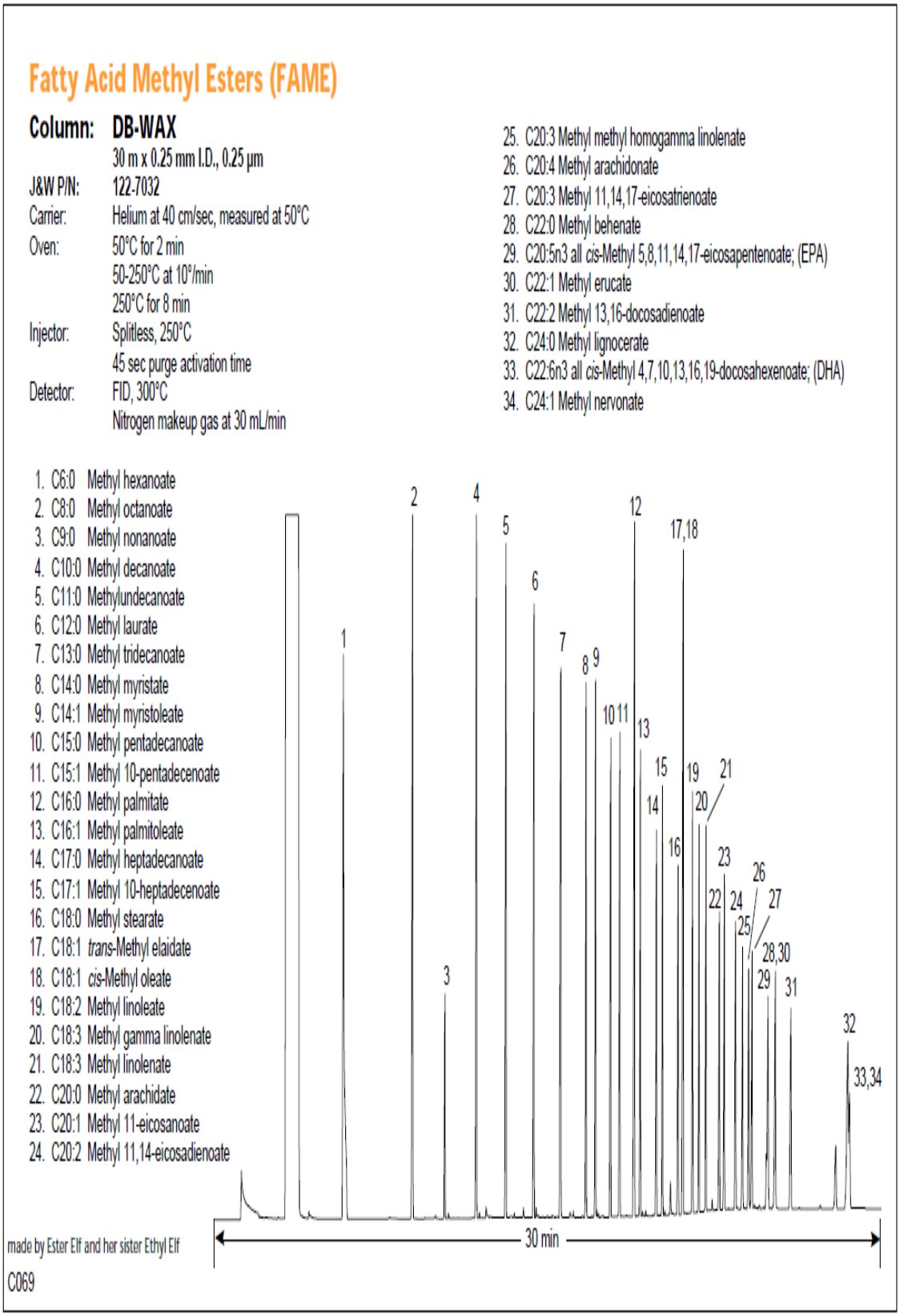

Figure 2.1: Standard GC peaks for fatty acid methyl esters (Ichihara, 2010)

2.5 Biodiesel Production Methods

Quite a lot of researches have been carried with the aim to overcome or minimize the problems associated with producing biodiesel. The popular methods that have been used for minimizing the viscosity of vegetable oils for practical application in internal combustion engines include: pyrolysis, micro-emulsification, blending (diluting) and transesterification.

2.6 Transesterification

Transesterification is a reversible reaction process, which is most widely employed for commercial production of biodiesel. It involves heating the oil to a designated temperature with alcohol and a catalyst, thereby restructuring its chemical structure (Sani *et al.,* 2016). This conversion reduces the high viscosity of the oils and fats. For the transesterification of triglyceride (TG) molecule, three consecutive reactions are needed (Sani *et al.,* 2016). In these reactions, FFA is neutralized by the TG from the alcohol. One mole of glycerol and three moles of alkyl esters are produced (for each mole of TG converted) at the completion of the net reaction. These separate into three layers, with glycerol at the bottom, a middle layer of soapy substance, and biodiesel on top (Fukuda *el at.,* 2001). Catalyzed transesterification process ensures a reasonably high conversion of triglycerides. The process conditions, feedstock compositional limits and post-separation requirements are predetermined by the nature of the catalyst used for transesterification (Sani *et al.,* 2016).

2.6.1 Transesterification raw materials

Biodiesel production comes mostly from both edible and non-edible oils extracted from oilseed plants especially jatropha, palm, neem, rapeseed and animal fats.

It is worthy of note that, any material that contains triglycerides can be used for the biodiesel production. In addition to the oil or fat, an alcohol and catalyst are required to produce biodiesel (Arbeláez & Rivera, 2007).

2.6.2 Transesterification alcohols

Primary and secondary alcohols with chain of 1-8 carbon length are used for biodiesel production, among the alcohols that can be used in this process are methanol and ethanol (Cujia & Bula, 2010). Propanol and butanol have also been reported in open literatures. Alcohols such as ethanol is more complicated to be recovered in the process because of the azeotrope it forms with water (Chen *et al.,* 2007). Also, the performance of ethyl esters is less compared to the methyl esters due to the fact that methanol has a lower molecular weight (32.04 g/mole) compared to ethanol (46.07 g/mole).On the other, methanol is made from natural gas, which is non-renewable, hence its usage would not contribute to sustainability and biodiesel would not be completely bio, by having the alcohol provided by a fossil fuel (Chen *et al.* 2007). A mechanical agitation is needed during transesterification to encourage the mass transfer of the alcohol (Arbeláez and Rivera, 2007). In the course of transesterification, emulsions were formed, using methanol is easy and quickly dissolved, forming a glycerol-rich bottom layer and a higher layer in methyl esters, while using ethanol these emulsions are more stable making the process of separation and purification of ethyl esters more difficult (Arbeláez and Rivera, 2007). Methanol is preferred in the biodiesel production because of its low viscosity (0.59 cP at 20 °C), compared to ethanol with high viscosity (1,074 cP at 20 °C). The usage of ethanol can increase the viscosity of biodiesel, thus hindering proper atomization of the fuel in injection system of diesel engines. Also, using ethanol in biodiesel production can increase the opacity of fumes produced from exhaust of diesel engines running the biodiesel (Benjumea *et al.,* 2007).

Transesterification reaction performance is observed to reach "higher conversions with methanol, while using ethanol makes the process more complex, expensive, requires a higher consumption of energy and time (Giron *et al.,* 2010).”We found that it requires less reaction time when using methanol rather than ethanol, either in acid or alkaline catalysis, reaching high yields” (Giron *et al.,* 2010). With the stated findings, methanol is widely preferred to be used in the biodiesel production due to its lower cost, better performance and less time and energy during the reaction.

2.6.3 Transesterification: side reactions

$$\underset{\textit{Fatty acid}}{RCOOH} + NaOH \longrightarrow \underset{\textit{Sodium carboxylate (Soap)}}{R\text{-}COO^{-}\,Na^{+}} + H_2O \qquad (2.1)$$

$$\underset{\textit{Fatty acid}}{2RCOOH} + CaO \longrightarrow \underset{\textit{Calcium carboxylate (Soap)}}{Ca^{2+}(RCOO^{-})_2} + H_2O \qquad (2.2)$$

$$\underset{\textit{Fatty acid}\ \text{methanol}}{RCOOH + CH_3\text{-}OH} \longrightarrow \underset{\textit{Methyl ester}}{CH_3\text{-}COOR} + H_2O \qquad (2.3)$$

2.6.4 Transesterification catalyst

Homogeneous, heterogeneous or enzyme catalysts are used in the biodiesel production. Homogeneous catalysts are soluble in the middle of reaction, i.e. they are in a single phase either liquid or gaseous. One of the advantages of homogeneous catalysis is the high speed of reaction, and moderate temperature and pressure conditions (Giron *et al.,* 2010). The catalysts can be acids or alkalis, the acid catalysts are effective but require a time interval extremely long and temperatures exceeding 100 °C for its action. Getting conversions of 99% with a concentration of 1% sulfuric acid in relation to the amount of oil, it takes about 50 hours (Giron *et al.,* 2010). We can use this catalytic process when the oils have a high degree of acidity and harm the action of alkali catalysts with acidity greater than 10% (Bournay *et al.,* 2005).

Heterogeneous catalysts are found in two phases and a contact area, the use of these catalysts simplifies and makes more economical the purification process due the easy separation of the products and reactants. The disadvantage is the difficulty to temperature control for very exothermic reactions, limitations on mass transfer of reactants and products, as well as high mechanical resistance to the catalyst (Arbeláez and Rivera, 2007). To achieve high yields the reaction must be carried out to a higher temperature increasing energy costs (Bournay *et al.*, 2005). High reaction times was reported by (Guan *et al.*, 2009), because the speed of transesterification reaction with these solid catalysts is lower in comparison with homogeneous catalysts, due to the mass transfer resistance. Enzymes are biocatalysts usable in the biodiesel production. The widely used enzymes are lipases, being effective for the transesterification reaction. This type of catalysis has the advantage of allowing the use of alcohol with high content of water (more than 3%), low temperatures, which is an energy-saving and high degrees of acidity in oils (Bournay *et al.*, 2005).

2.7 Homogeneous Catalyst for Transesterification

Homogeneous catalysts for transesterification could be acidic or alkali. Basic hydroxides and methoxides have been reportedly used for transesterification. Acid sulphides and chlorides have also been widely reported. Alkaline metal alkoxides (Freedman, 1986; 1987) and hydroxides (Vinatoru *et al.*, 2005; Meher *et al.*, 2006), as well as sodium and potassium carbonates have been reported to catalyze a transesterification process (Truterb and Varghaa, 2005). The alkaline catalysts normally show high performance when vegetable oils with high quality is used. However, when the oils contain significant amounts of free fatty acids, they cannot be converted into biodiesels but to a lot of soap (Furuta *et al.*, 2004).

However, these free fatty acids react with the alkaline catalyst to produce soaps that inhibit the separation of biodiesel, glycerin and wash water (Canakci and Garpen, 2003).

2.7.1 Homogeneous alkali-catalyzed transesterification

Homogeneous base catalysts are the numerous alkaline liquid such as sodium hydroxide, sodium methoxide, potassium hydroxide, or potassium methoxide. Alkaline metal alkoxides (as CH_3ONa for the methanolysis) are most active catalysts, since they give very high yields (98%) in short reaction times (30 min) even if they are applied at low molar concentrations (0.5 mol %). Alkaline metal hydroxides (KOH and NaOH) are cheaper than metal alkoxides, but less active. Nevertheless, they are a good alternative since they can give the same high conversions of vegetable oils simply by increasing the catalyst concentration to 1 or 2mol% (Vargas *et al.*, 1998). During transesterification, the glycerin that is formed needs to be removed so that it is not converted into formaldehyde or acetaldehyde when burned in a diesel engine because both would pose a health hazard (Meng, 2011). Base catalyzed transesterification is much faster than acid-catalyzed transesterification and is the most commonly used method commercially (Hanna *et al.,* 1998). Alkaline catalysts are less corrosive than acidic compounds, industrial processes usually favor base catalysts such as alkaline metal alkoxides and hydroxides as well as sodium or potassium carbonates (Helwani *et al.,* 2009). Potassium and sodium methoxides are the widely used base catalyst. The advantage of using sodium and potassium methoxides is that no water is formed and no saponification is occurring. The use of hydroxide involves the formation of water resulting in hydrolysis of the acylglycerides or alkyl esters with formation of soaps (Verhe *et al.,* 2011). Reaction scheme for a methoxide base-catalyzed transesterification is shown in the figure 2.8. Kinetic studies of this multiple phase reaction show that the formation of the diglyceride is the slowest, whereas the next steps are much faster (Mittelbach and Trathnigg, 1990).

The standard conditions for the alkaline transesterification are 6:1 molar ratio of methanol to oil, concentration of catalyst in the range of 0.5–1.5% (depending on the FFA content of the feedstocks) and temperature of 60°C (Verhe *et al.*, 2011). Reaction times can be shortened using a two-step procedure or a continuous reaction with simultaneous separation of the glycerol. In the alkaline catalyzed process, it is important that the feedstock is as much as possible water-free as well as with low FFA content in order to prevent hydrolysis (Verhe *et al.*, 2011). FFAs are not converted into esters but are transformed into soaps which cause problems in separating the glycerol layer and the water washing due to the formation of emulsions (Verhe *et al.*, 2011). In addition, FFAs are deactivating the catalyst with the soap formation. A feedstock with a high FFA content needs a higher concentration of catalyst (Verhe *et al.*, 2011). Preferably the FFA content should be less than 0.5% to ensure a complete conversion and efficient post-treatment. The glycerol layer separated from the biodiesel contains methanol, catalyst and soaps (Verhe *et al.*, 2011). After acidifying, the FFAs can be separated, the methanol evaporated and the sodium or potassium salts separated, purification steps which result in crude glycerol. Biodiesel is then dried and used as such without post-treatment (if the feedstock is a refined lipid) after recovering of the excess of methanol and water washing. Biodiesel can also be produced by transesterification of the oil in situ. In this procedure there is no need for the extraction of the oil from seeds. The liquid phase and solid oil containing feedstock are mixed and stirred. The disadvantage of this process is that large quantities of methanol and high concentration of catalyst are required. Furthermore, soaps are formed and additional solvent is needed to wash the seeds in order to ensure the complete separation of the oil and the transesterification reaction (Verhe *et al.*, 2011).

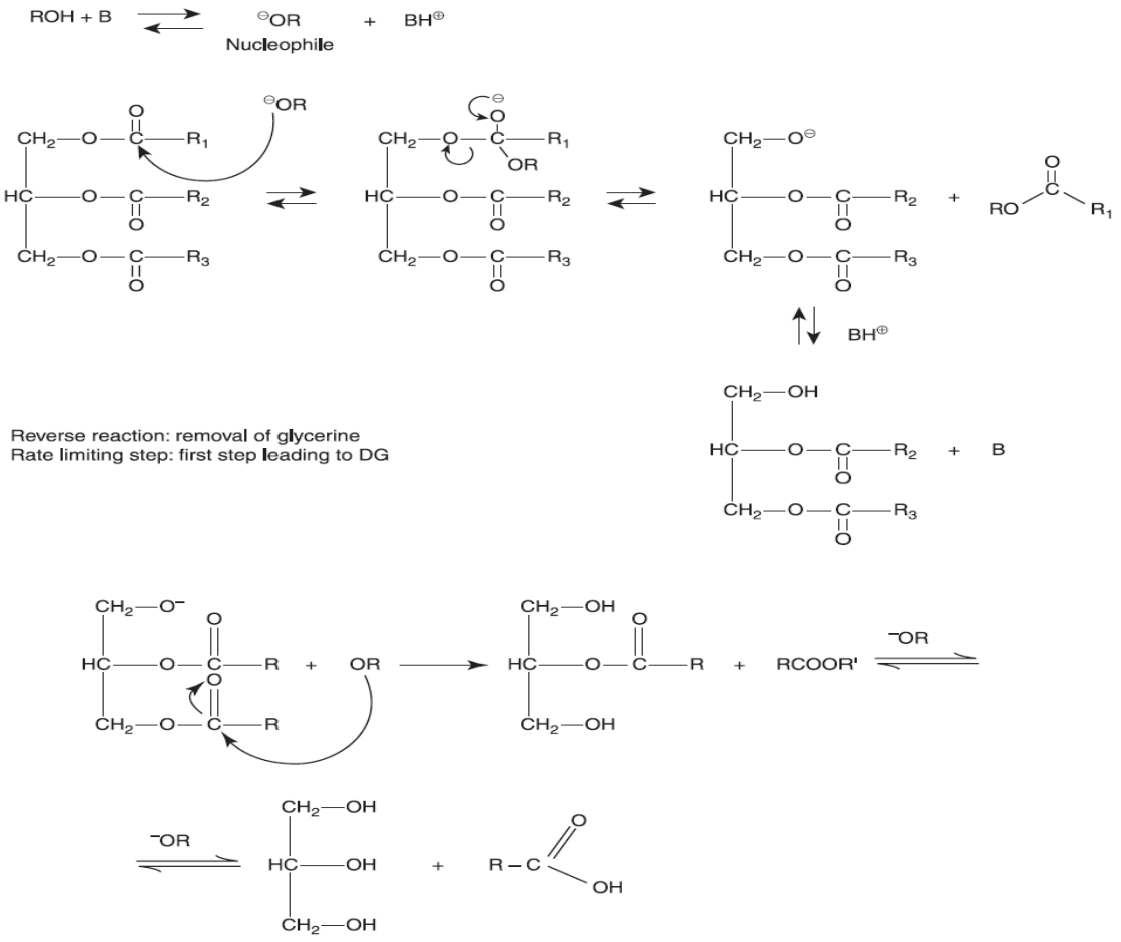

Figure 2.2: Reaction scheme for base-catalyzed transesterification (Verhe *et al.*, 2011)

2.7.2 Advantages of homogeneous base catalyst

1. Base catalysts enables faster transesterification reaction rates (Carlos *et al.*, 2016)

2. They are readily available at affordable prices (Sani *et al.*, 2016)

2.7.3 Disadvantages of homogeneous base catalyst

1. Basic catalysts produces soaps due to the high amounts of free fatty acids and water in oil (Carlos *et al.*, 2016).

2. Soap lowers the yield of the biodiesel and inhibits the separation of the esters from the glycerol (Leung *et al.*, 2010).

2.7.4 Homogeneous acid-catalyzed transesterification

Acid transesterification and esterification transesterification can also be performed in the presence of strong homogeneous acid catalysts such as sulfuric acid normally for feedstocks with high FFA (>0.5%).

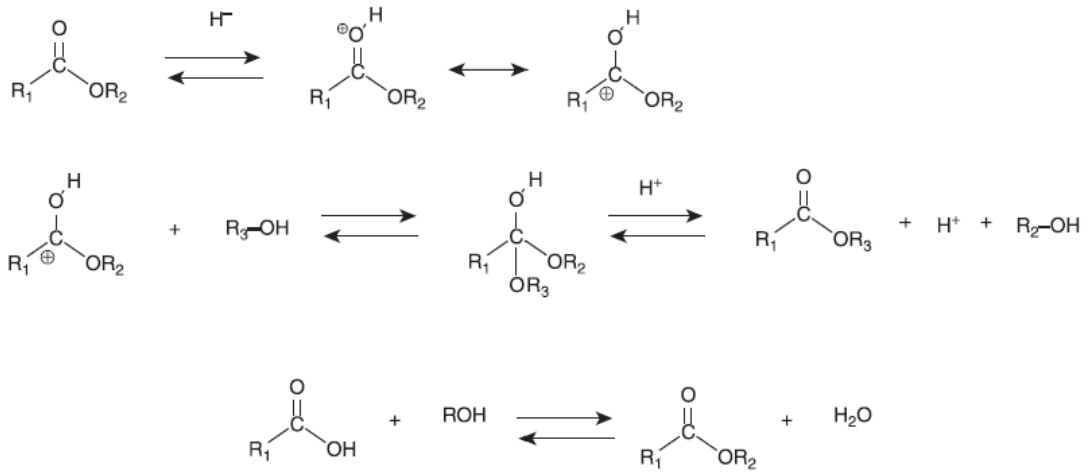

Figure 2.3: Reaction scheme for acid-catalyzed transesterification (Verhe *et al.*, 2011)

Methanesulfonic acid has been reported as an efficient catalyst for esterification of low quality oils (Verhe *et al.*, 2011). This acid is less corrosive, non-oxidizing and more environmentally friendly than sulfuric or phosphoric acid. It is also used as a neutralizing agent in the base-catalyzed transesterification (Verhe *et al.*, 2011). The advantage of the acid catalyzed process is that FFAs are simultaneously converted into esters. Therefore, acid-catalyzed transesterification can be used for feedstocks which are containing high amounts of FFAs such as crude palm oil (up to 8%), used frying oils (3–7%), animal fats (up to 30%), grease and side-streams from oil refining (10–90%) (Verhe *et al.*, 2011). The reaction mechanism involves protonation of the carbonyl function giving rise to a carbonium ion which is attached by the nucheophilic alcohol followed by splitting of the diglyceride and the aliphatic ester. The reaction is repeated with the diglyceride and monoglyceride (Verhe *et al.*, 2011).

2.7.5 Disadvantages of homogeneous acid catalysts

1. Acid-catalyze reaction is about 4000 times slower than the homogeneous base-catalyzed reaction (Sani *et al.,* 2016).

2. Due to the slow reaction rate higher temperatures and pressure have to be applied (100°C/5 bar) which can also result in formation of by-products (formaldehydes and glycerol ethers) (Verhe *et al.,* 2011).

3. This is because the use of strong acids such as H_2SO_4 (shiyi *et al.,* 2006), HCl, BF_3, H_3PO_4, and organic sulfonic acids (Lotero *et al.,* 2006), is associated with higher costs and environmental impacts

4. Acid-catalyzed transesterifications are especially sensitive to water concentration. It was demonstrated, previously, that as little as 0.1 wt. % water in the reaction mixture was able to affect ester yields in transesterification of vegetable oil with methanol, with the reaction almost completely inhibited at 5 wt.% water concentration (Helwani *et al.,* 2009)

5. During the esterification water is formed which causes hydrolysis of the triglycerides resulting in lower yields (Verhe *et al.,* 2011).

2.7.6 Advantage of homogeneous acid catalysts

1. The advantage of acid catalysts over base catalysts is their low susceptibility to the presence of FFA in the starting feedstock (Helwani *et al.,* 2009).

2.8 Heterogeneous Catalyst for Transesterification

Although homogeneous catalysis is the traditional and very efficient process to convert lipids into alkyl esters, it has a number of disadvantages. The catalyst cannot be reused and has to be discarded after the reaction. In addition, catalyst residues have to be removed from crude biodiesel using several water washing steps that increases the production cost and complicates the purification of the glycerol.

Various processes are available using heterogeneous catalysts which are simplifying the purification costs of the biodiesel and the glycerol. The advantage of heterogeneous catalysis is that the catalyst can be either recovered by filtration and/or decantation or applied in a fixed bed reactor and the post-treatment of the biodiesel and glycerol is easier (Veher *et al.,* 2011). Similar to homogeneous catalyst, heterogeneous catalyst could be acidic or alkaline.

2.8.1 Heterogeneous acid-catalyzed transesterification

Acid catalysis is simultaneously performing esterification of free fatty acids (FFAs) and transesterification of triglycerides (TGs). In this way, it is more economical to use low-quality feedstocks and lower processing costs. The reaction mechanism using solid Brønsted acids catalyzed esterifications is similar to that of the homogeneously catalyzed process. The reaction involves a nucleophilic attack of the adsorbed carboxylic acid with the free alcohol in the rate-determining step. The formation of a more electrophilic intermediate is also occurring with solid Lewis acids. The rate-determining step is dependent on acid strength. Desorption of the ester will be decreased if the strength of the acid sites is too high. This mechanism is valid for both homogeneous and heterogeneous catalyst (Bonelli *et al.,* 2007). Among the solid acids available are functionalized polymers, such as the acid forms of some resins, as well as inorganic materials, such as zeolites, modified oxides, clays, and others. Some of these solids have already been found to be effective in transesterification reactions of simple esters and b-ketoesters (Lotero *et al.*, 2006). Compared to sulfuric acid, the solid clay catalysts produced a cleaner biodiesel due to their bleaching activity. Thus, unrefined oils or waste cooking oils could be employed as feedstock without pretreatment. However, the performance of the clays diminished with repeated use and catalysts had to be reactivated after each run to maintain peak performance, suggesting that some leaching of sulfuric acid took place (Lotero *et*

al., 2006). Furuta *et al.,* (2004) tested a series of strong solid acids (alumina promoted sulfated zirconia, alumina promoted tungstated zirconia and sulfated tin oxide) for the transesterification of soybean oil with methanol at 200–300^{0}C. Reaction yields over 90% were obtained for the alumina promoted tungstated zirconia at reaction times of 20 h using a flow reactor (T = 250^{0}C). The activity of the same catalyst was maintained for up to 100 h (Furuta *et al.,* 2004). In general, the application of solid acid catalysts to produce biodiesel from oils and fats has been largely ignored. The possibility of unwanted side reactions has been in part blamed for this fact. Perhaps, a more important reason for the little research in this particular area is the slow reaction rate associated with acid catalysis in general (Lotero *et al.,* 2006). However, the ability of solid acids to catalyze both esterification and transesterification reactions simultaneously and the possibility for employing catalysts that are reusable and green, meaning that they do not pose a great environmental threat, are attractive aspects that make the study of these materials imperative (Lotero *et al.,* 2006).

2.8.2 Heterogeneous base-catalyzed transesterification

The transesterification of vegetable oils or animal fats to biodiesel by chemical catalysts, especially in the presence of a strong basic solution, such as sodium hydroxide and potassium hydroxide, has been widely used in industrial production of biodiesel. Such basic solutions can transform triglycerides to their corresponding FAMEs with higher yield at lower temperature and shorter time than those by acid catalysts. However, separating the catalysts from products is technically difficult (Feng and Fang, 2011). Moreover, natural vegetable oils and animal fats usually contain small amounts of FFAs and water, which can have significant negative effects on the transesterification of glycerides with alcohols, and also hinder the separation of FAMEs and glycerol due to saponification of FFAs.

Compared with basic solutions, solid base catalyst is preferred due to easy separation (Feng and Fang, 2011). Heterogeneous base catalysis has a shorter history than that of heterogeneous acid catalysis. Solid bases refer mainly to solids with Brønsted basic and Lewis basic activity centers, that can supply electrons (or accept protons) for (or from) reactants. Heterogeneous base catalyzed transesterification for biodiesel synthesis has been studied intensively over the last decade (Feng and Fang, 2011). Low-qualified oil or fat with FFAs and water can be used. However, the catalytic efficiency of conventional heterogeneous base catalysts is relative low and needs to be improved (Feng and Fang, 2011). Various types of catalytic materials have been studied to improve the transesterification of glycerides. Heterogeneous base catalysts, such as hydrotalcites, metal oxides, metallic salt, supported base catalyst and zeolites are well discussed herein details.

2.8.2.1 Metal oxides

Metal oxides are composed of cations possessing Lewis acid and anions with Brønsted base. Metal oxides used in transesterification are classified as single metal oxides (e.g., MgO, CaO and SrO) and mixed metal oxides [A-B-O type metal oxides, where A is an alkaline-earth metal (Ca, Ba, Mg), alkaline metal (Li), or rare earth metal (La) and B is a transition metal (Ti, Mn, Fe, Zr, Ce)] (Feng and Fang, 2011). Early studies on heterogeneously catalyzed transesterification were focused on the catalysis by single metal oxides. The basicity of oxides (especially, basic sites) directly depends on reaction rate (Feng and Fang, 2011). A comparison of several metal oxides (MgO, CeO_2, La_2O_3 and ZnO) indicated that the most basic one is La_2O_3, followed by MgO, CeO_2 and ZnO (Bancquart *et al.*, 2001). The order of activity among alkaline earth oxide catalysts is BaO > SrO > CaO > MgO.

2.9 Performance of Calcium Oxide (CaO) as a Catalyst in Biodiesel Production

CaO is the most frequently applied metal oxide catalyst for biodiesel preparation, due to its cheap price, relatively high basic strength and less environmental impacts (Feng and Fang, 2011). However, in most experiments using heterogeneous catalysts, the transesterification reaction proceeds at a relatively slow rate as compared to the transesterification reaction in those conducted with homogeneous catalysts. This typically slow reaction rate is due to diffusion problems accruing from the heterogeneous media's behavior as a three-phase system (oil/methanol/catalyst) (Xie and Huang, 2006). Among the solid base catalysts, CaO is one of the well-researched heterogeneous catalysts. Four reasons account for this: CaO has a higher basicity, lower solubility, and lower price than KOH/NaOH, and it is easier to handle (Krasae *et al.*, 2010).

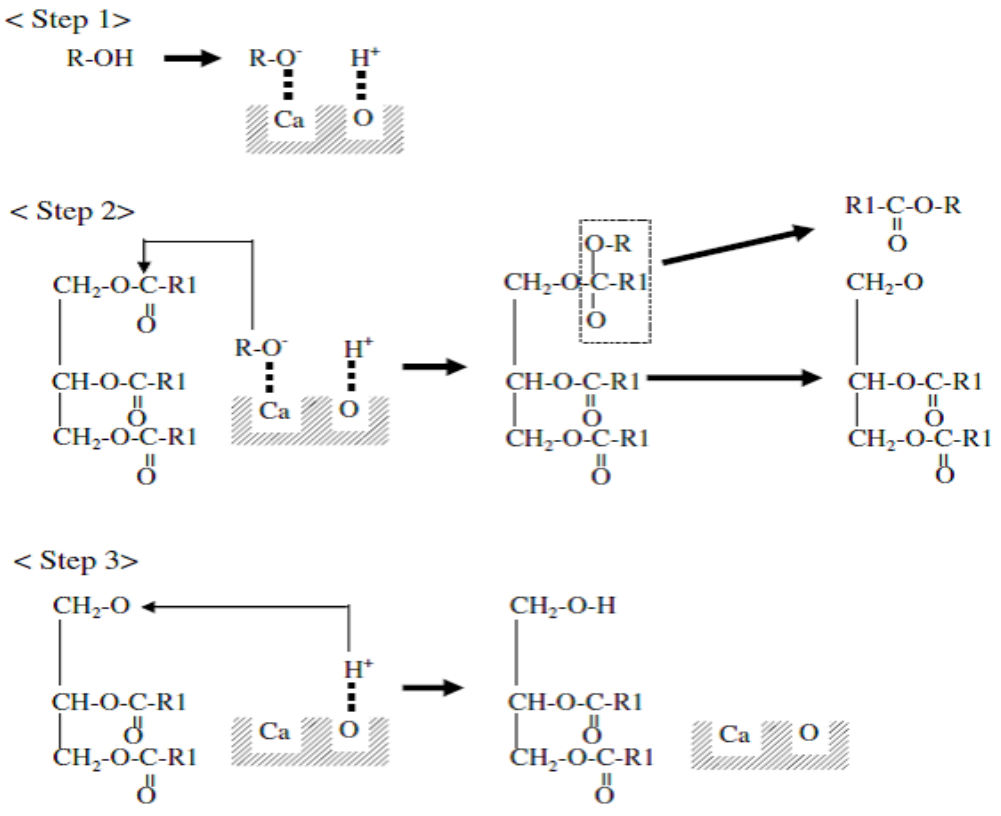

Figure 2.4: CaO-catalyzed transesterification reaction mechanism (Masato *et al.*, 2008)

The first step of the mechanism transesterification involving calcium oxide as the solid base catalyst is abstraction of proton from methanol by the basic sites to form methoxide anion. The methoxide anion attacks carbonyl carbon in a molecule of the triglyceride, leading to formation of the alkoxycarbonyl (tetrahedral) intermediate (step 1). Then, the alkoxycarbonyl intermediate divides into two molecules: a mole of FAME and anion of diglyceride (step 2) (Masato *et al.,* 2008; Pragas *et al.,* 2011). The charged-anion is then stabilized by a proton from the catalyst surface to form diglyceride and at the same time regenerates the catalyst (step 3) (Masato *et al.,* 2008; Pragas *et al.,* 2011). The cycle continues until all three carbonyl centres of the triglyceride have been attacked by the methoxide ions to give one mole of glycerol and three moles of methyl esters. Calcium diglyceride, a compound formed from the reaction between calcium oxide and glycerol, has also been recognized as a catalyst (Masato *et al.,* 2008).

2.9.1 Supported or loaded calcium oxide (CaO)

To enhance the performance of CaO, a few researchers have tried to load an active ingredient onto CaO. Watkins *et al.,* (2004) as reported by (Pragas *et al.,* 2011) evaluated Li-loaded CaO in the transesterification of glyceryl tributyrate to methyl butanoate. Experiments with lithium loading ranges from 0.26 to 4.0 wt. %. The authors found that the optimum loading amount of 1.23 wt.% exhibited maximum activity. The doping of lithium on CaO increases the basicity of the catalyst. Li-doped CaO was also examined by Granados *et al.,* (2007) in transesterifying sunflower oil into methyl esters. They concluded that an activated catalyst at 500^0C and a lithium loading of 4.5 wt.% onto CaO gave the highest catalytic activity. They noted that the catalyst activation temperature should be higher than the melting point of $LiNO_3$ (219^0C). However, catalyst activation above 500^0C caused the active species to leach into the reaction media, thus, affecting the heterogeneous catalytic route.

A series of alkali-doped CaO was tested by MacLeod *et al.* (2008). CaO and MgO were loaded with nitrate of Li, Na and K in the production of methyl esters using rapeseed oil. Dried (110^0C, 5 h) and calcined (600^0C, 5 h) catalysts, Na/CaO, K/CaO and Li/MgO at 5 wt.% loading, exhibited 100% methyl esters conversion in a 3 h reaction with 5% catalyst. Calcined Li/CaO gave 99% conversion; uncalcined Na, K and Li/CaO resulted in 98%, 90% and 85% conversions, respectively. The performance of these catalysts relates well with their basic strengths. As for species leaching, it was found that calcined Li/CaO gave the lowest metal leaching of 18ppm followed by uncalcined Li/CaO (22 ppm), calcined K/CaO (32 ppm) and uncalcined K/CaO (36 ppm). Calcined Li/MgO resulted in the highest metal leaching of 98 ppm, followed by uncalcined Na/CaO and calcined Na/CaO at 78 and 52 ppm, respectively. Thus, as far as lixiviation is concerned, lithium is the most stable loading species and calcination seems to further improve the stability of Li/CaO and K/CaO catalyst systems (MacLeod *et al.* 2008). In a related research, Ali and Kaur (2014) reported 99% yield of methyl ester from cottonseed oil having FFA of 5.8% in a transesterification involving a potassium fluoride (KF) loaded CaO/NiO catalyst. It was found that the reaction took 4h at 65^0C using 1:15 molar ratio of oil/MeOH and 5 wt. % catalyst to achieve such a high yield of biodiesel. The adequate KF loading was reported to be 20 wt. % and subsequent calcination temperature at 700^0C for 2h produced such a highly active catalyst. These authors concluded that, CaO doped with NiO, which was then impregnated with KF had its basic strength increased to H_=18.4, this was believed to be responsible for the high activity of the catalyst. KF/CaO nanocatalyst was prepared by using impregnation method and used to convert Chinese tallow seed oil to biodiesel (Wen *et al.,* 2010). The catalyst found to have a specific surface area of 109 m^2/g produced biodiesel yield of 98%. The transesterification process as well as the synthesis of the catalysts were optimized using orthogonal experimental design.

The researchers concluded that, the optimal conditions for biodiesel production from Chinese tallow seed oil under KF/CaO nanocatalyst were molar ratio 12:1 of alcohol to oil molar ratio, the catalyst 4% w/w of the oil, reaction temperature of 65^0C and reaction time of 2.5 h. Wen *et al.,* (2010) established that, the formation of an highly basic crystals of $KCaF_3$ was responsible for the activity of the catalyst. It was reported that the optimal synthesis conditions for the nanocatalyst were 25 wt. % KF loading rate, 600^0C calcination temperature for 3h.

2.9.2 CaO sourced from waste and organic materials

In order to make the biodiesel production more sustainable and cost-efficient, the use of heterogeneous catalysts sourced from spent materials continue to stir research interests. The shells of oysters and chicken eggs have been evaluated as effective catalysts in converting soybean oil to methyl esters. Nakatani *et al.,* (2009) showed that by using 25 wt.% of thermally activated (at 700^0C) oyster shell at 6:1 MeOH:oil molar ratio, a biodiesel product with a yield of over 70% and purity of 98.4 wt.% was achieved in a 5 h reaction time. The conversion at a moderate 6:1 (MeOH:oil) ratio was achievable at the expense of a higher catalyst and longer reaction time. With 3 wt. % of calcined egg shell (at 1000^0C), Wei *et al.,* (2009) transesterified soybean oil to produce biodiesel of over 95% yield using the following transesterification conditions; 3 h reaction time, 9:1 MeOH:oil molar ratio and reaction temperature of 65^0C. It was reported that, the catalyst obtained from waste material was capable of being reused up to 13 times without much loss in the activity. In addition, similar catalytic potential of mud crab shells in palm olein transesterification was reported by (Boey *et al.,* 2009; Pragas *et al.,* 2009). The crab shell was able to transesterify palm olein to 98.8% yield of biodiesel. The process conditions were; reaction temperature of 65^0C, reaction time of 2.5h, 5:1 MeOH:oil molar ratio and 5 wt.% catalyst concentration.

2.10 Waste Chicken Eggshell

Alkali-earth metal carbonates have been reported to be found in chicken eggshells (Stadelman, 2000). Eggshells are the hardest part of the reproductive cells of a bird. They are often described as a blue print of another animal (chicken) with sufficient building materials to make it. Eggshells vary widely in texture. The eggshell is secreted most actively during the last 15 hours that the egg spends in uterus. It is predominantly made up of calcium carbonate and glycoprotein matrix (2%). The crystalline part of the shell consists of columns materials embedded in the outer shell membrane. Pores that extend from the outside of the egg to the shell membranes and allow for gas exchange by the embryo separate these columns. Outside the shell is a thin proteinaceous layer, the cuticle that may block the entrance of bacteria (Al-awwal & Ali, 2015). Most good quality eggshells from commercial layers contain approximately 2.2 grams of calcium in the form of calcium carbonate. About 95% of the dry eggshell is calcium carbonate weighing 5.5 grams. The average eggshell contains about 29 – 35% water, 1.4 – 4% protein, 0.1 – 0.2% crude fat, 89.9 – 91.1% ash content, 35.1 – 35.4% calcium, 0.12% phosphorus, 0.15 – 0.17% sodium, 0.37 – 0.40% magnesium, 0.10 – 0.13% potassium and 0.09 – 0.19% sulphur and trace of iron, zinc and copper (Al-awwal & Ali, 2015).

2.10.1 Availability of eggshell resources in nigeria

The Nigerian poultry industry in particular has been rapidly expanding in recent years and is therefore one of the most commercialized (capitalized) subsectors of Nigerian agriculture (USDA 2013; Adene and Oguntade 2006) as reported in (Heise *et al.*, 2015). The popularity of poultry production can be explained by the fact that poultry has many advantages over other livestock. Finally, eggs, one of the major products of poultry production, are more affordable for the common person than other sources of animal protein (Heise *et al.* 2015).

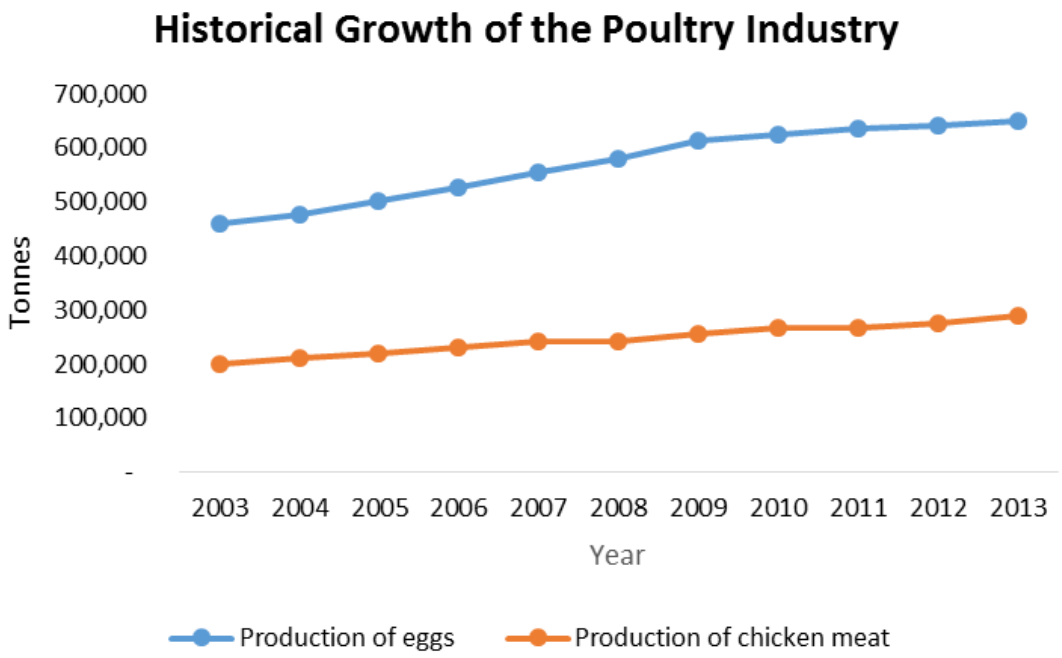

Figure 2.5: Nigerian poultry industry growth trend (USDA, 2013)

The Nigerian poultry industry is estimated at ₦80 billion ($600 million) and is comprised of approximately 165 million birds, which produced 650,000 MT of eggs and 290,000 MT of poultry meat in 2013. From a market size perspective, Nigeria's egg production is the largest in Africa (South Africa is the next largest at 540,000 MT of eggs) and it has the second largest chicken population after South Africa's 200 million birds (USDA, 2013). Chicken importation (with the exception of day-old-chicks) was banned by Nigeria in 2003, which spurred growth in domestic poultry production. Statistics from Eurostat, however, high-light that between 2009 and 2011 over 3 million MT worth of poultry products were imported into the Republic of Benin, with the preponderance of these products ending up in the Nigerian market. If this is reflected in overall assumptions, estimated poultry meat consumption in Nigeria is approximately 1.2 million MT (USDA, 2013).

2.10.2 Performance of eggshell as solid catalyst for biodiesel production

Table 2.3: Summary of eggshell catalyst for biodiesel production

Catalysts	Feedstock	Operating conditions	Biodiesel Yield (%)	References
CaO from waste eggshell	Waste cooking oil	T=25^{0}C, t=11h, MeOH/Oil=6:1, C=5.8 wt.%	97	Aharon *et al.*, 2016
CaO from waste eggshell	Palm oil	T=65^{0}C, t=2h, MeOH/Oil=12:1, C=1.5 wt.%	98^{cv}	Cho and Seo, 2010
CaO waste eggshell	Palm oil	T=60^{0}C, t=4h, MeOH/Oil=9:1, C= 9 wt.%	94	Muthu and Viruthagiri, 2015
Chicken eggshell	Sunflower waste oil	T=60^{0}C, t=30min, MeOH/Oil=6:1, C= 3 wt.%	97.5	El-Gendy *et al*., 2015
Waste eggshell	Soybean oil	T=65^{0}C, t=3h, MeOH/Oil=9:1, C= 3 wt.%	95	Wei *et al.*, 2009
Industrial waste eggshell	Palm olein oil	T=60^{0}C, t=3h, MeOH/Oil=12:1, C= 10 wt.%	94.1	Faungnawakij *et al.*, 2012
KF/Eggshell	Soybean oil	T=65^{0}C, t=2h, MeOH/Oil=12:1, C= 2 wt.%	99	Danlin *et al.*, 2015
Li/Eggshell	Nahor oil	T=65^{0}C, t=4h, MeOH/Oil=10:1, C= 5wt.%	94	Jutika *et al.*, 2014
Eggshell	Palm oil	T=65^{0}C, t=4h, MeOH/Oil=9:1, C= 20wt.%	94	Buasri *et al.*, 2013

T=temperature, t=time, MeOH/Oil=methanol-oil molar ratio, C=catalyst dosage and CV=reported as "conversion" by authors

2.11 Synthesis of Solid Catalyst

The catalytic properties of heterogeneous catalysts are strongly affected by every step of the preparation together with the quality of the raw materials. The choice of a laboratory method for preparing a given catalyst depends on the physical and chemical characteristics desired in the final composition. It is easily understood that the preparation methods are also dependent on the choice of the base materials and experience shows that several ways can be considered, even for a given selection of the base material (Carlo and Villa, 1997). Table 2.4 reports the main unit operations usually applied in solid catalyst preparation.

Table 2.4: Unit operations in catalyst synthesis

S/N	Unit operations	S/N	Unit operations
1	Precipitation	**7**	Calcination
2	Gelation	**8**	Forming operation
3	Hydrothermal transformation	**9**	Impregnation
4	Decantation, filtration and centrifugation	**10**	Crushing and grinding
5	Washing	**11**	Mixing
6	Drying	**12**	Activation

Source: (Carlo and Villa, 1997)

2.11.1 Main unit operations for solid catalyst preparation

2.11.1.1 Precipitation or co-precipitation

The aim of this step is to precipitate a solid from a liquid solution. While each intermediate in the preparation chain can be considered the precursor of the following one, precipitation gives rise to the basic precursor, because it creates the imprint or latent image of the final solid that subsequent operations will progressively reveal. Precipitation occurs in three steps: supersaturation, nucleation and growth. Precipitation procedures can be used to prepare single component catalysts, supports or mixed catalysts. The main purpose in the latter case is the intimate mixing of the catalyst components that can be achieved either by the formation of very small crystallites or by the formation of mixed crystallites containing the catalyst constituents (Carlo and Villa, 1997).

2.11.1.2 Calcination

Calcination is a further heat-treatment beyond drying. As with drying, this unit operation can be located before or after the forming operation, depending on the case (Carlo and Villa, 1997). Calcination in air, occur typically at temperatures higher than those used in drying operations.

Several processes occur during calcination: loss of the chemically bonded water or CO_2 modification of the texture through sintering (small crystals or particles which turn into bigger ones), modification of the structure, active phase generation and stabilization of mechanical properties (Carlo and Villa, 1997).

2.11.1.3 Impregnation

Supported catalysts are often applied because they combine a relatively high dispersion (amount of active surface) with a high degree of thermostability of the catalytic component. The preparation of supported catalysts aligns all the unit operations toward dispersing an active agent on a support that may be inert or catalytically active. The wetting of the support with a solution or a slurry of the active phase precursors is the operation that characterizes such a preparation. The active species are introduced into a porous support not in their final form but by impregnation with a solution containing a precursor, the choice of which is crucial for the final dispersion (Carlo and Villa, 1997).

The impregnation method involves three steps:

(1) Contacting the support with the impregnating solution for a certain period of time,

(2) Drying the support to remove the imbibed liquid, and

(3) Activating the catalyst by calcination, reduction or other appropriate treatment.

Two methods of contacting may be distinguished, depending on the total amount of solution.

(1) With excess of solution. The support is placed on a screen and dipped into an excess quantity of solution for the time necessary for total impregnation. The solid is then drained and dried (Satterfield, 1980).

(2) With repeated application of solution. A more precise control is achieved by this technique, termed dry impregnation or impregnation to incipient wetness.

The support is contacted with a solution of appropriate concentration, corresponding in quantity to the total known pore volume or slightly less (Satterfield, 1980).

2.11.1.3.1 Impregnation without chemical interaction

The impregnation will be called with no interaction when no specific interaction between the impregnating solution and the support is foreseen or no particular attention is given to following this aspect. In this case the greater dispersion of the active species observed for a supported catalyst must be ascribed to differences in the precipitation of the precursor occurring during drying. In fact, although the formation of the precipitate particles is ruled by the same laws for supported and unsupported catalysts, the heterogeneous nucleation is enormously enhanced inside the pores by the high surface area available of the support in contact with the solution. In the thermal treatments which follows the support acts as a 'spacer', i.e. separates the small crystals formed and slows down the process of crystal growth (not the transformation into the final active species) (Carlo and Villa, 1997). The final dispersion depends on many parameters, such as support texture, precursor solubility and drying velocity and on the nature of the starting salts. The interaction of the support with the active species is not only physical in nature, but there is always a more or less pronounced influence of its chemical nature.

2.11.1.3.2 Impregnation with chemical interaction

The impregnation with interaction tries to take advantage of a chemical interaction of the support with the impregnating solution so as to obtain a better dispersion of the active species: dispersion reaching almost the value of 1 (atomic dispersion) may be reached during this stage. Often the particle size of a metal supported by this procedure is of the order of 10Å, while by impregnation with no, interaction it is rare to reach values below 50Å (Carlo and Villa, 1997).

2.12 Characterization of Eggshell Derived Catalyst

2.12.1 SEM-EDS of eggshell derived catalysts

Scanning Electron Microscopy (SEM) is a method for high-resolution imaging of surfaces. The electrons interact with the atoms that make up the sample, producing signals that contain information about the sample's surface topography, composition, and other properties such as electrical conductivity (Amaral, 2011). Energy Dispersive X-ray Spectroscopy (EDS) is an analytical technique used for the elemental analysis or chemical characterization of a sample. It is used to study the interaction between a source of X-ray excitation, and a sample. It is based on the fundamental principle that each element has a unique atomic structure allowing X-rays that are characteristic of an element's atomic structure to be identified uniquely from one another (Amaral, 2011).

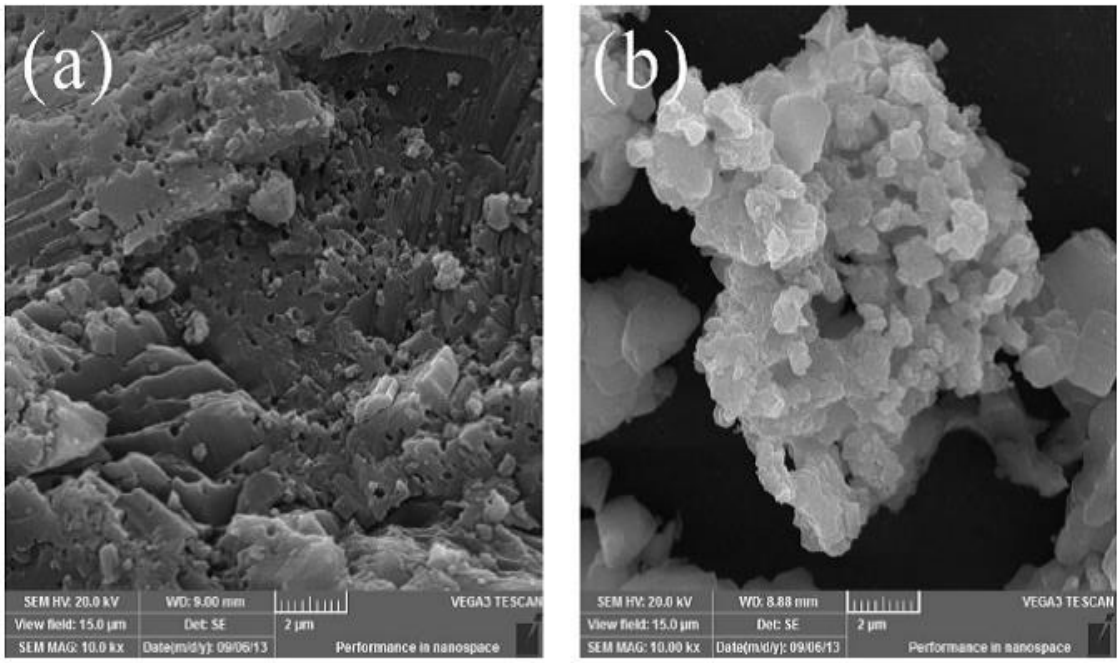

Figure 2.6: SEM micrographs of (a) CaO derived from eggshell (b) KF/eggshell catalyst calcined at 800^0C for 12h (Danlin *et al.*, 2015)

2.12.2 X-ray fluorescence (XRF)

X-ray fluorescence (XRF) is the emission of characteristic "secondary" (or fluorescent) X-rays from a material that has been excited by bombarding with high-energy X-rays or gamma rays. The phenomenon is widely used for elemental analysis and chemical analysis, particularly in the investigation of metals, glass, ceramics and building materials, and for research in geochemistry, forensic science, archaeology and art objects (Beckhoff *et al.,* 2006).

Table 2.5: Chemical composition of eggshell

Components	Percentage composition	
	Raw Eggshell	Calcined Eggshell at 900^0C for 4h
CaO	70.7	89.8
SiO_2	0.12	0.10
Al_2O_3	0.04	0.32
MgO	0.01	0.01
Fe_2O_3	0.03	0.03
Na_2O	0.23	0.21
P_2O_5	0.24	0.26
SO_3	0.63	0.63
LOI	28.2	11.5

Source: (Eletta *et al.*, 2016), LOI: Loss on ignition

2.12.3 X-ray diffraction (XRD)

Solid matter can be described as:

Amorphous: The atoms are arranged in a random way similar to the disorder we find in a liquid. Glasses are amorphous materials.

Crystalline: The atoms are arranged in a regular pattern, and there is as smallest volume element that by repetition in three dimensions describes the crystal. E.g. we can describe a brick wall by the shape and orientation of a single brick. This smallest volume element is called a unit cell (Hull, 1919). The dimensions of the unit cell is described by three axes: a, b, c and the angles between them alpha, beta and gamma.

About 95% of all solids can be described as crystalline. When x-rays interact with a crystalline substance (phase), one gets a diffraction pattern. Hull (1919) reported that every crystalline substance gives a pattern; the same substance always gives the same pattern; and in a mixture of substances each produces its pattern independently of the others. The x-ray diffraction pattern of a pure substance is, therefore, like a fingerprint of the substance (Hull, 1919). The main use of powder diffraction is to identify components in a sample by a search/match procedure. Furthermore, the areas under the peak are related to the amount of each phase present in the sample (Hull, 1919).

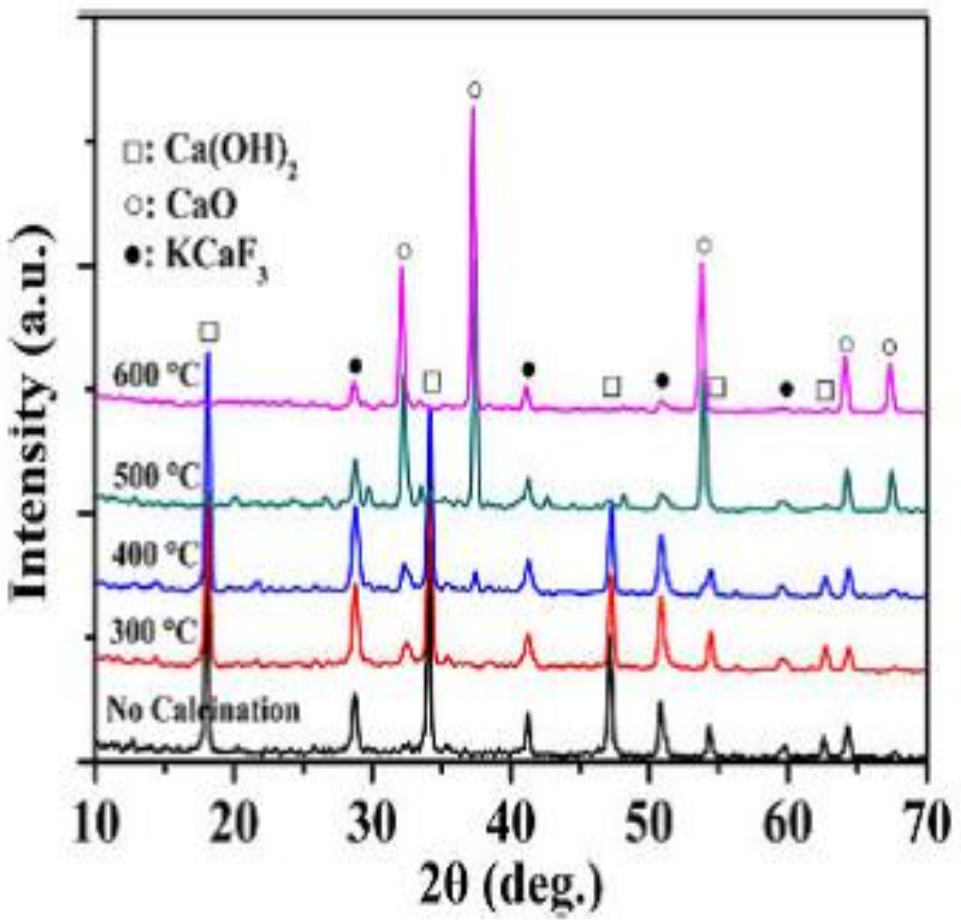

Figure 2.7: XRD patterns of KF/CaO prepared under various temperature (Wen *et al.*, 2010)

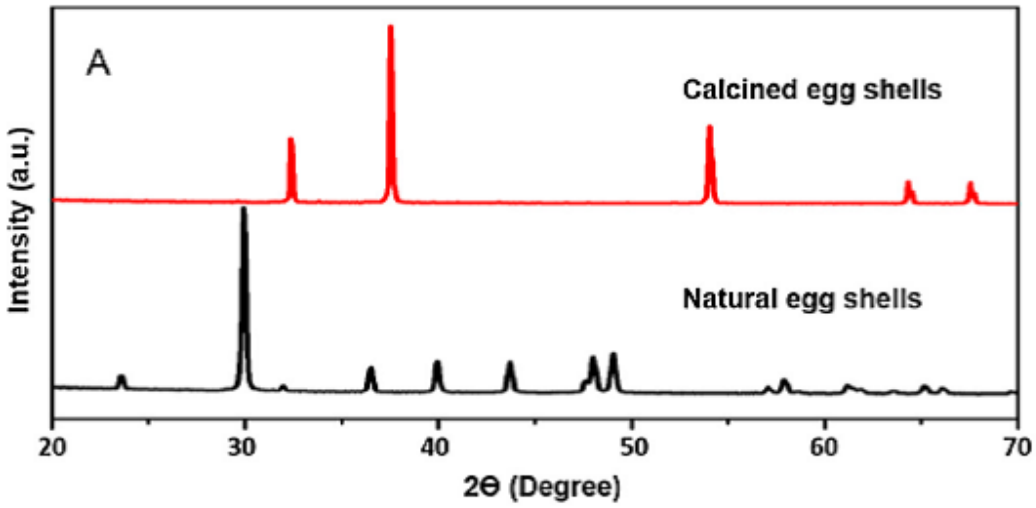

Figure 2.8: XRD patterns of natural eggshells and eggshells calcined at 900^0C for 3h (Aharon *et al.*, 2016)

2.12.4 Surface area and pore-size distribution

To elucidate the pore parameters and surface area, the well-known method is the sorption of probe molecules on a porous solid. Surface area, pore volume, and pore-size distribution were obtained by measuring volume adsorbed at different P/Po (where P and Po denote the equilibrium and saturation pressures of nitrogen, respectively) values and by applying different methods. The adsorption of a nitrogen gas on a solid catalyst can be quantitatively described by an adsorption isotherm, which represents the amount of condensed molecules (the adsorbates) in a porous solid catalyst (the absorbent) as a function of the partial pressure of the gas phase at a constant temperature. An array of computational procedures has been proposed by various authors to calculate the pore-size distribution from the nitrogen adsorption data (Ramesh *et al*. 2014). The surface area can be calculated from Brunauer–Emmett–Teller (BET), cumulative pore volume using Dollimore–Heal (DH) and Barret–Joyner–Halenda (BJH) models, while maximum pore volume can be evaluated from Horvath–Kawazoe (HK) model (Ramesh *et al.* 2014).

2.12.5 Basicity and acidity of solid surfaces

Number of methods for determining acidity and acid strength of solid surfaces have been reported recently and extensively used for the study concerning the correlation between catalytic activity and acidic property of solid catalyst. Very little work, however, has been made on basic property of solid surfaces. Only two methods for measuring basicity have been reported: i) Method to observe the color change of bromthymol blue adsorbed on solid suspended in decalin or in benzene. ii) Method to measure the amount of phenol vapor adsorbed on solid. Basic property of MgO, CaO, K_2CO_3, ZnO, ZnS etc. has been measured by these methods (Yamaguchi and tanabe, 1963). The basic strength (H_) of a solid base could be assessed using Hammett indicators. The following Hammett indicators could be used: bromthymol blue (H_=7.2), phenolphthalein (H_=9.8), 2, 4-dinitroa-niline (H_=15.0), and nitroaniline (H_=18.4). Approximately 50 mg of the catalyst sample should be shaken with 10 mL of anhydrous ethanolic solution of Hammett indicator and allowed to equilibrate for 2h. Then the color change of the solution should be observed. When the solution exhibits a color change, this indicates that the basic strength of the catalyst is stronger than the indicator used. However, when the solution produces no color change, the basic strength of the catalyst is weaker than that of the indicator used. It should be noted that Hammett indicator titration can only give qualitative information about the basic properties of catalysts (Song *et al.*, 2009)

2.12.6 Fourier transform infrared spectroscopy (FTIR)

Fourier transform infrared spectroscopy is a technique which is used to obtain an infrared spectrum of absorption or emission of a solid, liquid or gas. FTIR spectra reveal the composition of solids, liquids and gases. An FTIR spectrometer simultaneously collects spectral resolution data over a wide spectra range (Griffiths and Hasseth, 2007).

2.13 Reusability and Leaching: challenge of solid catalyst

As far as solid catalysts are concerned, catalyst active species leaching into the reaction media is always the prime concern. The extent of the catalyst leachability is the yardstick, inversely, for the solid catalysts practical usage as well as their ability to be reused. For the case of CaO, past results indicate that it has a considerably low leaching property and lower (0.035%) solubility in methanol (Pragas *et al.,* 2011). A work by Granados *et al.,* (2007) revealed that the contribution of CaO heterogeneity is more crucial and relevant to obtain a higher yield. For reutilization of the catalyst, the leaching of CaO was not so intense (able to be reused eight times with a yield ranging from 81 to 73%), as long as a sufficient amount of catalyst is employed in each reuse (Granados *et al.,* 2007). The rate of leaching is proportionate with the reaction time, hence, reaction conditions with a shorter catalyst residing time could be the possible solution without compromising the purity and yield of the final product (Pragas *et al.,* 2011). Summarily, although there is CaO lixiviation into reaction media, the heterogeneity of CaO still plays a dominant role over the homogeneity route and by controlling the reaction duration, the degree of catalyst leaching can be further minimized (Pragas *et al.,* 2011).

2.14 Design of Experiment

Design of experiment (DOE) is a statistical method for systematically planning and conducting scientific studies that investigate independent experimental variables of interest altogether at a time in order to determine their effects on a given response. It is a more efficient approach than the traditional method of changing "one variable at a time" in order to observe the variable's impact on a given response (Montgomery and Rupp, 2005).

2.14.1 Response surface methodology

Response Surface Methodology (RSM) is a well-known up to date approach for constructing approximation models based on either physical experiments, computer experiments (simulations) and experimented observations (Box *et al.,* 1978; Montgomery *et al.,* 1994). RSM, invented by Box and Wilson, is a collection of mathematical and statistical techniques for empirical model building (Raissi and Eslami, 2009). RSM involves two basic concepts: (1) The choice of the approximate model, and (2) The plan of experiments where the response has to be evaluated.

2.14.1.1 Design procedure for response surface methodology

Optimization of processes is used to determine the levels of the design parameters at which the response reaches its optimum. The optimum could be either a maximum or a minimum of a function of the design parameters (Raissi and Eslami, 2009). In this technique, the main objective is to optimize the response surface that is influenced by various process parameters. Response surface methodology also quantifies the relationship between the controllable input parameters and the obtained response surfaces (Raissi and Eslami, 2009).

The design procedure of response surface methodology is as follows:

1. Designing of a series of experiments for adequate and reliable measurement of the response of interest.
2. Developing a mathematical model of the second order response surface with the best fittings.
3. Finding the optimal set of experimental parameters that produce a maximum or minimum value of response
4. Representing the direct and interactive effects of process parameters through two and three dimensional plots.

If all variables are assumed to be measurable, the response surface can be expressed as follows:

$$Y = \beta_0 + \sum_{j=1}^{n} \beta_j X_j + \sum_{j=1}^{n} \beta_{jj} X_{jj}^2 + \sum_{i} \sum_{j=2}^{n} \beta_{ij} X_i X_j + e_i \qquad (2.4)$$

Where e_i is a random error. The β coefficients, which should be determined in the second-order model, are obtained by the least square method. The mathematical models were evaluated for each response by means of multiple linear regression analysis. The significant terms in the model were found by analysis of variance (ANOVA) for each response. Significance was judged by determining the probability level that the F-statistic calculated from the data is less than 5%. The model adequacies were checked by R^2, adjusted-R^2, predicted-R^2 and prediction error sum of squares (PRESS) (Raissi and Eslami, 2009). A good model will have a large predicted R^2, and a low PRESS.

2.14.2 Optimization using RSM: desirability function approach

The desirability function was originally developed by (Harrington, 1965) as reported in (Raissi and Eslami, 2009) to simultaneously optimize the multiple responses and was later modified by (Derringer and Suich, 1980) to improve its practicality (Raissi and Eslami, 2009). The desirability lies between 0 and 1 and it represents the closeness of a response to its ideal value. If a response falls within the unacceptable intervals, the desirability is 0, and if a response falls within the ideal intervals or the response reaches its ideal value, the desirability is 1. Meanwhile, when a response falls within the tolerance intervals but not the ideal interval, or when it fails to reach its ideal value, the desirability lies between 0 and 1. The more closely the response approaches the ideal intervals or ideal values, the closer the desirability is to 1.

2.15 Summary

Homogeneous catalyzed transesterification is the preferred choice for producing biodiesel commercially. Nevertheless, the numerous disadvantages of homogeneous catalyst cannot be over looked. The interest in solid catalysis for biodiesel production is increasing daily, hence a breakthrough in solid catalysis that can completely replace homogeneous system of catalysts remains a subject of research focus. The cost determinant for final biodiesel product in the production chain is the vegetable oil. The high cost of edible refined vegetable oil with very low free fatty acids is an integral part of the overall cost of biodiesel production, therefore means to reduce this cost is most sought after. This quest has generated a lot of interest in non-edible vegetable oil, but this type oil usually have high free fatty acids. The established process route for producing biodiesel using this type of oil remains, esterification-transesterification. The esterification is usually carried out with acid catalysts to reduce the free fatty acids, followed by a base catalyzed transesterification to produce the biodiesel. These two-step process could become cumbersome when dealing with vegetable oil with very high free fatty acids content. In this research, synthesizes of a catalyst capable of circumventing these several steps was carried out. The catalyst was able to esterify and transesterify in a single stage.

CHAPTER THREE

MATERIALS AND METHODS

3.1 Materials and Apparatus

Table 3.1: Materials for the catalyst synthesis and transesterification reaction

S/N	QUANTITY	MATERIALS	REAGENT QUALITY	MANUFACTURER
1	5 litres	Neem oil	Crude	NARICT
3	1 litre	Waste cooking oil	Waste	Not applicable
4	5 litres	Methanol	Analytical grade (99%)	Sigma Aldrich
5	3.5 kg	Spent eggshell	Not applicable	Not applicable
8	10 litres	Distilled water	Analytical grade	ABU Chem. Eng Dept.
9	500g	($KF.2H_2O$)	Analytical grade	Sigma Aldrich
10	500g	($FeCl_3.6H_2O$)	Analytical grade	Sigma Aldrich
11	500g	($FeCl_2.4H_2O$)	Analytical grade	Sigma Aldrich
12	250ml	(NH_4OH)	Analytical grade	Sigma Aldrich
13	5 litres	Deionized water	Analytical grade	ABU Chem. Eng Dept.
14	50g	(KOH)	Analytical grade	Sigma Aldrich
15	50ml	(H_2SO_4)	Analytical grade	Sigma Aldrich
16	50g	(NaCl)	Table salt	Sigma Aldrich
17	25ml	Phenolphthalein	Analytical grade	Sigma Aldrich
18	250ml	Ethanol	Analytical grade (99%)	Sigma Aldrich
19	500g	CaO	Analytical grade (99%)	Sigma Aldrich

Neem oil was obtained at National Research Institute of Chemical Technology (NARICT), all analytical grade chemicals used in this research were obtained from Sigma Aldrich through their Nigerian distributor; Zayo Chemicals Limited, Jos. Nigeria.

Table 3.2: Equipment/Apparatus for catalyst synthesis and transesterification process

S/N	APPARATUS	MANUFACTURER/ MODEL
1	Electric furnace	Nabertherm/LH12014
2	Ball milling machine	Kera
3	Viscometer	Brookfield/RVT43320
4	Flash point apparatus	Cleveland/HZKS-3
5	Magnetic hot-plate stirrer	Stuart/SB162
6	Electric oven	Gallenkamp/PA2345
7	Sieve-shaker	Sieve-tronic
8	BET Machine	Quantachrome/4200e
9	XRF Machine	Shidmadzu/XRF-1800
10	FTIR Machine	Agilent/Cary 630
11	GCMS Machine	Shimadzu QP2010PLUS
12	EDS Machine	Shidmadzu/EDX-720
13	SEM Machine	Hitachi/S-4500
14	XRD Machine	Shidmadzu/XRD-6000
15	Refrigerator	Thermofisher
16	Glasswares	Pyrex
17	Digital weighing balance	AEAdam/PW184
18	Reflux condensers	Pyrex
19	Desiccator	Pyrex
20	Filtration apparatus	-
21	pH meter	Agilent

3.2 Physicochemical Characterization of Neem Oil

3.2.1 Determination of saponification value of neem oil

The saponification value of the neem oil sample was evaluated using the (ASTM D5558, 1995) analytical method. Two grams of the neem oil weighed using a digital weighing balance was transferred into a 250ml round-bottom flask using a pipette. Freshly prepared 0.5 N alcoholic potassium hydroxide solution (25ml) was added to the sample by means of pipette, and the mixture gently refluxed on a water bath using an air-condenser for 60 minutes. Then the flask was cooled, the condenser tip was washed with little distilled water, and the contents was titrated with 0.5 N hydrochloric acid solution using 2 drops of phenolphthalein as an indicator. A Blank titration was simultaneously conducted under same conditions without the oil sample to serve as a controlled experiment.

$$\text{Saponification value} = \frac{(V_b - V_s) \times 28.05}{W} \quad (3.1)$$

Where Vb = titre value for blank, Vs = titre value for sample, W = weight of sample in gram and 28.05 = the equivalent weight (mg) of KOH required to neutralize 1ml of 0.5N HCl. The difference between the blank and test sample reading gives the number of millilitres of 0.5N KOH required to saponify 1g of fat.

3.2.2 Determination of acid value of neem oil

The acid number and free fatty acid of the oil was determined by the procedures of (ASTM D664-11ae1, 2011) Two grams of the neem oil was weighed using a digital weighing balance, which was transferred into a 250ml conical flask using a pipette. Propan-2-ol (25ml) was added by means of a pipette, and the flask was heated on a steam bath for 3 minutes. Then the flask was cooled, and the contents was titrated with 0.1N potassium hydroxide solution using 2 drops of phenolphthalein as an indicator.

$$\text{Acid value} = \frac{V \times N \times 56.1}{W} \quad (3.2)$$

Where, V = volume of potassium hydroxide used, N = normality of potassium hydroxide, W = weight in gram of the oil and 56.1= the equivalent mass (mg) of KOH.

3.2.3 Determination of percentage free fatty acid (%FFA) from acid value

The percentage free fatty acid is usually calculated in terms of oleic acid, 1000g of sample contains 282 g of oleic acid. The method enumerated in (ASTM D5555, 2011) was employed for the calculation of the free fatty acid content of the neem oil.

$$\frac{Acid\ value}{56.1} = \frac{V \times N}{W} \quad (3.3)$$

$$\frac{\%FFA}{28.2} = \frac{V \times N}{W} \quad (3.4)$$

$$\frac{\%FFA}{28.2} = \frac{Acid\ value}{56.1}$$

$$\frac{Acid\ value}{\%FFA} = \frac{56.1}{28.2}$$

$$\%FFA = \frac{Acid\ value}{1.99} \quad (3.5)$$

3.2.4 Determination of specific gravity of neem oil

The procedure of hydrometer method (ASTM D1298, 2012), was used to measure specific gravity of the neem oil. A clean dry empty 25ml density bottle was weighed and the mass recorded as W_1, it was then filled up with distilled water and subsequently with the neem oil. The mass of the bottle and water was taken and recorded as W_2 and that of neem oil as W_3 respectively. The experiment was conducted at 40°C. The specific gravity was evaluated using the equation 3.6

$$\text{Specific gravity of the neem oil sample} = \frac{(W_3 - W_1)}{(W_2 - W_1)} \quad (3.6)$$

3.2.5 Determination of iodine value of neem oil

The WIJS method reported in the Journal of European Committee for Standardization (EN-14111, 2003) was adopted in determining the iodine value of the neem oil. One gram of the oil was measured into a 250 ml conical flask followed by addition of 30 ml of Hanus solution; the content was well mixed and placed in fume cupboard for exactly 30

minutes. Potassium iodide solution (10 ml of 15% w/v) was added to the flask washing down any iodide that was found on the stopper. This was titrated against 0.12 M $Na_2S_2O_3$ until the solution became light yellow. Starch indicator (1%, 2 ml) was added which turned the mixture to blue, and the titration continued until the instant at which the blue colour disappeared. A blank titration was also carried out under the same conditions. The titre value was recorded and used to calculate the iodine value.

$$I_v = \frac{(V_b - V_s) \times N \times 12.96}{Weight\ of\ sample} \quad (3.7)$$

I_v = iodine value of sample to the nearest whole number, N = normality of $Na_2S_2O_3$

V_b = titre value of blank, V_s = titre value of sample and 12.96 = correlation factor derived from equivalent weight of iodine.

3.2.6 Determination of viscosity of neem oil

The viscosity of the neem oil was measured using Brookfield Synchro-Electric RVT-43320 viscometer at 40^{o}C. Exactly 200 ml of the oil was transferred into a beaker. The spindle, No. 2 attached to the viscometer, was lowered into the beaker and allowed to attain same temperature with the sample. The viscometer was operated at a speed of 60 rpm by which the spindle rotates in the sample. With the viscometer on, the reading at 25% shear rate was taken and recorded.

3.2.7 Determination of moisture content in neem oil

In other to determine the moisture content (%) in the oil, standard test method for direct moisture content measurements (ASTM D5556, 2011) was used. Exactly 100g of the oil was weighed and filtered using muslin cloth to remove solid particles. Precisely 50g of the filtered oil was measured and poured into a moisture pan. The weight of the pan and oil was taken. The oil was heated in an oven for 1 h at a temperature of 120^{o}C. The sample was cooled and weighed, this procedure was repeated until the weight before and after heating was accurately measured. Loss in weight is assumed to be moisture loss.

3.2.8 Molecular weight determination

The saponification and acid value of the neem oil were determined. The molecular weight of the oil was calculated according to the formular given by Xu *et al.,* (2007);

$$M_w = \frac{168300}{SV - AV} \quad (3.8)$$

Mw = molecular weight of oil, SV = saponification value of oil and AV = acid value of oil.

3.3 Eggshell Pre-treatment for Catalyst Synthesis

The overall process flow diagram for the non-magnetic catalyst synthesis is shown in figure 3.1. Spent chicken eggshell is the major raw material in this research from which CaO compound is synthesized. The stepwise synthesis processes from raw eggshell to the catalyst are discussed as follows;

3.3.1 Eggshell collection

Spent eggshells were collected at Frizlers restaurant in Ahmadu Bello University main campus, Zaria. The total collected spent eggshell weighed 3.5 kg.

3.3.2 Beneficiation of eggshell (Boiling, washing and drying)

The eggshells were boiled at a temperature of about 120^{o}C for 30 minutes to solidify the gelatinous materials adhering to the inner wall of the eggshell for easy removal. Also, to kill the microorganism possibly growing in the eggshell. The boiled eggshells were soaked in a distilled water at room temperature for 20 minutes. The eggshells were vigorously washed and crushed for size reduction, the less dense inner wall linings floated in the water, while the denser shells sunk in the water. This step was repeated eleven times until all the gelatinous materials were satisfactorily removed. The crushed eggshells were then dried in hot air oven at 105^{o}C for 24 h.

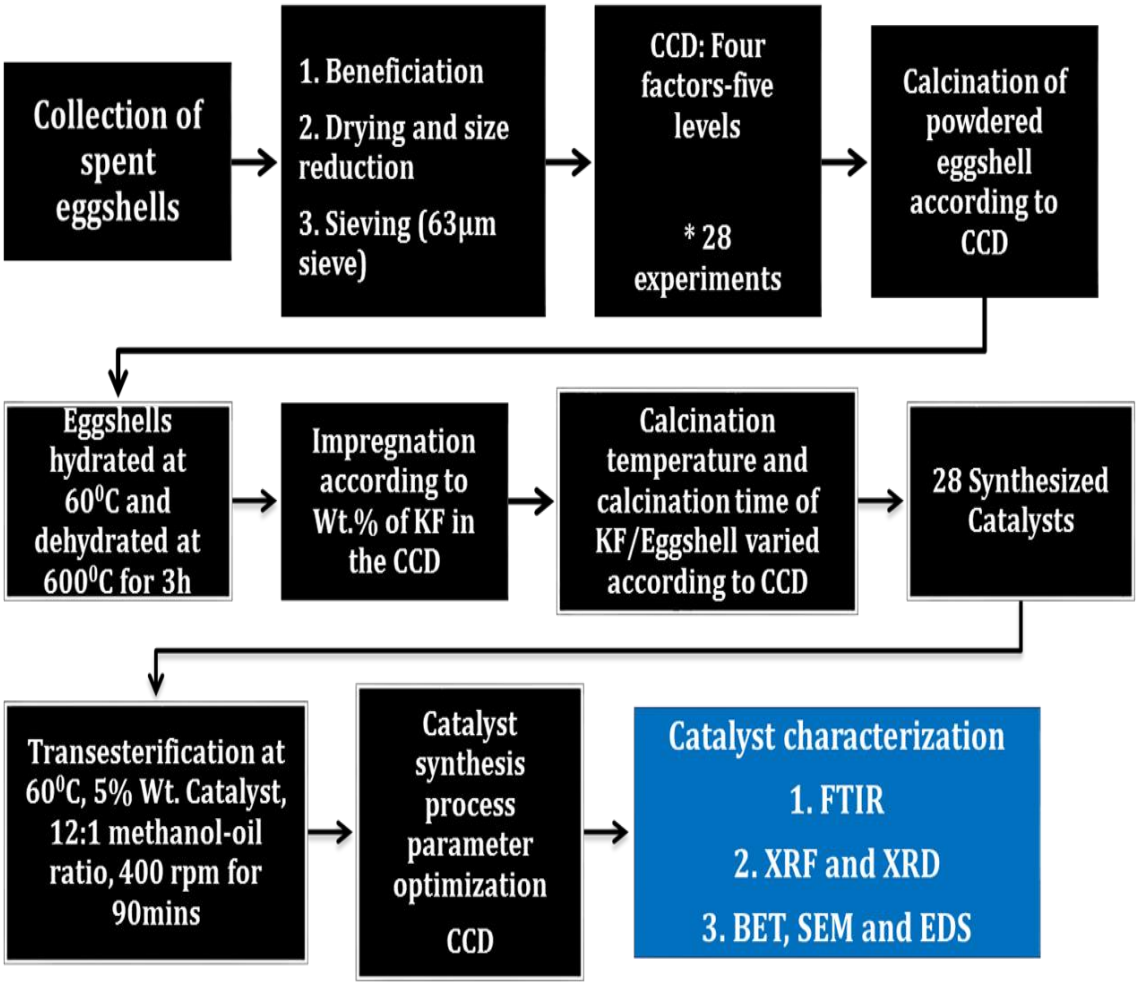

Figure 3.1: General procedure used for catalyst synthesis, performance testing and characterization

3.3.3 Milling and sieving of eggshell

The dried eggshells were ball milled for 16h to reduce the particle size and increase the surface area. The particle size was further reduced using a 63µm mesh sized sieve mounted on a sieve- shaker. The sieve-shaker was operated for 20 minutes per batch to obtain fine brown coloured particles. The powdered eggshell was weighed to be 3.1 kg, designated as beneficiated and kept in the desiccator for further treatment.

3.3.4 Central composite design of experiment for catalyst synthesis

Design Expert software version 10 already installed on a DELL Laptop running windows 10 operating system was utilized. The option “new design” was clicked upon to design new experiments for the catalyst preparation process. The “response surface” menu on the upper left hand corner was clicked. The central composite design (CCD) was selected. Four factors having the specified levels as presented in Table 3.3 was formulated. The required response for the experiment was designated to be the biodiesel yield. A total of 28 experiments were obtained, this included; 16 factorial points, 8 axial points and 4 centre points. The developed experimental matrix is shown in Table 3.4.

Table 3.3: Catalyst synthesis process factors for Response Surface Methodology using a rotatable CCD

S/N	Process Factors	Units	Low Level (-)	High Level (+)
Eggshell calcination temperature fixed at 900^{o}C				
1	Eggshell calcination time	h	2	4
2	Dosage of KF in calcined eggshell	wt.%	15	35
3	Calcination temperature of KF/Eggshell	^{o}C	300	600
4	Calcination time of KF/Eggshell	h	2	4

Block = 1 Alpha = 2

Table 3.4: Design of catalyst synthesis experiment

		Factor 1	Factor 2	Factor 3	Factor 4
Std	Run	A:Eggshell Calcination time	B:KF/Calcined Eggshell Impregnation	C:Calcination Temperature of KF/Eggshell	D:Calcination time of KF/Eggshell
		h	wt.%	^{o}C	h
14	1	4	15	600	4
25	2	3	25	450	3
18	3	5	25	450	3
7	4	2	35	600	2
21	5	3	25	150	3
17	6	1	25	450	3
26	7	3	25	450	3
11	8	2	35	300	4
27	9	3	25	450	3
3	10	2	35	300	2
13	11	2	15	600	4
28	12	3	25	450	3
16	13	4	35	600	4
6	14	4	15	600	2
15	15	2	35	600	4
8	16	4	35	600	2
1	17	2	15	300	2
2	18	4	15	300	2
20	19	3	45	450	3
12	20	4	35	300	4
22	21	3	25	750	3
23	22	3	25	450	1
5	23	2	15	600	2
10	24	4	15	300	4
9	25	2	15	300	4
4	26	4	35	300	2
24	27	3	25	450	5
19	28	3	5	450	3

3.4 Laboratory Synthesis of the Catalyst

The synthesis of the catalyst was carried out in the laboratory according to the designed parameters in Table 3.4 of the central composite design. The general block diagram follows from that given in figure 3.1; the stepwise procedures are enumerated as follow;

3.4.1 Calcination of beneficiated eggshell

Five suitable crucibles labelled A-E each containing 500g of the beneficiated eggshell were marked for calcination. Crucible A was marked 5 h, B-4 h, C-3 h, D-2 h and E-1 h. Calcination of the eggshell was carried out in a muffle furnace under static air condition at 900^{o}C using the eggshell calcination times specified in the Table 3.4 to decompose the calcium carbonate species in the eggshell into CaO molecules. The five samples of calcined beneficiated eggshell in the marked crucibles were kept in the desiccator for further use.

3.4.2 Hydration-dehydration of calcined eggshell

The CaO derived from the five samples of the calcined beneficiated eggshell was hydrated with distilled water and stirred on a magnetic stirrer at 150rpm for 3 h. This mixture was allowed to settle for 24 h. The whitish solid product obtained was filtered and dried in a hot air oven at 105^{o}C for 24 h. The dried sample was further dehydrated by calcination at 600^{o}C for 3 h to convert the hydroxides to highly porous calcium oxide. The dehydrated samples in the marked crucible were designated refined eggshell, and were kept in the desiccator.

3.4.3 Synthesis of KF/Eggshell by wet impregnation method

Exactly 50g each of the stored refined eggshell samples were measured. An aqueous solution of potassium fluoride (KF) was prepared according to the weight specified in the design, (5-45wt. % KF dosage based on refined eggshell weight). The measured refined eggshell sample was dissolved in the various KF solutions according to the DOE. The mixture was dried at 105^{o}C for 24 h in an electric oven and was subsequently calcined according to the temperature and time specified in the design. This resulted in the production of 28 different samples of the catalyst that were stored in desiccator for catalyst performance studies.

3.5 Catalyst Performance Testing: synthesis parameter studies

The 28 set of prepared catalysts were applied in a transesterification reaction to determine the efficacy of the catalyst in the transesterification of neem oil having FFA of 4.2%. This study is also meant to analyze optimum combination of parameters for synthesizing the catalyst based on the obtained biodiesel yield per experiment. The transesterification reaction was conducted using process conditions obtained from (Wen *et al.,* 2010) with little modifications. The reaction temperature and time used in this catalyst performance studies were different from those reported by Wen *et al.,* (2010). Briefly, the oil-methanol ratio used was 1:12, catalyst weight of 5wt. % was employed, reaction temperature of 60^{o}C and reaction time of 90 minutes were used, and the agitation speed was 400 rpm. Precisely 23g of the neem oil was measured into 100ml beaker and heated to 105^{o}C for 30 minutes in order to remove the moisture content of the oil. Exactly 10.71g of methanol was measured and mixed with 1.15g of the catalyst for 5 minutes in a 2-necked round-bottom flask. The heated oil was added to the methanol-catalyst mixture in 2-necked flat bottom flask, this was mounted with reflux condenser on a magnetic hot plate stirrer. The reaction proceeded for 90 minutes under constant stirring and heating. The mixture was allowed to cool down before been transferred into the clamped separating funnel. The glycerol, biodiesel and solid catalyst phase separated into three different distinct layers after 24 h. The topmost biodiesel layer was decanted, and was washed with warm distilled water until a clear solvent was obtained. The washed biodiesel was heated to 80^{o}C for 15 minutes to evaporate both the methanol and water molecules that may still be remaining in the mixture. The dried biodiesel was stored in a corked specimen bottle, then placed in a desiccator at room temperature for analytical purposes.

3.5.1 Optimization of catalyst synthesis parameters

The optimization feature of the design expert software was used based on the biodiesel yields obtained per experiment conducted. Profitability of the synthesis process was the objective function upon which an optimal solution was selected among the numerous solutions provided by the software. A predicted biodiesel yield was obtained based on the computed optimal synthesis parameters. The catalyst was synthesized using the selected optimal parameters. The synthesized catalyst was employed in a verification experiment for biodiesel production. The verification experiment was repeated three times and average of the biodiesel yield was recorded as the actual yield. The difference between the predicted yield and the actual yield was recorded and discussed in chapter four. Catalyst produced using these optimal parameters was designated as ***"OCAT"*** catalyst, was stored for characterization and applied in subsequent transesterification experiments.

3.6 Synthesis of Magnetic KF/Eggshell-Fe_3O_4 Catalyst

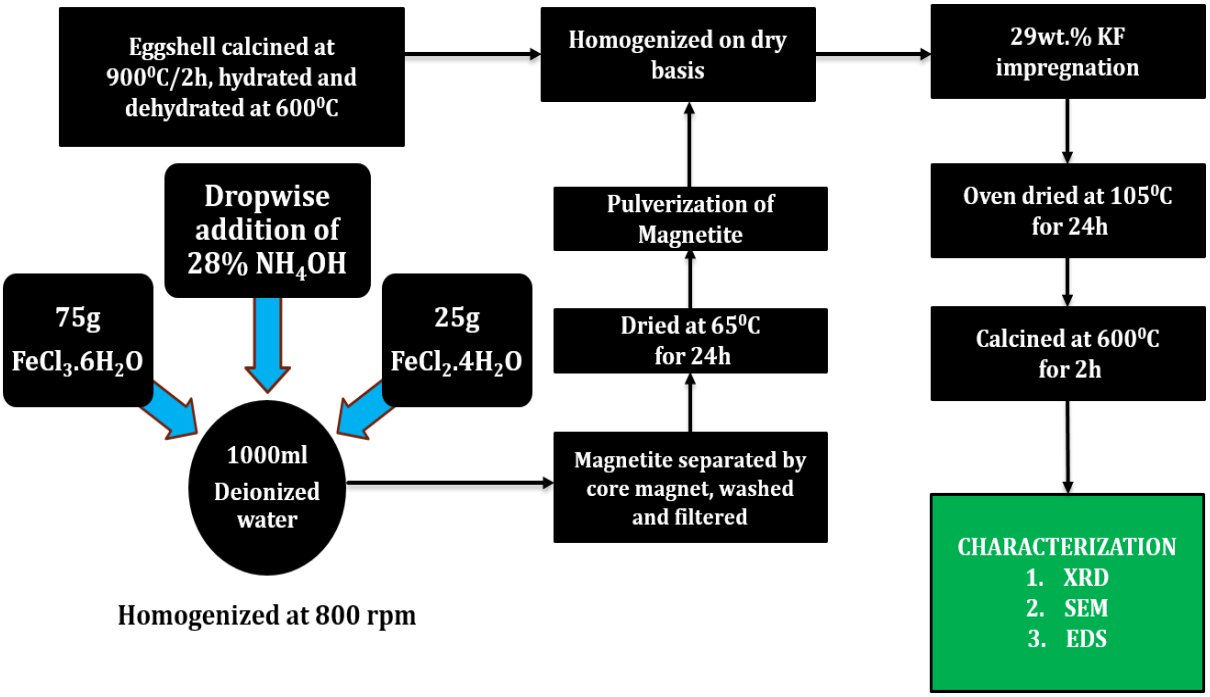

Figure 3.2: General procedure for synthesis and characterization of magnetized form of KF/Eggshell catalyst

3.6.1 Synthesis of magnetite (Fe_3O_4) by co-precipitation

Exactly 75g of Iron (III) chloride hexahydrate ($FeCl_3.6H_2O$) and 25g of iron (II) chloride tetrahydrate ($FeCl_2.4H_2O$) were measured and dissolved in 1000ml of deionized water. Precisely 100ml of 28% ammonium hydroxide (NH_4OH) solution was measured in a clamped burette. The NH_4OH solution was added drop wisely to the Fe^{2+} and Fe^{3+} solution at 60^{o}C, the solution was stirred at 800 rpm for 30 minutes. The pH of the solution was intermittently measured and was maintained at 12.0 by using the NH_4OH solution to control it. The mixture was allowed to cool down for 1 h. A black solid magnetite was formed, then separated by a permanent magnet core, washed with distilled water until the pH value of the mixture was 7.0. The mixture was filtered and the residue was dried at 65^{o}C in an electric oven for 24 h, after which it was pulverized and stored in the desiccator for further use. This procedure used for co-precipitation was slightly modified from that reported by Hu *et al.,* (2011). The basic medium used in here was different, also speed and time of agitation were different. Choice of basic medium here and agitation properties were based on research curiosity.

3.6.2 Synthesis of KF/Eggshell-Fe_3O_4 by wet impregnation

Exactly 20g of the stored refined eggshell was mixed with 1g of stored magnetite (Fe_3O_4) in a crucible. Precisely 29% aqueous solution of potassium fluoride (KF) established as optimum potassium fluoride (KF) dosage was prepared, and the fully mixed eggshell-Fe_3O_4 was dissolved in the prepared KF solution. The mixture was dried at 105^{0}C for 24 h in an electric oven, and was subsequently calcined at 600^{o}C for 2 h, which was established as optimal calcination condition for KF/Eggshell catalyst. The catalyst was designated as ***"MCAT"***, and stored in the desiccator for characterization and reusability studies.

3.7 Catalyst Characterization

Fourier Transform Infrared Spectroscopy (FTIR), X-ray Fluorescence Spectroscopy (XRF), X-Ray Diffraction Spectroscopy (XRD), Scanning Electron Microscopy (SEM), Electron Dispersive Spectroscopy (EDS) and Brunauer-Emmett-Teller (BET) were used for the characterization of the catalyst and raw materials according to the standard analytical procedures.

3.7.1 XRF characterization of the eggshell

The chemical compositions of the beneficiated eggshell was determined by XRF spectrometry using Shidmadzu XRF-1800 spectrometer.

3.7.2 SEM-EDS characterization of the catalyst

The morphology and specific composition of the beneficiated eggshell, refined eggshell, OCAT and MCAT catalysts were observed under Scanning Electron Microscopy with Energy Dispersive X-ray Spectroscopy (SEM-EDS) using Hitachi S-4500 field emission SEM with a quartz PCI X-one SSD X-ray analyzer.

3.7.3 XRD characterization of the catalyst

The crystalline phase of each stage of the transformation of eggshell into the desired catalysts was studied using Shidmadzu XRD-6000 Diffractometer. The XRD patterns were identified and analyzed by comparing their diffraction lines and intensities using the Joint Committee on Powder Diffraction Standards (JCPDS).

3.7.4 BET analysis of the catalyst

Quantachrome Nova 4200e BET machine was employed to determine the specific surface area, pore diameter and pore volume of the OCAT catalyst using the N_2 general adsorption-desorption technique.

3.8 Transesterification Process: parametric studies

Factors affecting the yield of biodiesel in a typical transesterification process were investigated using CCD (table 3.5). The CCD procedure followed that of the catalyst synthesis discussed in section 3.4.4. The general transesterification methodology is presented in figure 3.3. The stepwise transesterification process methodology is as explained in the section 3.6. A total of twenty-eight experiments were carried out, but the transesterification conditions employed per experiment were according to that specified in Table 3.6.

Table 3.5: Transesterification process factors for response surface methodology using rotatable CCD

S/N	Process Factors	Units	Low Level (-)	High Level (+)
1	Weight of catalyst	wt. %	3	5
2	Oil-methanol	Ratio	9	15
3	Reaction time	h	1.5	3
4	Reaction temperature	^{o}C	55	65

Block = 1 Alpha = 2

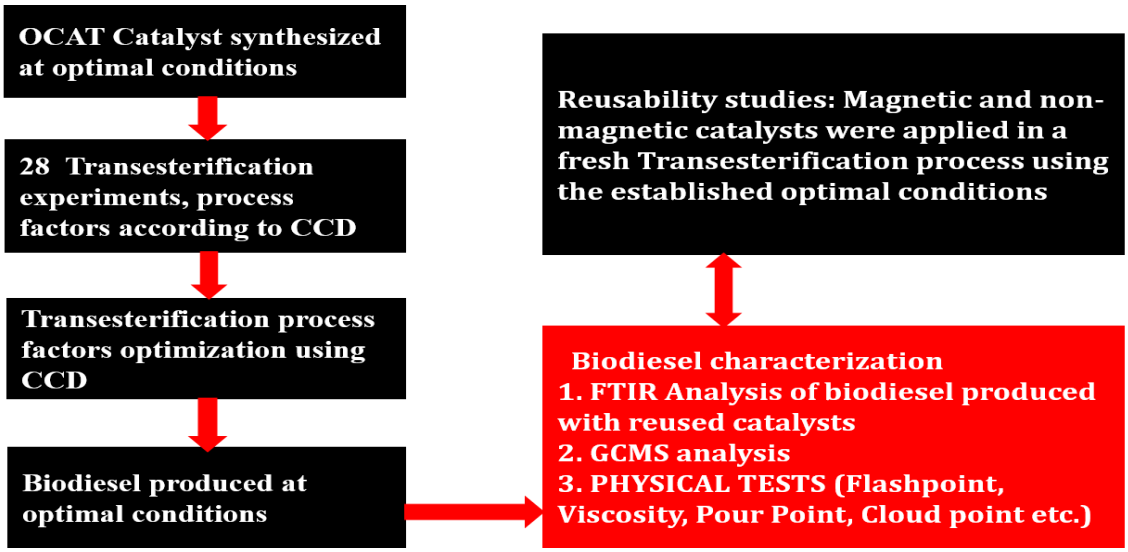

Figure 3.3: General procedure for transesterification experiment

Table 3.6: CCD of transesterification process experiments

		Factor 1	Factor 2	Factor 3	Factor 4
Std	Run	A:Weight of catalyst wt.%	B:Methanol-Oil Ratio	C:Reaction time h	D:Reaction temperature ºC
19	1	4	6	2.25	60
20	2	4	18	2.25	60
2	3	5	9	1.5	55
18	4	6	12	2.25	60
6	5	5	9	3	55
16	6	5	15	3	65
23	7	4	12	2.25	50
21	8	4	12	0.75	60
22	9	4	12	3.75	60
17	10	2	12	2.25	60
4	11	5	15	1.5	55
12	12	5	15	1.5	65
27	13	4	12	2.25	60
15	14	3	15	3	65
28	15	4	12	2.25	60
9	16	3	9	1.5	65
13	17	3	9	3	65
25	18	4	12	2.25	60
11	19	3	15	1.5	65
10	20	5	9	1.5	65
3	21	3	15	1.5	55
5	22	3	9	3	55
7	23	3	15	3	55
1	24	3	9	1.5	55
26	25	4	12	2.25	60
24	26	4	12	2.25	70
8	27	5	15	3	55
14	28	5	9	3	65

3.8.1 Optimization of transesterification parameters

As discussed in section 3.6.1, the optimization feature of the design expert software was employed for the purpose of optimizing the factors affecting transesterification reaction using the OCAT catalyst.

Based on the yield together obtained per transesterification experiment, a predicted yield of biodiesel was calculated. The predicted yield of biodiesel was calculated from a quadratic model equation developed using the software, its variables are the investigated transesterification factors. Three verification experiments were conducted using the selected optimal factors from which a predicted yield was calculated. The average of the biodiesel yield obtained in the verification experiment was taken as the actual yield. The difference between the predicted yield and the actual yield was recorded and discussed in chapter four. Biodiesel produced using these optimal factors was designated as neat biodiesel. The neat biodiesel was characterized thereafter.

3.9 Biodiesel Characterization

Fourier Transform Infrared Spectroscopy (FTIR) was used for the identification of methyl ester peaks present in the neat biodiesel. Gas Chromatography-Mass Spectroscopy (GC-MS) was used for qualitative identification of the chemical profiles of the neat biodiesel.

3.9.1 FTIR qualitative analysis of the neat biodiesel sample

The Agilent Cary 630 FTIR spectrometer employed for analysis of the produced neat biodiesel uses a helium-neon laser operating in the visible region at 632.8 nanometers. The main liquid ATR GE method was used for the analysis. A blank background analysis was run, thereafter a drop of the liquid biodiesel sample, which is approximately 5.0µl was placed on the cleaned crystal surface. A spectrum of the biodiesel sample was obtained after a background scan by the machine. The spectrum is presented and discussed in chapter four.

3.9.2 GC-MS qualitative identification of the ester content

Shimadzu GCMS-QP2010 PLUS machine was used for the chemical analysis of the neat biodiesel sample. The column temperature was 60^{o}C. The injection mode was split with a split ratio of 20, and the injection temperature is 200^{o}C.

The column pressure was 112.8 kPa, the column flowrate was 1.28mL/min and the total flowrate was 41.2mL/min. The gas velocity in the column was 49.2 cm/sec. The purge flowrate was recorded to be 3.0mL/min. Nitrogen gas was used as the mobile-phase which was laced with the neat biodiesel sample. The detector gain mode was relative with a threshold of 2000. The ion source temperature was 200^{o}C and the interface temperature was 250^{o}C.

3.9.3 Physicochemical properties of biodiesel

The ASTM was used where appropriate for the characterization of the produced biodiesel. The detailed procedures are explained in section 3.2.1 – 3.2.8 with the exception of flashpoint which was carried out using the Cleveland Flash Point Apparatus. Cloud point and pour points were measured using refrigeration method.

3.9.3.1 Determination of cloud point of the neat biodiesel

Cloud point determination was done manually using a refrigerator. Approximately 25ml of produced neat biodiesel was poured into a test tube and corked. The test tube was placed in a laboratory refrigerator. The test tube was cooled, the temperature inside the freezer segment of the refrigerator was taken every 15 minutes. The cooling was continued until a cloud (crystal) was detected using a laboratory optical aid, the temperature at that point was measured and recorded.

3.9.3.2 Determination of pour point of the neat biodiesel

Pour point determination was also carried out manually using a refrigerator. Approximately 25ml of produced neat biodiesel was poured into a test tube and corked. The test tube was placed in a laboratory refrigerator. The test tube was cooled, the temperature inside the freezer segment of the refrigerator was taken every 15 minutes. The test tube was shaking every 15 minutes, the cooling was continued until the liquid biodiesel turned solid. At that point, the temperature was measured and recorded.

3.9.3.3 Determination of flash point of the neat biodiesel

The Cleveland apparatus was used for the determination of flashpoint temperature of the produced neat biodiesel. Firstly, a brass test cup of the apparatus was filled to a certain level with approximately 100ml of the sample. Then, the temperature of the sample was increased rapidly and then at a slow, constant rate as it approaches the theoretical flash point of 130^{o}C. The increase in temperature caused the biodiesel to produce flammable vapor in increasing quantities and density. The lowest temperature at which the flame passing over the surface of the biodiesel causes the vapor to ignite was noted and considered its flash point temperature

3.10 Comparative Reusability Studies: KF/Eggshell- Fe_3O_4 and KF/Eggshell

The magnetic KF/Eggshell- Fe_3O_4 (MCAT) and the non-magnetic KF/Eggshell (OCAT) catalysts were repeatedly applied independently in a transesterification reaction whose optimal process conditions had been established. The aim was to study reusable efficacy of these catalysts in catalyzing neem oil for biodiesel production. Precisely 6 wt. % (based on weight of neem oil) of the non-magnetic (KF/Eggshell) catalyst was mixed with exactly 12.71g of methanol in a 2-necked flat bottom flask. Exactly 23g of the neem oil was added, and transesterification was carried out using established optimal conditions in section 3.9.1. At the end of the first transesterification process, the used catalyst was recovered after decantation of the liquid products. The recovered catalyst was washed with methanol, dried at 70^{o}C, and reused for transesterification of a freshly prepared neem oil. The same catalyst was reused for seven consecutive times. This process was repeated using the magnetic catalyst. The weight of catalysts recovered and yield of the biodiesel produced per experiment were recorded. The findings were analyzed and presented in chapter four.

3.11 Commercial CaO and Eggshell Comparative Performance

Analytical grade CaO obtained from commercial vendor was used in lieu of the eggshell to synthesize a catalyst KF/CaO similar to KF/Eggshell following the procedure enumerated in subheadings 3.4 – 3.5. The catalysts KF/CaO and KF/Eggshell were used in the transesterification of the neem oil having FFA of 4.2% to study the possible difference in their catalytic activities. The results of the observation is presented in chapter four.

CHAPTER FOUR

RESULTS AND DISCUSSION

4.1 Neem Oil Characterization

Table 4.1: Neem oil physicochemical characterization

Properties	Measured values	Literature values (Djibril *et al.*, 2015)
Density at 25^{o}C (g/cm^{3})	0.92	0.92
Acid value (mg KOH/g)	8.36	10.20
Free fatty acid (%)	4.20	NR
Iodine value (mg I/100g oil)	71.40	72.82
Viscosity at 40^{o}C (mm^{2}/s)	36.09	49.79
Saponification value (mg KOH/g oil)	206	200
Molecular weight (g/mol)	870	NR
Moisture content (%)	0.04	No moisture

NR= Not reported

Some of the measured values were within the range of the reported literature values, the variations in some could be attributed to differences in the origin of the vegetable oil. Neem oil used by Djibril *et al.* (2015) was sourced from Senegal, while that used in this research was sourced in Nigeria. Also, allowable error of experimentation may be responsible for the observed variations. Iodine value is an indicator of the oil saturation level, saturation of vegetable oil may not have negative impact on transesterification, but it determines the oxidative stability of the biodiesel produced. The neem is highly viscous which makes it unsuitable for direct use in diesel engine due to possible fuel atomization challenges. The measured acid value is about 700% higher than the standard 1mg KOH/g oil stipulated for direct biodiesel production over alkali catalyst. The modified solid base catalyst synthesized was utilized to produce biodiesel from the oil directly.

4.2 Response Surface Modelling of Catalyst Synthesis and Testing Process

The effect of catalyst synthesis factors on the performance of the twenty-eight synthesized catalysts was studied using a central composite design through a transesterification process explained in sections 3.5 - 3.5.1.

Biodiesel yield was used as a response and basis to evaluate the catalytic activity. The biodiesel yield was defined as a ratio of the weight of separated and dried biodiesel layer to the weight of oil used for the transesterification reaction as reported by Leung and Guo (2006).

$$\text{Biodiesel Yield} = \frac{\boldsymbol{Weight\ of\ biodiesel\ layer}}{\boldsymbol{Weight\ of\ oil\ used}} \times \mathbf{100} \qquad (\mathbf{4.1})$$

4.2.1 Analysis of variance for catalyst synthesis

Table A.1 containing design matrix for the investigated catalyst synthesis factors and their corresponding responses is presented in the appendix A. Table 4.2 shows the ANOVA for the quadratic response surface model fitting of the catalyst synthesis factors using regression coefficients. A full quadratic model for predicting percentage yield of biodiesel was obtained. The major indicators demonstrating the significance and adequacy of this model include the model "F-value" (Fisher variation ratio), "P-value" (Prob>F) and adequate precision (Montgomery *et al.*, 1994; Tureli, 2009). The p-value of less than 0.05 (5% significance level), indicates that the model or model term is significant, meanwhile values greater than 0.50 indicates that the model is insignificant (Montgomery *et al.*, 1994). The F-value and P-value of the obtained quadratic model presented in table 4.2 were found to be 42.8 and 0.0001 respectively. These imply that the response surface quadratic model is significant. Consequentially, the model can adequately predict the yield of biodiesel production based on the investigated catalyst synthesis variables affecting its catalytic activity. In this study, A, B, C, BC, A^2 and B^2 are significant model terms based on their p-values. The P-values of B, C, BC and B^2 were the most significant, this implies that, the amount of potassium fluoride impregnated and the temperature at which the catalyst is calcined are highly important to the overall activity of the catalyst. Accordingly, insignificant model terms contained in equation 4.2 were stepwisely removed as seen in equation 4.3 to improve the accuracy of the model equation.

$$\%\text{Biodiesel Yield} = 50.9 - 5.64A + 2.16B - 0.015C - 3.04D + 0.013AB + 0.0016AC - 0.125AD + 0.0014BC - 0.00005BD + 0.00083CD + 0.979A^2 - 0.05B^2 + 0.00002C^2 + 0.6D^2 \quad (4.2)$$

The reduced final quadratic model is given as equation 4.3.

Table 4.2: Analysis of variance (ANOVA) for catalyst synthesis

Full Quadratic Model					Model Accuracy	
Terms	Mean Square	F-value	P-value	Remarks	Correlation Coefficients	Values
Model	181.2	42.77	0.0001	Significant	R-squared	0.9757
A-Eggshell calcination time	20.2	4.76	0.0481	Significant	Adj. R-squared	0.9559
B- KF dosage	486.0	114.70	0.0001	Significant	Pred. R-squared	0.8807
C- Catalyst calcination temperature	1204.2	284.29	0.0001	Significant	Adeq. Precision	28.32
D- Catalyst calcination time	8.2	1.93	0.1884	Insignificant		
AB	0.3	0.06	0.8119	Insignificant		
AC	1.0	0.24	0.6352	Insignificant		
AD	0.3	0.06	0.8119	Insignificant		
BC	72.3	17.05	0.0012	Significant		
BD	0.0	0.00	1.0000	Insignificant		
CD	0.3	0.06	0.8119	Insignificant		
A^2	23.0	5.43	0.0365	Significant		
B^2	546.3	128.92	0.0001	Significant		
C^2	5.5	7.30	0.2747	Insignificant		
D^2	8.8	2.07	0.1741	Insignificant		
Residual	4.2	-	-	-		
Lack of fit	5.3	7.96	0.0572	Insignificant		
Pure error	0.7	-	-	-		

$$\%\text{Biodiesel Yield} = 37.68 - 3.66A + 2.31B + 0.012C + 0.00142BC + 0.76A^2 - 0.05B^2 \quad (4.3)$$

Equations 4.2 and 4.3 are given in terms of actual factors. These can be used to make predictions about the response for given levels of each factor. The levels should be specified in the original units for each factor. These equations should not be used to determine the relative impact of each factor because the coefficients are scaled to accommodate the units of each factor and the intercept is not at the center of the design space.

After the insignificant model terms have been reduced stepwisely using the software, about 60% increase was observed in the adequate precision value. The initial value before noise reduction was 28.32, while it rose to 45.18 thereafter. The “Adeq. Precision value" measures the model signal to noise ratio.

Table 4.3: ANOVA for response surface reduced quadratic model for catalyst synthesis

Full Quadratic Model					Model Accuracy	
Terms	Mean Square	F-value	P-value	Remarks	Correlation Coefficients	Values
Model	419.3	115.07	0.0001	Significant	R-squared	0.9705
A-Eggshell calcination time	20.2	5.53	0.0285	Significant	Adj. R-squared	0.9620
B- KF dosage	486.0	133.38	0.0001	Significant	Pred. R-squared	0.9105
C- Catalyst calcination temperature	1204.2	330.48	0.0001	Significant	Adeq. Precision	45.18
BC	72.3	19.83	0.0002	Significant		
A^2	15.5	4.26	0.0500	Significant		
B^2	663.3	182.05	0.0001	Significant		
Residual	3.64	-	-	-		
Lack of fit	4.14	6.21	0.0788	Insignificant		
Pure error	0.67	-	-	-		

Joglekar and May, (1987) established that for a good fit of a model, the correlation coefficient should be at a minimum of 0.80. Higher value of R^2 expresses excellent agreement between the predicted and actual results within the range of experiment. In this study, the values for the correlation coefficient (R^2) and adjusted coefficient (Adj. R^2) were found to be 97% and 96% respectively. The predicted correlation coefficient (Pred. R^2) was found to be 91%, this is in a reasonable agreement with the (Adj. R^2) as their difference is below 20%.

It is required for a good model that, the difference between (Pred. R^2) and (Adj. R^2) should not be above 20%. The P-value (Prob>F) for "Lack of Fit" was found to be 0.0788, which implies that the “Lack of Fit” is not significant relative to the pure error. Insignificant lack of fit is good as it is desired that the model fits perfectly. Lack of fit results and correlation coefficients provided sufficient approximation of the quadratic model to the real system.

4.2.2 Normal distribution

Generally, a normal probability plot demonstrates if the residuals follow a normal distribution, i.e if the responses follow a straight line with little possibility of scattering. From figure 4.1, the data is presumed to follow a normal distribution for the percentage biodiesel yield. Figure 4.2 evidently shows that, the predicted values of the percentage biodiesel yield obtained from the model in equation (4.2) and the observed values are reasonably in agreement.

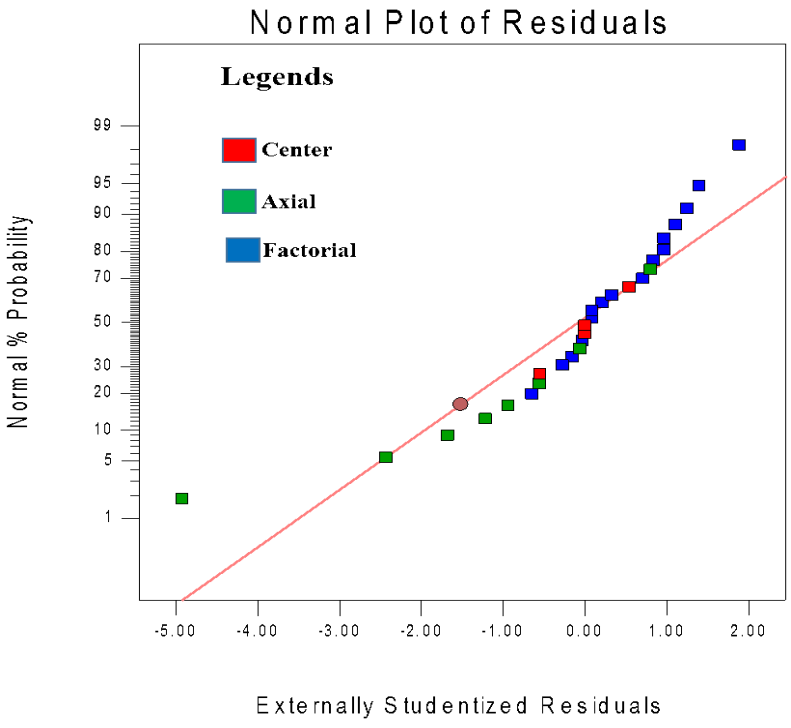

Figure 4.1: Normal probability plot of studentized residuals for percentage biodiesel yield

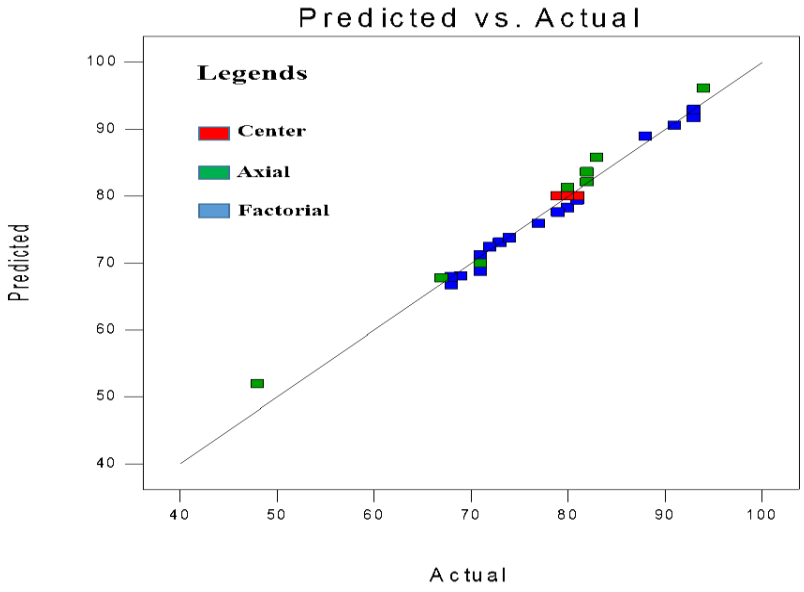

Figure 4.2: Predicted versus actual values plot for percentage biodiesel yield

4.2.3 Main effects of investigated catalyst synthesis factors

4.2.3.1 A-eggshell calcination time: significant factor

The effect of calcination time of eggshell on the catalytic activity of catalyst was investigated using percentage biodiesel yield as a response. The temperature of calcination was 900^{o}C but the time was varied according to the specifications in Table 4.2. The p-value of this independent variable was found to be 0.0285 (Table 4.4), this indicates that based on 95% confidence level, the eggshell calcination time has only a little effect on the catalytic activity of the catalyst relative to the significant factors B and C having p-values of 0.0001. Manop and Juthagate (2011) established that, the smaller the magnitude of the p-value, the more significant is the corresponding coefficient. The possible explanation of this observation is that, calcination time of eggshell alone was not sufficient to increase the activity of the catalyst without the impregnation of potassium fluoride and other factors. It is believed based on these values that, dosage of potassium fluoride and temperature of calcination after the impregnation process are the determining factors for the onward activity of the catalyst.

This observation proved that, the minimum time of calcination of eggshell at 900°C was adequate for the decomposition of $CaCO_3$; the major constituent of the eggshell.

4.2.3.2 D-catalyst calcination time: insignificant factor

The p-value for this factor was found to be 0.1884 as given in Table 4.2 which depicts no significant effect on the catalytic activity. It follows that, the time of exposure of the catalyst to heat was not as significant as the temperature being exposed to. This occurrence may be due to high sensitivity of the material to heat, thus inducing its transformation momentarily.

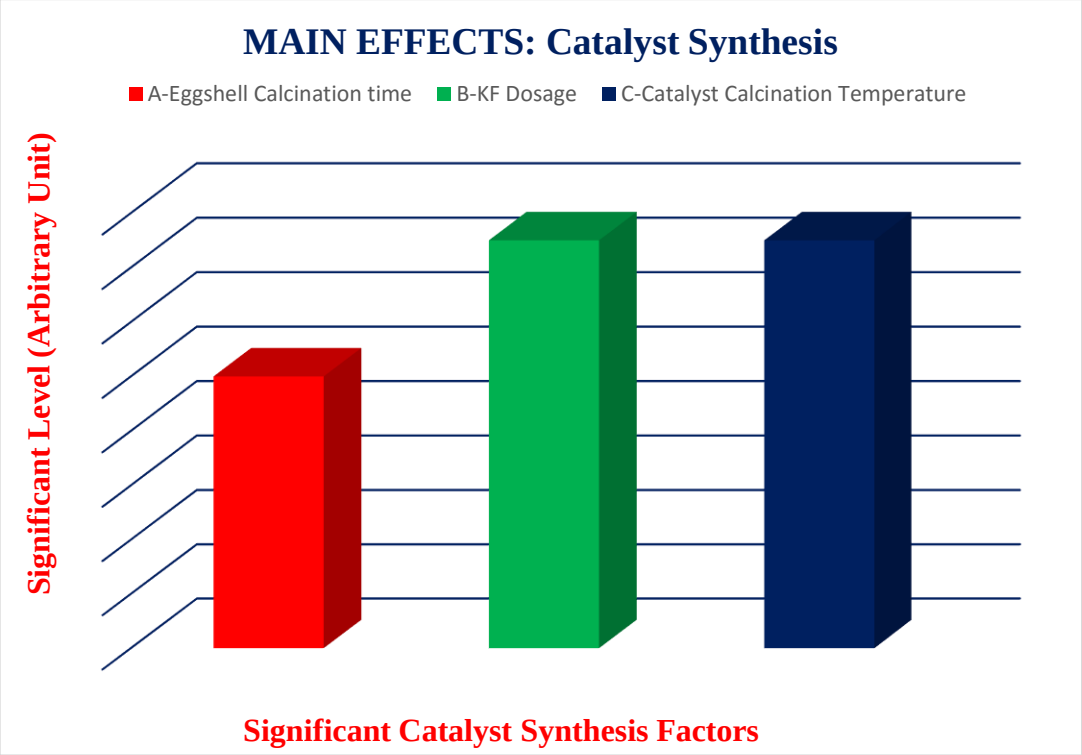

Figure 4.3: The level of significance of catalyst synthesis factors on catalytic activity

4.2.4 Interaction effects

4.2.4.1 A-eggshell calcination time and B-potassium fluoride dosage (AB)

AB represents the interaction between eggshell calcination and potassium fluoride dosage, these variables have no significant interaction based on their p-value presented in Table 4.2. This observation is quite explainable; calcination time of eggshell alone and impregnated potassium fluoride were not sufficient to increase the activity of the catalyst

without the formation of the $KCaF_3$ crystals. The strong basic sites and possible acidic centres of $KCaF_3$ were believed to be largely responsible for the high activity of the catalyst. This suggests that, there is a possibility of interactions if three variables are combined together at once. Figure 4.4 confirms that there is no statistical interaction between eggshell calcination time and the KF dosage. At 3 h calcination time of eggshell and 25 wt.% KF dosage, 80% biodiesel yield was predicted (fig 4.4).

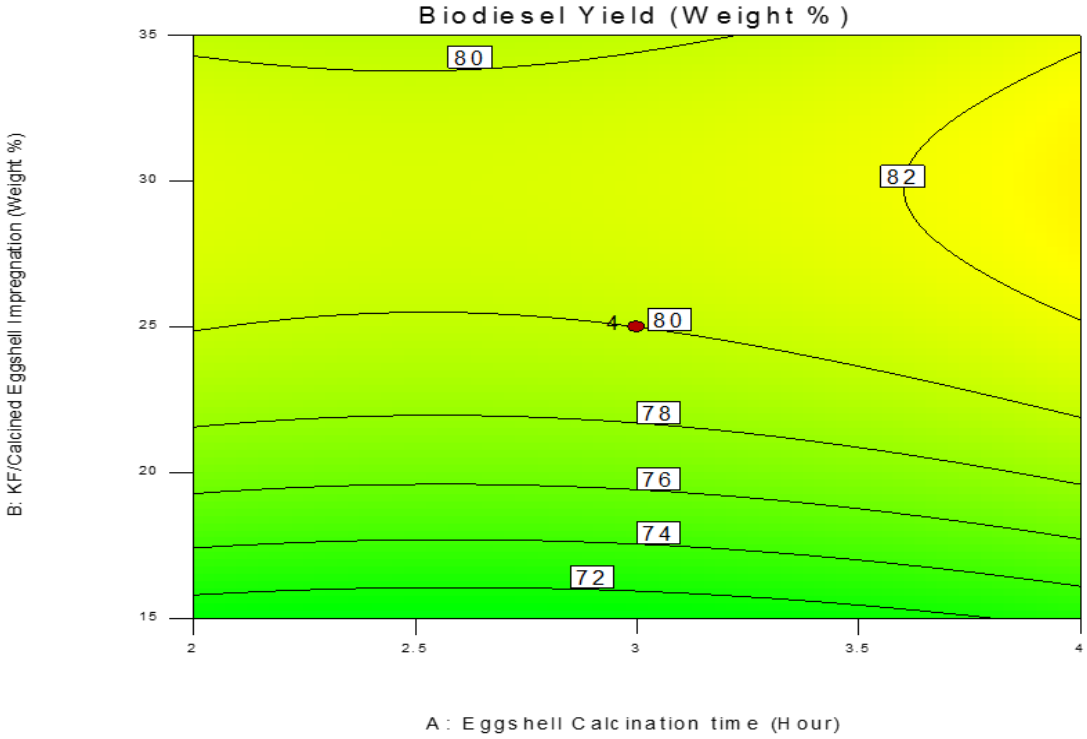

Figure 4.4: Contour plot of interaction effect between A and B

The same yield of 80% was recorded at 33 wt.% KF dosage and 2.7 h eggshell calcination time. The almost flat profile observed in 3D response surface plot of A and B shown in figure 4.4 depicts the initial observation that, there is no significant interactions between A and B. A similar observation was recorded for all the interaction effects that have their p-values indicating insignificant influence on the catalytic activity of the catalysts.

4.2.4.2 B-potassium fluoride dosage and C-calcination temperature of catalyst (BC)

The P-value for the BC interaction is 0.0002 (table 4.3), this indicates a very good level of significant interaction between these variables.

The p-values of all the interaction effect show that, based on the confidence level of 95%, there is a negligible interaction between the variables when considered on a pair basis except for BC. BC represents the interaction between potassium fluoride dosage and the calcination temperature to form the catalyst crystal. Figure 4.5 and 4.6 are the plots of the interaction effect between B and C. Figure 4.5 shows a stepwise increase in the yield of biodiesel as the dose of potassium fluoride increases together with the temperature of calcination of the catalyst. The maximum yield observed was 89% at approximately 580^{o}C and 33 wt.% of KF. A yield of 85% was observed at 26 wt.% of KF dosage and 530^{o}C. These observations indicate that towards the extreme points of the investigated factors, difference in yield obtainable may not be significant. Figure 4.6, depicts the 3D response surface plot of this observation having a steep curvature towards the extreme end of the coordinates. At 600^{o}C and 15 wt.% yield of about 74% was recorded while 89% was observed at 580^{o}C and 33wt.% KF dosage. The obvious difference in elevation between these two points supports already stated findings that there is an impressive interaction between B and C.

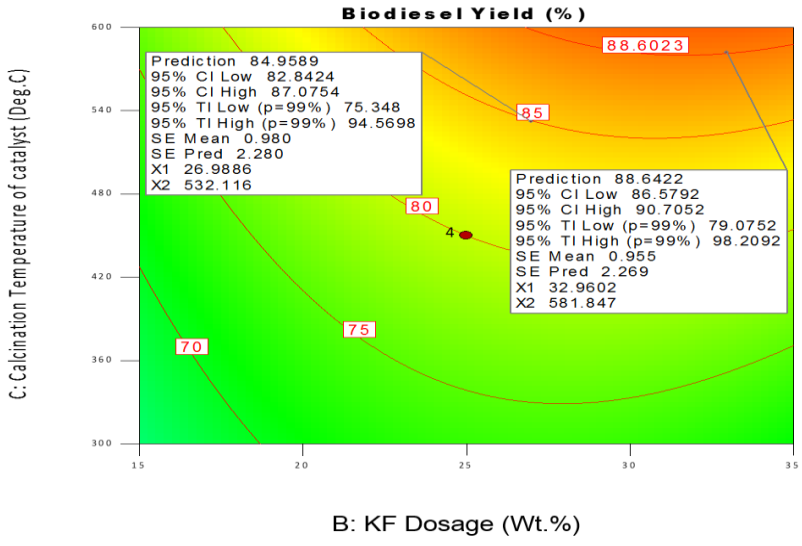

Figure 4.5: Contour plot of interaction effect between B and C

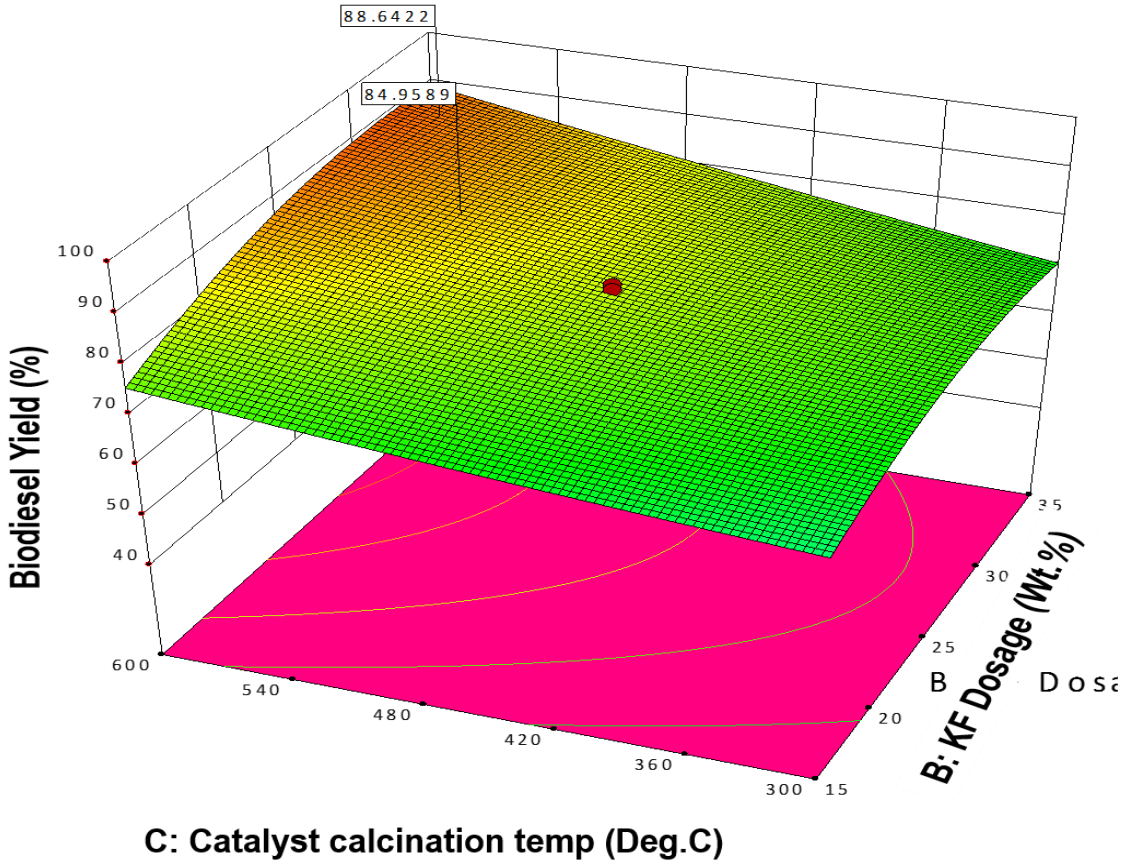

Figure 4.6: 3D response surface plot of interaction effect between B and C

4.3 Optimization of the Catalyst Synthesis Factors

High yield of biodiesel was desired, hence the goal of optimization in this study was to find optimal points among the independent variables that maximize desirability function of the yield. It is evident from section 4.2.3.1 that, minimum time was sufficient for calcination of eggshell. The same observation applies to the calcination time of the catalyst as explained in 4.2.3.2. Figure 4.4 shows that KF dosage of less than 20 wt.% was not adequate for good yield of biodiesel over the catalysts. Figure 4.5 showed that, dosage close to the extreme (35 wt.%) and slightly above (25 wt.%) had no significant effect on the biodiesel yield. Therefore, the goal for KF dosage was set to be a range between the two points. Therefore, optimal range was set within the range whose yields have been predicted as shown in the contour and 3D plot of figure 4.4-4.5.

The observations guided the optimization decision, such that both factors were set to minimum to reduce overall cost of the production.

Table 4.4: Desirability specifications for independent variables and response

		Constraints				
Variables	Optimization Goal	Lower Limit	Upper Limit	Lower Weight	Upper Weight	Importance
A-Eggshell calcination time	Is in range	2	3	1	1	3
B-KF dosage	Is in range	25	30	1	1	3
C-Catalyst calcination temperature	Is in range	500	600	1	1	3
D-Catalyst calcination time	Is in range	2	3	1	1	3
Biodiesel yield	Maximize	48	90	1	1	3

Set of 50 optimal solutions were generated and presented in table 4.5. The selected solution was based on its closeness to our optimization set goals and maximum combined desirability. The adopted optimal conditions were resolved using the modified equation 4.2, and a biodiesel yield of 90% was predicted.

Table 4.5: Optimization results for catalyst synthesis process

Fifty optimal solutions found						
S/N	A (h)	B (wt. %)	C (^{o}C)	D (h)	Biodiesel Yield (%)	Desirability function
1	2.93	28.98	597.86	2.56	90.0607	1.000
2	2.16	29.60	599.82	2.04	90.1345	1.000
3	2.34	29.79	597.65	2.46	90.0131	1.000
4	2.72	29.05	599.33	2.98	90.0134	1.000
5	2.11	29.08	599.31	2.50	90.0081	1.000
6	2.50	29.86	598.60	2.04	90.0802	1.000
7	2.13	29.19	599.30	2.91	90.0268	1.000
8	2.12	29.32	598.37	2.65	90.0113	1.000
9	2.89	29.27	599.11	2.02	90.1678	1.000

10	2.99	29.85	598.17	2.61	90.3151	1.000
11	2.70	29.54	599.46	2.46	90.1272	1.000
12	2.26	29.81	597.36	2.14	90.0126	1.000
13	2.10	29.69	597.24	2.69	90.0379	1.000
14	2.85	28.74	599.26	2.19	90.0029	1.000
15	2.23	29.83	596.93	2.44	90.001	1.000
16	2.22	29.72	599.44	2.37	90.1195	1.000
17	2.65	29.18	599.24	2.57	90.0125	1.000
18	2.99	28.74	599.16	2.31	90.108	1.000
19	2.10	29.74	597.33	2.59	90.0513	1.000
20	2.92	29.23	597.79	2.82	90.1029	1.000
21	2.01	28.91	599.90	2.53	90.047	1.000
22	2.92	29.00	597.94	2.06	90.0604	1.000
23	2.08	29.06	599.87	2.72	90.0472	1.000
24	2.44	29.33	599.88	2.37	90.0375	1.000
25	2.96	29.19	599.10	2.66	90.1999	1.000
26	2.30	29.63	599.86	2.91	90.1063	1.000
27	2.09	29.78	596.37	2.10	90.0097	1.000
28	2.61	29.70	598.80	2.47	90.0897	1.000
29	2.90	29.60	599.68	2.53	90.2756	1.000
30	2.91	29.73	599.84	2.40	90.3197	1.000
31	2.17	29.31	599.19	2.05	90.034	1.000
32	2.98	29.75	598.84	2.63	90.3269	1.000
33	2.74	29.79	598.63	2.88	90.1492	1.000
34	2.99	28.33	599.78	2.17	90.0185	1.000
35	2.59	29.72	599.08	2.25	90.102	1.000
36	2.98	29.41	599.26	2.78	90.2755	1.000
37	2.04	29.84	596.08	2.58	90.0304	1.000
38	2.10	29.08	599.14	2.83	90.006	1.000
39	2.08	29.50	597.35	2.41	90.0151	1.000

40	2.00	28.96	599.48	2.04	90.0394	1.000
41	2.44	29.22	599.78	2.50	90.0054	1.000
42	2.79	29.17	598.24	2.39	90.0261	1.000
43	2.60	29.99	596.30	2.00	90.0003	1.000
44	2.42	29.36	599.29	2.50	90.011	1.000
45	2.96	29.16	597.57	2.54	90.108	1.000
46	2.56	29.95	598.46	2.98	90.1009	1.000
47	2.60	29.22	599.54	2.45	90.0229	1.000
48	2.67	29.15	599.21	2.55	90.0105	1.000
49	2.87	29.85	598.82	2.12	90.2543	1.000
50	3.00	27.93	600.00	2.61	89.8947	0.997

A catalyst designated as “OCAT” was synthesized using the selected optimal conditions for the purpose of characterization and further use. Triplicate transesterification experiments were carried out over the “OCAT”. An average of 93% biodiesel yield was obtained. The 3% deviation could be attributed to experimentation error (pure error) or lack of fit error.

Table 4.6: Results of predicted and actual experiments using optimized conditions

Predicted optimal conditions and yield					Validation experiments				Deviation		Error
A h	B Wt.%	C ^{0}C	D h	Yield (%)	Yield I (%)	Yield II (%)	Yield III (%)	Average Yield (%)	Predicted Yield (%)	Actual Yield (%)	± 3%
2	29	600	2	90.08	92.40	93.41	93.33	93.05	90.1	93.05	

4.4 Characterization of Catalyst

4.4.1 Chemical composition of eggshell (XRF)

Table 4.7: Chemical composition (%) of raw eggshell

Composition	$CaCO_3$	H_2O	Na_2O	Al_2O_3	Fe_2O_3	CeO_2	$BaCO_3$	$SrCO_3$	TiO_2	Others
Percent	98.04	1.00	0.08	0.28	0.08	0.03	0.06	0.36	0.02	0.05

Table 4.7 presents result of XRF analysis of the beneficiated raw eggshell, this indicated that it is a very rich source of $CaCO_3$ as this constitute 98% of the eggshell. Chemical compositions are widely reported in their oxide forms with regards to X-ray Fluorescence (XRF) analysis. Eletta *et al.* (2016) reported that eggshell contains 78% $CaCO_3$ before calcination. Hunton (2005) reported that the chicken eggshell is 97% calcium carbonate compound, which are stabilized by a protein matrix, he also mentioned that an amount as low as 78% has been reported. 96% calcium carbonate was reported by Sirivat (2012) as the major constituent of eggshell while Buasri *et al.* (2013) reported 98% $CaCO_3$. The variance in the values presented in Table 4.7 with those reported in various literature can be attributed to difference in the chicken feed composition and probably location.

4.4.2 X-ray diffraction (XRD)

XRD was used to investigate phase transformation, crystallite size and shape of the samples. The diffraction patterns of the beneficiated raw eggshell samples is shown in figure 4.7(A). It was obtained with Cukα radiation (λ = 0.15406 nm) in a 2θ scan range of $10^0 – 80^0$. The most intense peak observed occur at $2\theta = 29.32^0$ having crystalline plane of (104). Other major peaks were noted at 35.95^0(110), 39.37^0(113), 43.08^0(202). The observed peaks were compared with the standard pattern of JCPDS file for calcium carbonate. They were found to match well with the calcite ($CaCO_3$) of the R-centred hexagonal lattice system having (JCPDS) card number; 01-085-1108; R-3c.

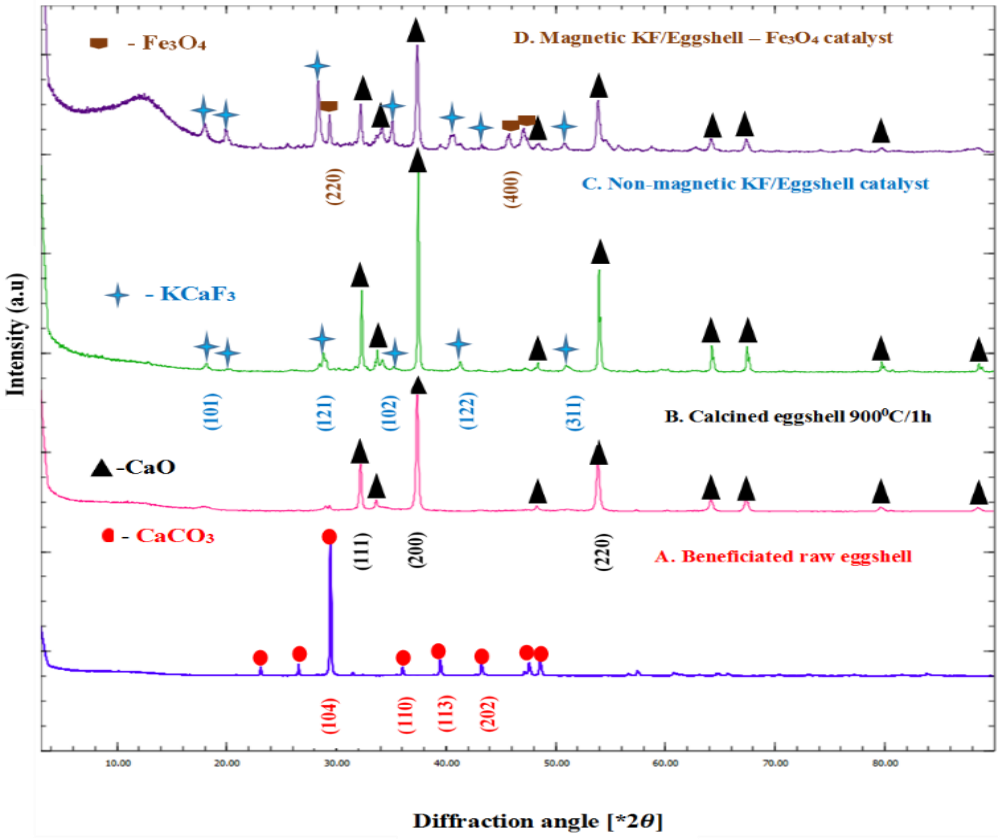

Figure 4.7: XRD patterns of the (A) raw eggshell, (B) calcined eggshell (C) non-magnetic catalyst and (D) magnetic catalyst

This compliments the XRF result in Table 4.7 which showed that beneficiated raw eggshell is majorly composed of $CaCO_3$. Upon calcination of the calcite at the optimum calcination condition, complete decomposition of the $CaCO_3$ into lime was observed as depicted by figure 4.7(B). The most notable peaks of the obtained lime were observed at 2θ = 32.03^0(111), 37.26^0(200), 53.71^0(220). These peaks matched precisely with the JCPDS's reported pattern of face-centred cubic lattice system of lime having card number; fm-3m: 01-077-2376. The phase transformation of the optimal catalyst (OCAT) is as shown in figure 4.7(C), the two major phases present in the catalyst were that of lime and $KCaF_3$. Critical observation of intensity of the peaks corresponding to CaO in figure 4.7(C) revealed that, it increased compared to those shown in figure 4.7(B).

This increment in crystallinity is possibly due to the hydration-dehydration technique subsequently applied to the already calcined eggshell before impregnation. The peaks corresponding to the $KCaF_3$ were consistent with the standard pattern reported in JCPDS file (3-567) for $KCaF_3$ crystal. The magnetic catalyst (MCAT) showed three distinct phases as depicted in figure 4.7(D); predominantly lime, $KCaF_3$ and magnetite (Fe_3O_4).

Table 4.8: the crystallite sizes and shape of the samples

Samples	Crystallinity (%)	Crystal size (nm)	Crystal shape
Raw eggshell	94	100	R-centred hexagonal
Calcined eggshell	92	84	Face-centred cubic
Non-magnetic catalyst	87	79	R-centred hexagonal
Magnetic catalyst	98	108	Orthorhombic

The most intense peaks of the magnetite were observed at $2\theta = 30.04^0(220)$, $43.08^0(400)$, these magnetite peaks were consistent with the JCPDS's reported pattern upon matching as contained in the file number (79-0417). The observed presence of Fe_3O_4 peaks are responsible for the magnetic properties of the MCAT catalyst being a ferromagnetic material. The peaks are sharp with broad base indicating ultra-fine nature and small crystallite size of the particles.

4.4.3 Scanning electron microscopy (SEM)

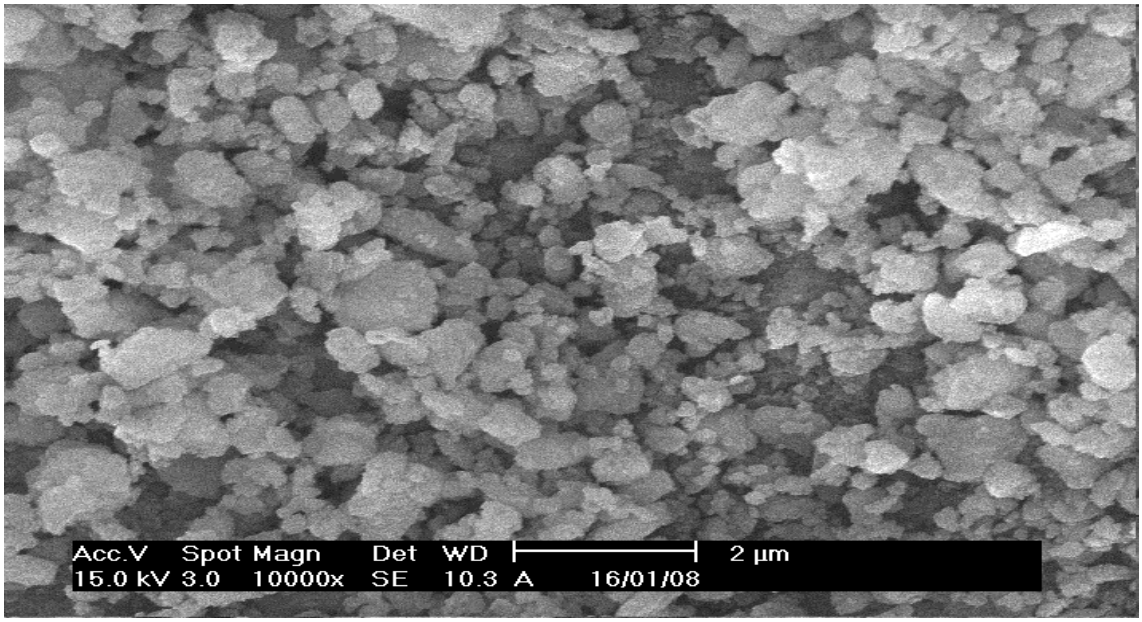

Plate I: SEM micrograph of the beneficiated raw eggshell

SEM Analysis was performed to elucidate the morphology of the sample surface. Plate I is the SEM image of the beneficiated eggshell, it shows irregular agglomerates of rod-like particles of eggshell. Faungnawakij *et al.,* (2012) and Meera *et al.,* (2014) reported a similar observation. After calcination at optimal conditions, the calcined eggshell was modified as explained in section 3.4.2 The calcination-hydration-dehydration process changed the morphology of the eggshell as seen in plate II. A mixture of small and big distinctive cubical-like particles with definite structure was observed. The morphology of the non-magnetic "OCAT" catalyst prepared using the optimal conditions is presented in plate III. Compacted hexagonal-like plates with smooth surface can be seen, the initial cubical-like shaped particles have taken a wider but concise shape indicative of possible formation of crystals of a new compound in the structure. The wide hexagonal-like plates suggest availability of high surface area to the reacting species.

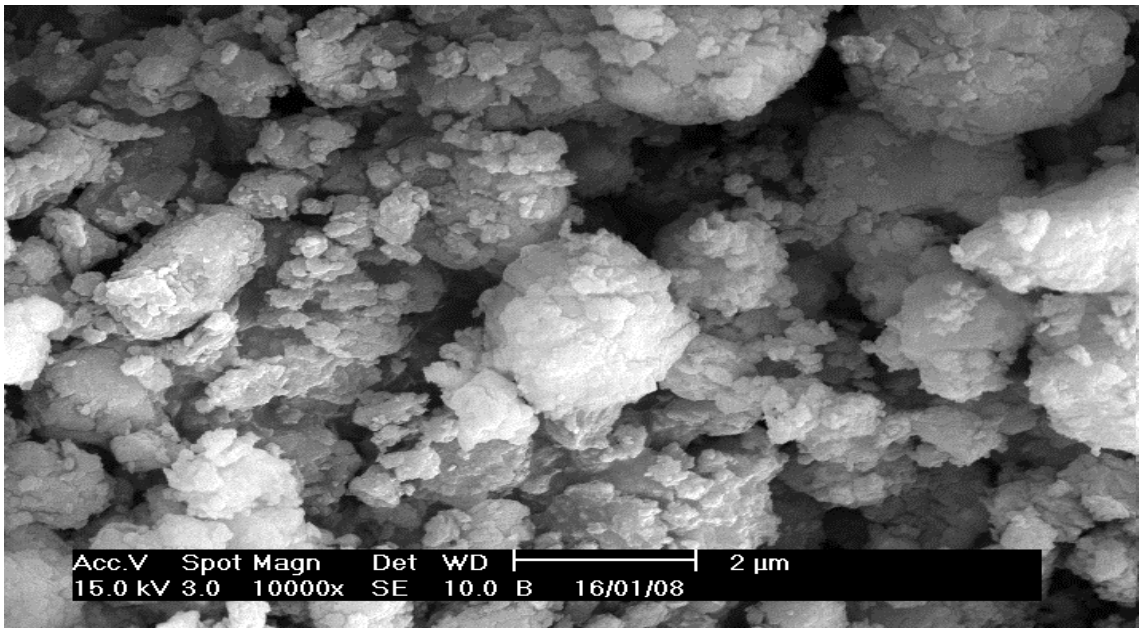

Plate II: SEM micrograph of calcined eggshell at (900^0C/2h/600^0C/3h)

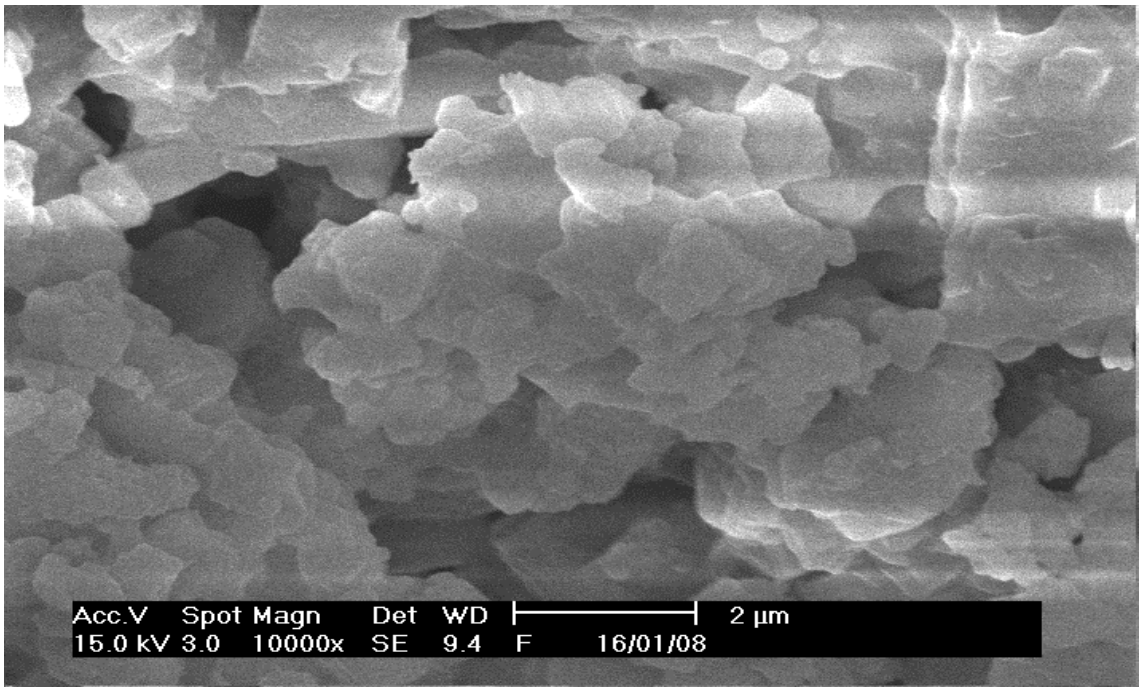

Plate III: SEM micrograph of OCAT catalyst prepared under optimal conditions

The systemic arrangement of these plates as seen in plate III suggests the probable reason behind the high activity of the catalyst as diffusing reactants were likely exposed to the active sites of the catalyst thus leading to almost complete conversion of the oil to methyl ester. Danlin *et al.*, (2015) reported a similar micrograph for KF/CaO catalyst.

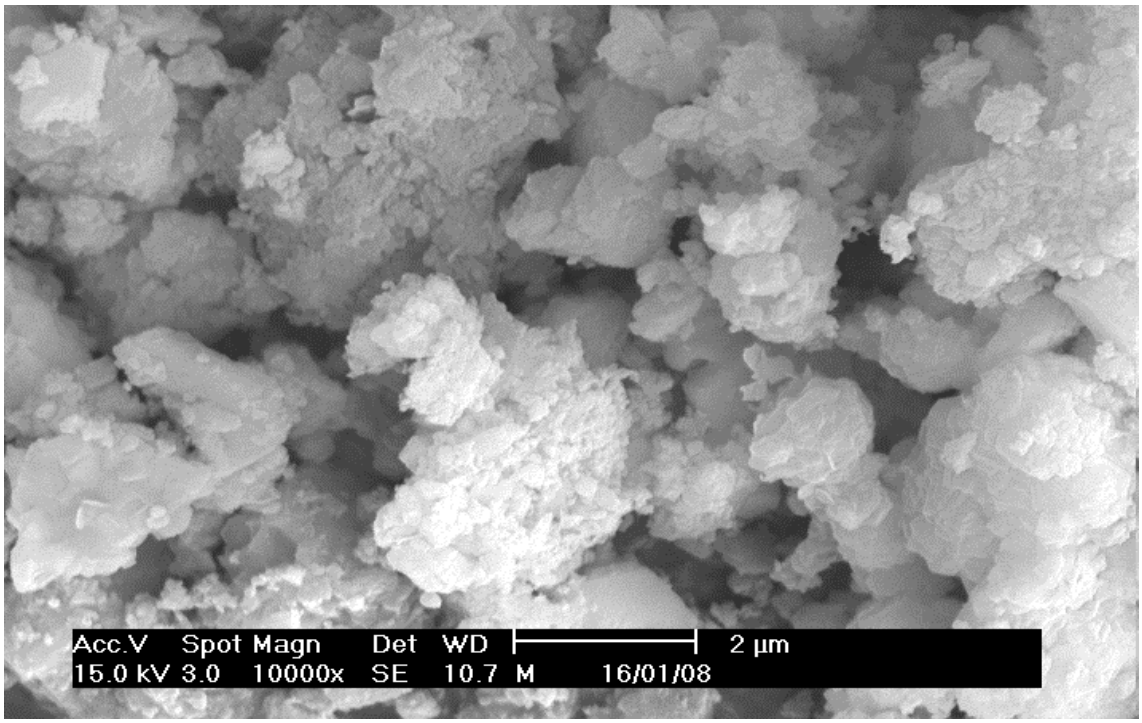

Plate IV: SEM micrograph of MCAT catalyst prepared under optimal conditions

Plate IV is the SEM micrograph of the magnetic catalyst (MCAT), slightly uniform hexagonal-like plates of the non-magnetic catalyst has been modified due to the formation of magnetite crystal in the non-magnetic catalyst structure. The particles of this catalyst were observed to be well fussed together unlike those in plate IV, this fusion may be due to the newly acquired magnetic property of the catalyst.

4.4.4 Energy dispersive x-ray spectroscopy (EDS)

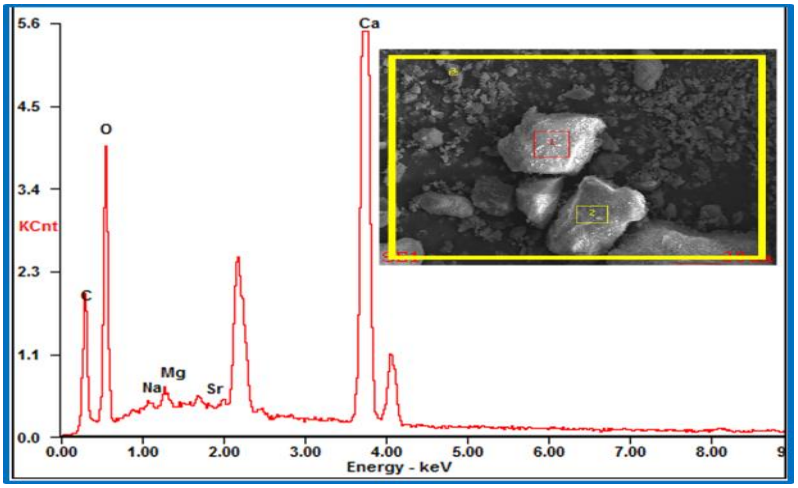

Figure 4.8: EDS of beneficiated eggshell

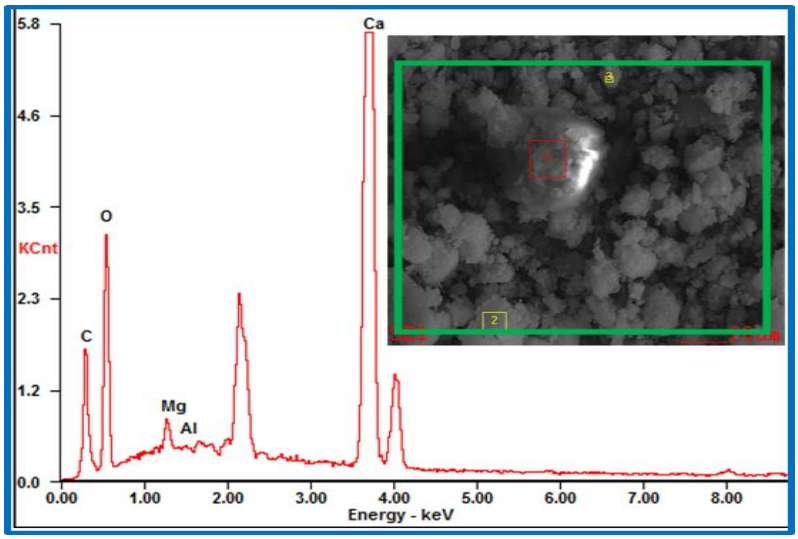

Figure 4.9: EDS of calcined eggshell

The EDS analysis is an incorporated feature of SEM. It was used to evaluate the composition of the structure of beneficiated raw eggshell, calcined eggshell, non-magnetic and magnetic catalyst. The marked areas in the figure 4.8-11 were the pinged points of the surface whose compositions were analyzed.

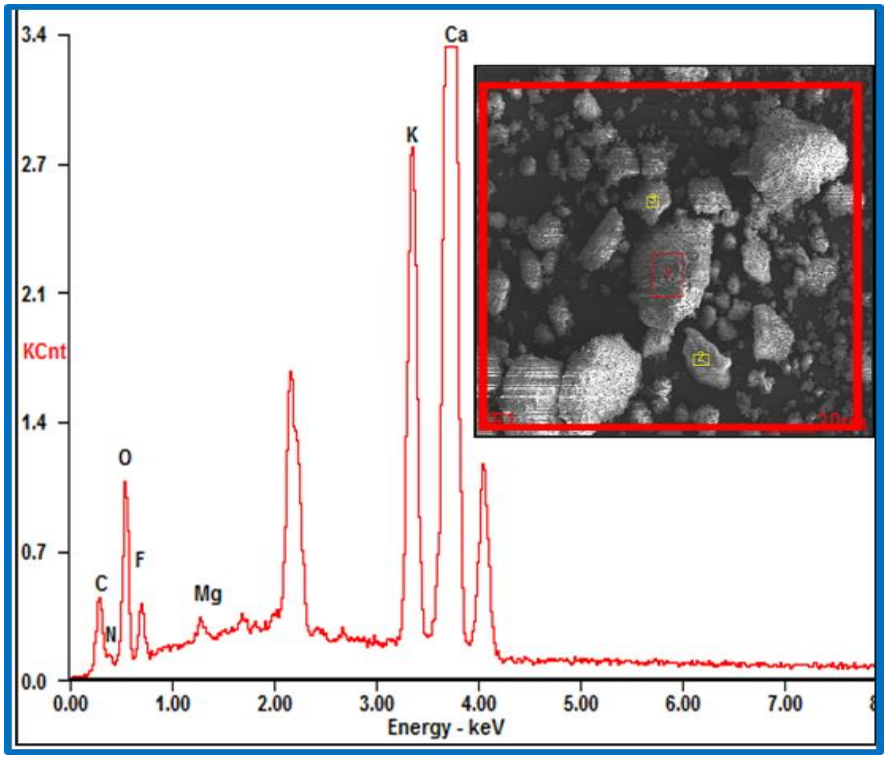

Figure 4.10: EDS of OCAT

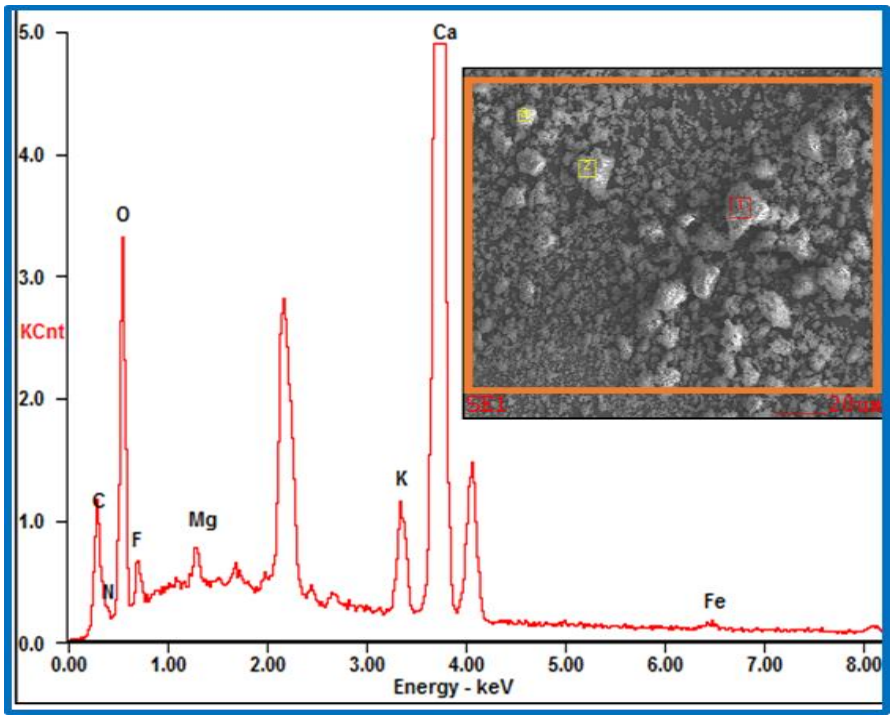

Figure 4.11: EDS of MCAT

The intensity of the Calcium (Ca) from $CaCO_3$ as shown in figure 4.8 scan be observed to be the highest. This result is complemented with the XRF analysis presented in Table 4.8, and there it was found that $CaCO_3$ is 98%. The presence of the other elements shown in figure 4.8 are corroborated by the result of XRF presented in Table 4.8. Figure 4.9 presents the EDS of the calcined eggshell. A significant decrease in the percentage of oxygen and carbon was observed which implies occurrence of decomposition reaction of the calcite at 900^{o}C. The calcium (Ca) element in figure 4.9 is evidently from CaO and the carbon is likely to have resulted from the carbon coating. Figure 4.10 shows the composition at the pinged point of the non-magnetic catalyst. Potassium (K) and fluoride (F) were observed, these are mainly from the potassium fluoride (KF) impregnated on the calcined eggshell. Further decrease in percentage of oxygen and carbon noticed may be due to additional calcination of the KF/Eggshell catalyst after impregnation. Also, this may be due to loss of oxygen during the formation of a new $KCaF_3$ crystal when CaO combined with KF.

Presence of magnetite (Fe_3O_4) in the magnetic catalyst is depicted in figure 4.11, iron (Fe) was observed and the percentage of oxygen was also noticed to have increased, this may be attributed to the introduction of the magnetite containing oxygen in the matrix of the catalyst. These results are consistent with those of the XRD and XRF.

4.4.5 Surface area, pore size and volume of the OCAT catalyst

Surface area is a principal attribute of a solid catalyst that plays a vital role in its catalytic activity. The specific surface area of the non-magnetic catalyst was calculated using BET (Brunauer-Emmett-Teller) method. The BET equation is given by;

$$\frac{1}{W((P_o/P)-1)} = \frac{1}{W_m C} + \frac{C-1}{W_m C}\left(\frac{P}{P_o}\right) \qquad (4.4)$$

W is the weight of gas adsorbed at a relative pressure of P/P_o, and W_m is the weight of the adsorbate constituting a monolayer of surface coverage.

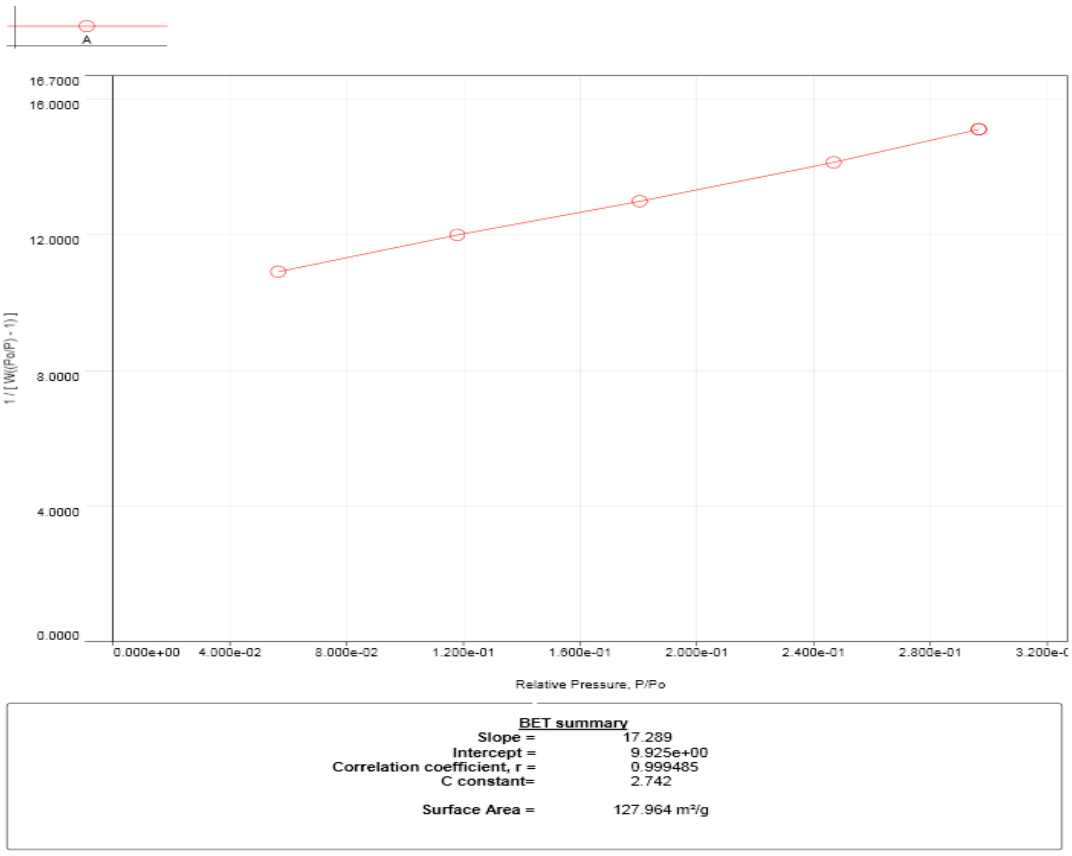

Figure 4.12: Specific surface area plot obtained by multipoint BET method

The constant C is related to the energy of adsorption in the first adsorbed layer. Its value shows the magnitude of the adsorbent and adsorbate interactions. (P and Po denote the equilibrium and saturation pressures of nitrogen, respectively). The total surface area of the catalyst is based upon the nitrogen gas (adsorbate) adsorbed by the catalyst matrix (adsorbent) and that which is condensed in its pores.

$$S_t = \frac{W_m N_{avg} A_N}{M_w} \qquad (4.5)$$

$$S_s = \frac{S_t}{W_s} \qquad (4.6)$$

S_t is the total surface area, Ss is the specific surface area of the catalyst, W_s is the sample weight, N_{avg} is Avogadro's number (6.023×10^{23} molecules/mol), M_w is the molecular weight of the adsorbate (N_2) and A_N is the area occupied by one adsorbate molecule given by Dong *et al.* (2006) as $16.2 \times 10^{-20}\ m^2$ for N_2. Figure 4.12 is the BET plot based on multipoint approach, the specific surface area of the **OCAT** catalyst was determined to be 128m^2/g using the AUTOSORB-1 (QUANTACHROME) software. The hydration-dehydration technique after initial calcination was reported by Yoosuk *et al.,* (2010) to play an important role in improving the specific surface of CaO catalyst. This technique was employed and may be the reason for the high surface area recorded. Sirivat *et al.,* (2012) reported 136m^2/g as the specific surface area of CaO after similar treatment. The pore size of the OCAT catalyst was determined to be 3.24 nm with pore volume of 0.046 cm^3/g. According to the IUPAC classification, pores are classified as macropores for pore widths greater than 500 Å, mesopores for the pore range 20 to 500 Å and micropores for the pores in the range less than 20 Å (Sing, 1985). This implies that the **OCAT** is mesoporous having a pore width of 3. 24nm which falls within the mesopores size range of 2 nm – 50 nm.

4.5 Analysis of Variance for Transesterification Process

Table 4.9 presents the ANOVA of the investigated transesterification factors. Table B.1 containing the experimental design matrix is presented in the appendix B. As explained earlier, non-significant model terms were stepwisely removed to increase the precision of the model. The F-value and P-value of the obtained modified quadratic model presented in Table 4.10 were found to be 86.09 and 0.0001 respectively. These imply that the quadratic model is significant. As a result of that, the model can sufficiently predict the yield of biodiesel based on the investigated factors affecting transesterification process. In this study, A, B, C, D, BC, BD A^2, B^2, C^2 and D^2 are significant model terms.

Table 4.9: ANOVA for response surface modified quadratic model of transesterification process

	Mean	F-value	p-value	Remarks	Model Accuracy	
Source	Square	Value	Prob > F		Correlation coefficients	Values
Model	170.91	86.09	0.0001	significant	R-Squared	0.9806
A-Catalyst dosage	210.04	105.80	0.0001		Adj R-Squared	0.9692
B-Methanol-Oil	975.37	491.30	0.0001		Pred R-Squared	0.9297
C-Reaction time	222.04	111.84	0.0001		Adeq Precision	34.913
D-Reaction temp	176.04	88.67	0.0001		PRESS	122.46
BC	27.56	13.88	0.0017			
BD	14.06	7.08	0.0164			
A^2	39.40	19.85	0.0003			
B^2	47.46	23.91	0.0001			
C^2	25.52	12.86	0.0023			
D^2	32.09	16.16	0.0009			
Residual	1.99					
Lack of Fit	2.21	2.42	0.2544	not significant		
Pure Error	0.92					

There are significant interactions between oil-methanol ratio and reaction temperature, oil-methanol ratio and reaction time. This observation is in total agreement with some of the reviewed literatures, where significant improvement have been recorded in the yield of biodiesel produced from transesterification monitored for long hours, relatively high

catalyst dosage, oil-methanol ratio and reaction temperature. R^2 value of 0.98 means that, the fit explains 98% of the total variation in the data about the average. Adj. R^2 value of 0.96 obtained in this study after the reduction of the model equation. Also, the adequate precision of 34 implies that, there is a high adequate signal from the model relative to the noise which has been reduced in the model.

$$\%\text{Biodiesel Yield} = 157.32 - 7.29A + 3.44B + 2.81C - 4.26D - 0.58BC - 0.063BD + 1.28A^2 + 0.16B^2 + 1.83C^2 + 0.046D^2 \quad (4.7)$$

The model equation given in equation 4.7 is in terms of actual factors. It can be used to make predictions about the yield of biodiesel for given levels of each factor. "Lack of Fit P-value" of 0.2544 implies that, the Lack of Fit is not significant relative to the pure error. Non-significant lack of fit is good as it is desired for the model to fit perfectly. The model terms A - D have a p-values of <0.0001, this is fundamentally correct. It follows that all the factors investigated; catalyst dosage, oil-methanol ratio, reaction temperature and time cumulatively affect biodiesel yield.

Plate V: a) freshly prepared neem oil biodiesel under separation b) decanted biodiesel and fresh neem oil

4.5.1 Main effects of investigated transesterification factors

The p-values of all the factors investigated showed that, they are equally significant to the production of biodiesel. This observation is a true reflection of reality; as it is technically explainable, this is because methanol is an alcohol which is a reactant in the course to produce biodiesel. Also, by principle, favourable amount of biodiesel is produced only when the molar ratio between the oil and the alcohol is 1:3 minimally. The high molar ratio of the alcohol is meant to drive the reversible transesterification reaction towards the forward direction where production of methyl ester is favoured according to the Le Chatlier's principle of chemical equilibrium. Even though a catalyst does not have effect on the equilibrium position of a reaction, it can conveniently increase the rate at which the reaction attains the equilibrium. Therefore, significant effect of catalyst on the yield of biodiesel cannot be over-emphasized, that possibly explains why the dosage of catalyst is observed to be significant to the amount of biodiesel produced. Molecules of reactant usually gain energy to overcome the invisible activation energy barrier, after which they collide with themselves to form the product molecules. Temperature is one of the means by which molecules gain kinetic energy. Having said that, reaction temperature is found to be significant to the yield of biodiesel, this is so because, by increasing the temperature, the molecules of the triglycerides and the alcohol gain kinetic energies, they thus collide faster, this positively affect the rate of the reaction. Moderately high time of reaction have been widely reported to positively affect the yield of the biodiesel, this is because reactions involving solid catalysts usually present mass transfer problem which over time, the reaction system will have to reach homogeneity through adequate stirring.

4.5.1.1 Perturbation

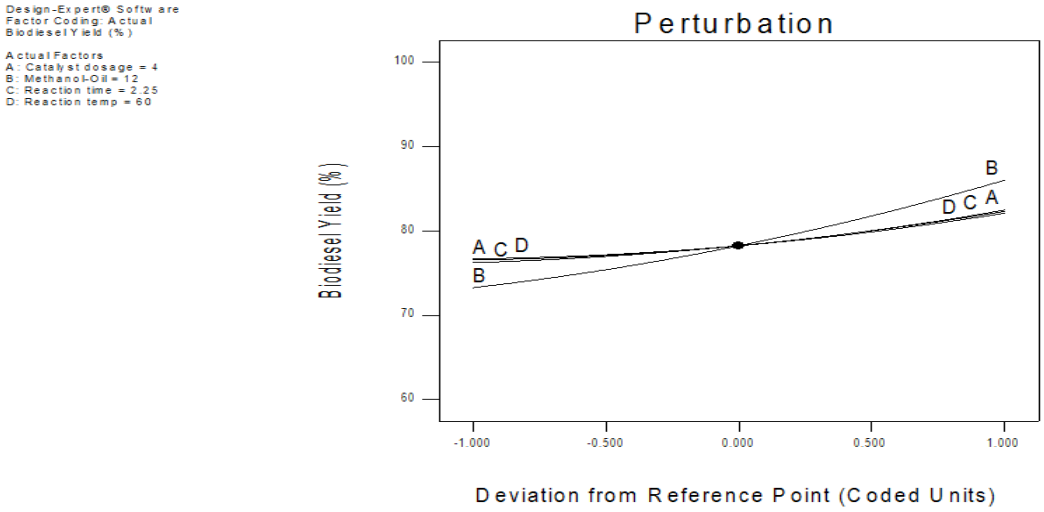

Figure 4.13: Perturbation plots of the main effects for transesterification process

Even though, the P-values for the main effects showed that, all the factors are significant equally, perturbation plot can show the comparative effects of all the investigated independent variables on biodiesel yield. From the plot in figure 4.13, catalyst dosage, reaction time and temperature show a consistent lumped curvature indicating that there is equality in their effect on the biodiesel yield. Within the range of this experimental design, it is evident that, the effect of these three lumped factors will seize to be significant beyond 80% yield of biodiesel. Meanwhile, increase in the oil-methanol molar ratio can possibly increase the yield of biodiesel up to 90%. From this observation, it can be said that, amount of methanol have the highest positive effect on the yield of the biodiesel, synergy among these factors contributed immensely to the yield of the biodiesel as well.

4.5.2 Interaction effects for transesterification factors

4.5.2.1 B-oil-methanol ratio and C-reaction time

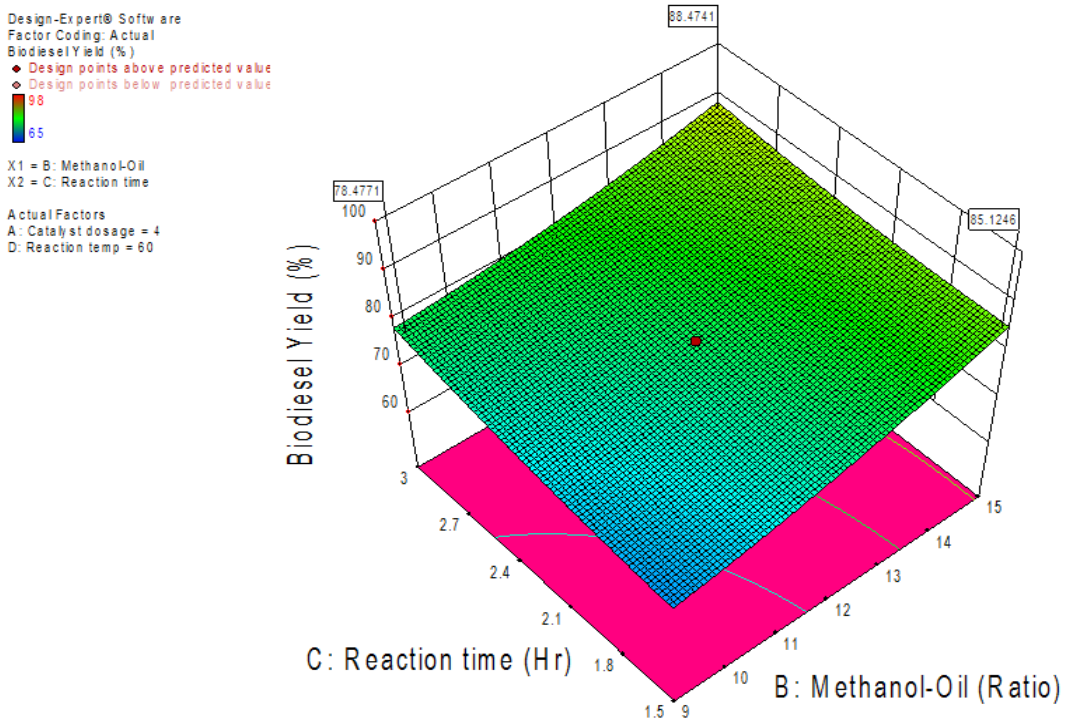

Figure 4.14: 3D response surface plot between oil-methanol ratio and reaction time interaction

The interaction between oil-methanol molar ratios with reaction time was observed to have significant effect on the biodiesel yield given their P-value. The plot in figure 4.14 shows that using 1:15 oil-methanol molar ratio for 1.5 h reaction time, the obtained biodiesel yield was 85% as shown on the flag, meanwhile using 1:15 for 3 h, 88% was obtained. At 1:9 oil-methanol molar ratio for 3h, 78% biodiesel yield was obtained. These observations are connected to the fact that, low amount of alcohol which is a limiting reactant in this reaction scheme would limit biodiesel production. A downward sloppy shaped surface plot with almost flat top profile indicates that, when the molar ratio of methanol is high, the effect of reaction time becomes relatively low. The difference between the yield of 88% and 85% does not justify the extra cost that would be incurred to run the experiment for an extra 1.5 h. Having said that, this observation would be put into consideration when setting the optimization goals.

4.5.2.2 B-oil-methanol ratio and D-reaction temperature

It is observed that biodiesel yield obtained at a temperature below the boiling point of methanol, was slightly lower than the yield obtained at a temperature of 65^{o}C for the same molar ratio. At temperatures around 55^{o}C, the methanol molecules were not as excited as those at 65^{o}C which is near the boiling point of methanol. As it can as well be observed in figure 4.15, at 1:15 oil-methanol ratio and 65^{o}C reaction temperature, about 90% of biodiesel yield was recorded. Meanwhile at 1:15 oil-methanol ratio and 55^{o}C reaction temperature, 85% was obtained.

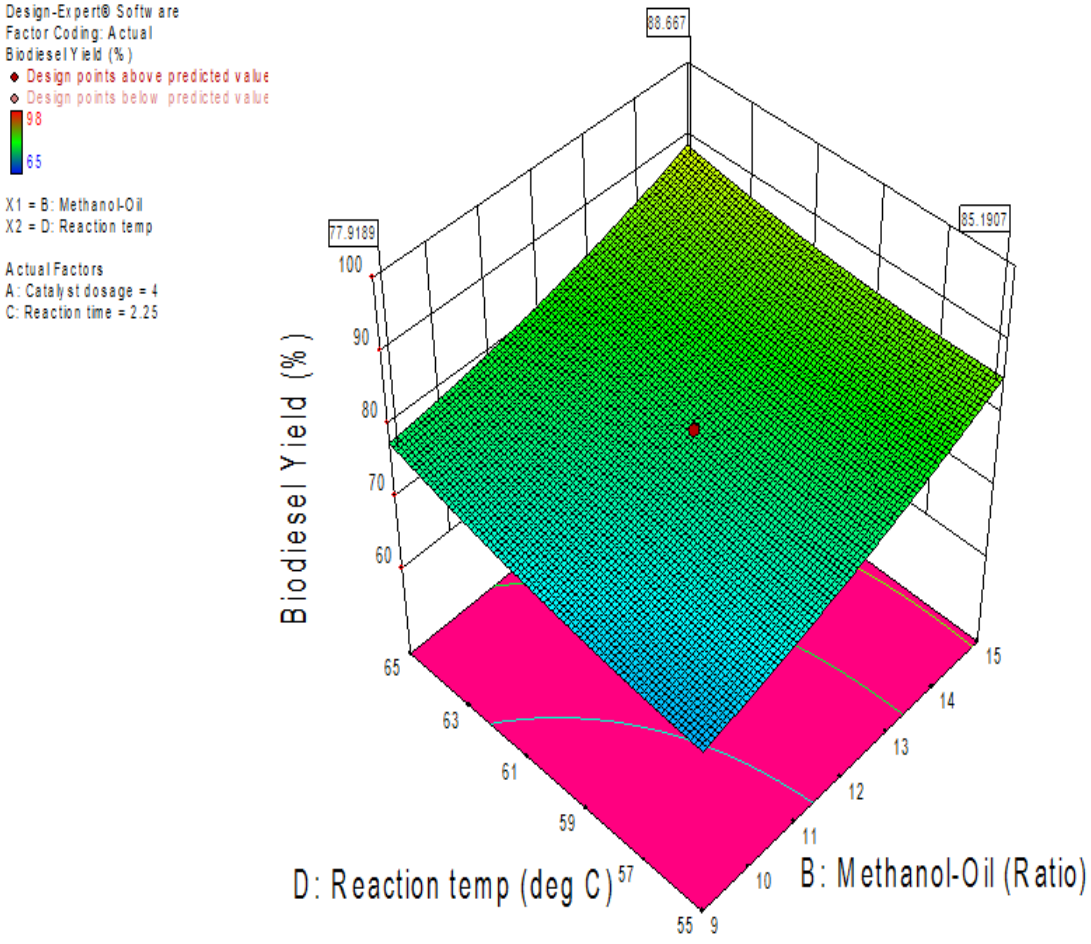

Figure 4.15: 3D response surface plot between oil-methanol ratio and reaction temperature interaction

4.6 Optimization of Transesterification Process Factors

The optimally prepared KF/Eggshell catalyst designated as OCAT was characterized and used in the transesterification of fresh neem oil having FFA of 4.2% in order to establish the optimal transesterification process conditions. Using a central composite design of experiment technique, four process factors including; weight of catalyst, oil-methanol ratio, reaction time and temperature were varied and studied for establishing the optimal process conditions. High yield of biodiesel was desired, hence the goal of optimization was to find optimal setting among the independent factors that maximize desirability of the yield. Minimal reaction time and temperature are sufficient for the transesterification using sufficient amount of oil-methanol molar ratios as shown in figures 4.14 - 15. Very high dosage of solid catalyst can negatively impacts the biodiesel yield due to mass transfer limitation. These observations guided the optimization decision, such that high yield of biodiesel will be produced at minimal cost.

Table 4.10: Desirability specifications for transesterification variables and response

	Constraints					
Independent factors	Optimization Goal	Lower Limit	Upper Limit	Lower Weight	Upper Weight	Importance
A-Catalyst dosage	Is in range	4	6	1	1	3
B- Oil-methanol	Is in range	12	15	1	1	3
C-Reaction time	Is in range	2	3	1	1	3
D-Reaction temp	Is in range	60	65	1	1	3
Biodiesel yield	Maximize	65	96	1	1	3

Set of 50 optimal solutions were found after the rigorous calculation and presented in Table 4.11. The selected solution was based on its closeness to the set optimization goals and maximum combined desirability function value.

Table 4.11: Optimization results for transesterification

Fifty Optimal Solutions Found						
S/N	Catalyst dosage (wt.%)	Methanol Oil (Ratio)	Reaction time (h)	Reaction temp (^oC)	Biodiesel Yield (%)	Desirability function
1	5.85	14.46	2.69	61.27	96.3643	1.000
2	5.97	14.94	2.05	60.68	96.4782	1.000
3	5.74	14.86	2.98	62.21	98.3579	1.000
4	5.86	14.97	2.27	61.02	96.3287	1.000
5	5.99	14.97	2.34	64.70	99.7998	1.000
6	5.89	14.31	2.84	64.54	99.1598	1.000
7	5.19	14.92	2.93	64.79	96.3214	1.000
8	5.98	13.96	2.24	64.36	96.5967	1.000
9	5.95	14.09	2.20	64.30	96.5291	1.000
10	5.70	14.78	2.56	62.73	96.398	1.000
11	5.42	14.67	2.89	64.84	97.1006	1.000
12	5.95	13.96	2.99	61.40	97.5115	1.000
13	5.46	14.97	2.58	64.28	96.3744	1.000
14	5.99	13.73	2.64	62.97	96.5305	1.000
15	6.00	14.67	2.24	60.07	96.0649	1.000
16	5.91	14.72	2.19	62.76	96.762	1.000
17	5.76	14.95	2.72	60.22	96.6146	1.000
18	5.78	14.84	2.10	64.74	97.2942	1.000
19	5.09	14.95	2.97	64.91	96.1419	1.000
20	5.66	13.39	2.96	64.93	96.536	1.000
21	5.96	14.89	2.01	61.69	96.7379	1.000
22	5.80	13.39	2.78	64.55	96.2588	1.000
23	5.97	13.49	2.77	63.59	96.8973	1.000
24	5.98	14.62	2.39	61.08	96.6452	1.000
25	5.74	14.88	2.43	63.61	97.1191	1.000
26	5.96	13.56	2.94	62.82	97.3221	1.000
27	5.98	14.47	2.44	60.66	96.1369	1.000
28	5.94	14.64	2.57	62.56	97.7384	1.000
29	5.91	14.41	2.99	60.03	97.5718	1.000
30	5.99	14.13	2.41	62.15	96.0296	1.000
31	5.92	14.24	2.17	64.04	96.4194	1.000
32	5.93	13.79	2.98	60.04	96.1843	1.000
33	5.96	13.52	2.71	63.35	96.3952	1.000
34	5.99	14.76	2.26	64.51	98.8798	1.000
35	5.74	14.32	2.60	63.34	96.0383	1.000
36	5.87	14.99	2.15	62.45	96.9403	1.000
37	5.98	14.03	2.27	64.74	97.1029	1.000
38	5.84	14.69	2.48	63.61	97.5065	1.000
39	5.56	14.12	2.98	64.80	97.3043	1.000
40	6.00	14.19	2.14	64.74	97.3457	1.000
41	5.55	13.98	2.94	64.89	96.8052	1.000
42	5.95	14.52	2.90	62.72	99.0607	1.000
43	5.61	14.94	2.97	60.83	96.9197	1.000
44	5.58	14.85	2.96	61.40	96.6937	1.000

45	5.99	14.52	2.04	62.41	96.253	1.000
46	5.66	14.62	2.27	64.46	96.0034	1.000
47	5.84	13.81	2.96	64.97	98.7319	1.000
48	5.96	13.40	3.00	60.00	95.7029	0.990
49	6.00	13.52	2.00	65.00	95.6035	0.987
50	6.00	12.76	2.97	60.00	94.5314	0.953

Fresh biodiesel was produced using the selected optimal process factors over the OCAT. Triplicate transesterification experiments were carried out. An average of 95% biodiesel yield was obtained. The 2% deviation could be attributed to experimentation error (pure error) or lack of fit error. The physicochemical properties of the optimally produced biodiesel was characterized and presented in table 4.13.

Table 4.12: Optimized conditions and validation for transesterification process

Predicted optimal conditions and yield					Validation experiments				Deviation		Error
A Wt.%	B ratio	C h	D ^{0}C	Yield (%)	Yield I (%)	Yield II (%)	Yield III (%)	Average Yield (%)	Predicted Yield (%)	Actual Yield (%)	± 2%
6	1:15	2	60	97	94.6	95.1	95.6	95.1	97	95	

4.7 Biodiesel Characterization

Table 4.13: Physicochemical properties of produced biodiesel under optimal conditions

Properties	Neem Oil Measured value	Biodiesel (B100) Measured value	ASTM (6751-12) Standard B100
Density at 40^{o}C (g/cm^{3})	0.92	0.89	0.86 – 0.89
Iodine value (mg I/100g oil)	71.4	42.5	-
Viscosity at 40^{o}C (mm^{2}/s)	36.09	4.78	1.9 – 6.0
Acid value (mg KOH/g)	8.36	0.264	0 – 0.5
Saponification value (mg KOH/g oil)	205.5	-	-
Flash point ^{o}C	-	137	93 -170
Cloud point ^{o}C	-	10	(-3) - 12
Pour point ^{o}C	-	4	(-15) - 10
Moisture content (%Vol)	-	0.02	0 – 0.05
Molecular weight (g/mol)	870	-	-

The biodiesel fuel produced using the validated optimal conditions was evaluated for the biodiesel (B100) quality characteristics specified in the American Standards and Testing Methods (ASTM D6751, 2002). The major shift from direct use of vegetable oil in diesel engines to transesterified oil is because of its high viscosity; this fuel property affects the flow and atomization characteristics of a liquid fuel. 4.78 mm^{2}/sec kinematic viscosity of the produced biodiesel is within the standard range, this can ensure a superior injection and atomization performance with added advantage of lubrication for the moving engine parts. High flash point temperatures for fuels ensure safe handling and storage. About 40% reduction was observed in the iodine value of the biodiesel fuel produced as compared with the iodine value of the neem oil. The lower this value, the higher the oxidative stability of the fuel, which implies that the biodiesel may be stored for a longer time without losing its originality.

A similar reduction was observed in the density of the fuel. The cloud and pour points are used to evaluate the cold weather performance of biodiesel, the observed cloud point was slightly close to the upper limit in the standard specification, this may be due to presence of wax or trace of glycerol in the oil which began to solidify as the temperature decreases, be as it may, this problem can be mitigated thorough hot water washing of the biodiesel or blending with petro diesel as opined by Vyas *et al.*, (2009).

4.7.1 Qualitative chemical analysis of the biodiesel fuel using FTIR

Qualitatively conversion of triglycerides to methyl ester have taken place when the molecules of triglycerides lost their unique identity, as a result molecules of methyl esters are formed. The presence of these molecules of methyl esters can be detected by the FTIR and GC-MS analyses.

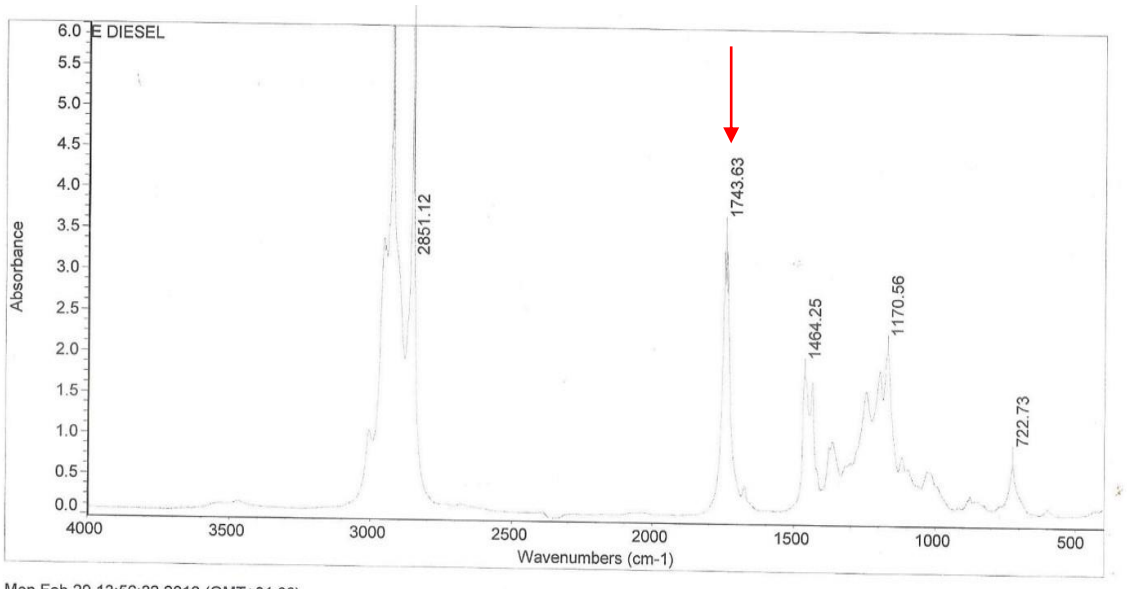

Mon Feb 29 13:56:32 2016 (GMT+01:00)
FIND PEAKS:
Spectrum: E DIESEL
Region: 4000.00 400.00
Absolute threshold: 0.090
Sensitivity: 12
Peak list:

Position:	722.73	Intensity:	0.717
Position:	1170.56	Intensity:	2.104
Position:	1464.25	Intensity:	1.791
Position:	1743.63	Intensity:	3.486
Position:	2851.12	Intensity:	6.145
Position:	2855.46	Intensity:	6.118
Position:	2922.96	Intensity:	6.122

Figure 4.16: FTIR spectra of biodiesel fuel produced using optimal process factor

Table 4.14: FTIR functional groups of biodiesel components

Wave numbers cm^{-1}	Functional Groups	Class of Compounds
3600 - 3300	OH	Water or Alcohol
3190 - 3050	=C-H	Alkene
2925 - 2850	$-CH_2$	Alkane
1750 - 1730	>C=O	Ester
1580 - 1557	COO^-	Li^+ Soap
1577 - 1541	COO^-	Ca^{2+} Soap
1570 - 1550	COO^-	Na^+ Soap
1470 - 1420	$-CH_2$, -C-H, =C-H	Alkene, Alkane
1155 - 995	C-O	Ether
730 - 721	$-CH_2$	Alkane

Source: (Tanwar *et al.,* 2013; Mouloungui *et al.,* 2003; Rohman and Man, 2011)

The spectra of the biodiesel produced using optimally synthesized OCAT is presented in figure 4.15. The most intense and broad peaks occur at $2851cm^{-1}$, $1743cm^{-1}$, $1464cm^{-1}$, $1170cm^{-1}$ and $722cm^{-1}$. Using the data presented in Table 4.14, it is evident that saponification did not occur during the single stage biodiesel production process. The peaks corresponding to presence of metal carboxylates were absent as depicted by a flat profile within the expected range of $1580 – 1541cm^{-1}$. Tanwar *et al.,* (2013); Mouloungui *et al.,* (2003); Rohman and Man, (2011), independently reported that peaks corresponding to $1750 – 1730cm^{-1}$ represent the presence of fatty acid methyl esters which are essentially biodiesel. In this case, the produced biodiesel shows the presence of these esters as depicted by the peak of $1743cm^{-1}$.

4.7.2 Qualitative chemical analysis of the biodiesel fuel using GC-MS

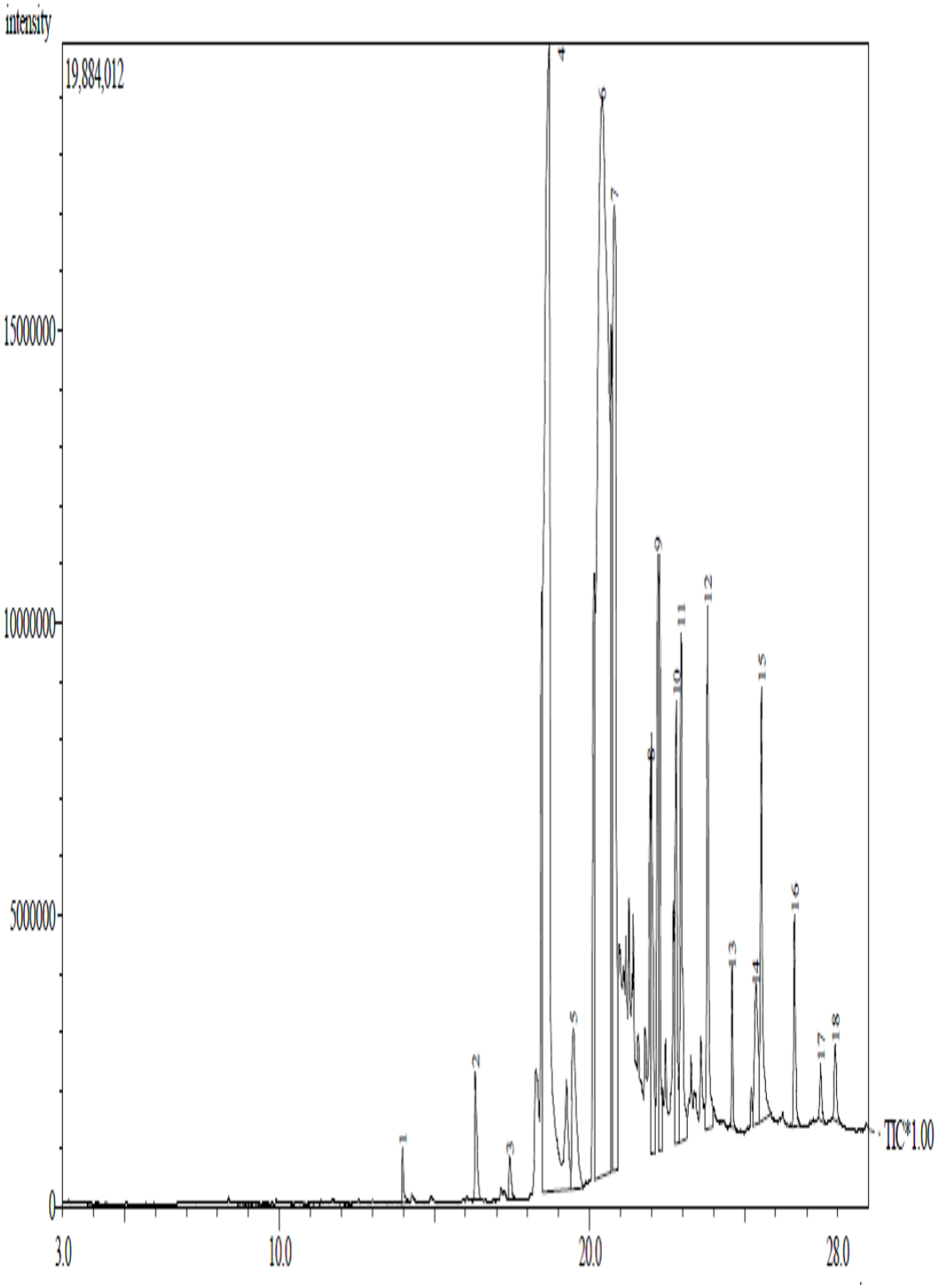

Figure 4.17: Chromatogram of the produced biodiesel fuel using optimal conditions

Table 4.15: Percentage compositions of the produced biodiesel

Peak No	IUPAC Name	Molar mass (g/mol)	Retention time (minutes)	Percentage compositions
1	Methyl Tridecanoate	228	14.0	0.25
2	Methyl Myristate	242	16.3	0.84
3	Methyl Pentadecanoate	256	17.4	0.35
4	Methyl Palmitate	270	18.7	22.94
5	Methyl Margarate	284	19.5	2.15
6	Methyl Oleate	296	20.4	39.61
7	Methyl Stearate	298	20.8	11.56
8	Methyl Eicosatrienoate	320	22.0	2.47
9	Methyl Eicosadienoate	322	22.3	2.56
10	Methyl 11-eicosanoate	324	22.8	3.01
11	Methyl Arachidate	326	23.0	3.69
12	Methyl Heneicosanoate	340	23.8	3.18
13	Methyl Behenate	354	24.6	0.65
14	Glycerin 1-monooleate^{NE}	356	25.4	1.61
15	Methyl Lignocerate	382	25.5	3.04
16	n-Octacosane^{NE}	394	26.6	1.23
17	Squalene^{NE}	410	27.5	0.34
18	Methyl Melissate	466	27.9	0.53
	Total composition			100
	Total NE			3.18
	Total ester content			96.82

NE = Non ester components

Figure 2.1 shows a GC chromatogram for fatty acid methyl esters, the standard chromatogram contains about 34 methyl ester compounds. Eleven ester compounds out of the 15 observed and presented in Table 4.15 were matched to the standard. Four ester peaks observed could not be identified on the standard chromatogram, this may be due to variance in the type of oil used. Molecules of glycerine that are present in the biodiesel may be due to insufficient purification after production. Squalene and the Octacosane are inherent compounds found in vegetable oils. The total ester content of the produced was found to be 96.82%, the standard stipulated by ASTM is 96.5% according to the information in Table 2.2

4.8 Reusability Studies: KF/Eggshell and KF/Eggshell-Fe_3O_4

Comparative reusability tests were conducted between the OCAT and the MCAT catalysts, the findings are presented in figure 4.18. The essence of the magnetism is to enhance the reusability of the catalyst by improving its lixiviation. As observed, it is evident that dosage of catalyst significantly affect the yield of biodiesel. As the weight(s) of catalysts reduce, so do the yield (s). Possibly because of the magnetic property of the MCAT, more of the catalysts were able to be recovered per experiment, this contributed to the differences seen in the yields compared to the runs transesterified by OCAT. Using the magnetic variant of the catalyst, yield of 92% was obtained after the fifth run, whereas the yield dropped to about 79% in the fifth run for the OCAT. The reason being that, while 1g of the MCAT catalyst was recovered and reused, only 0.7g of the OCAT was recovered and reused for the reaction in the fifth runs. This observation is in agreement with the ANOVA information presented in Table 4.9 which revealed that, catalyst dosage significantly affect the yield of biodiesel. The yield of biodiesel produced using recovered OCAT dropped to 55% in the seventh run, this can be attributed to the reduced catalyst dosage of 0.47g used, leaching of the active impregnated KF components and blockage of the catalyst pores. Similar reason can be inferred to be responsible for the 66% biodiesel yield obtained while using MCAT for the seventh run.

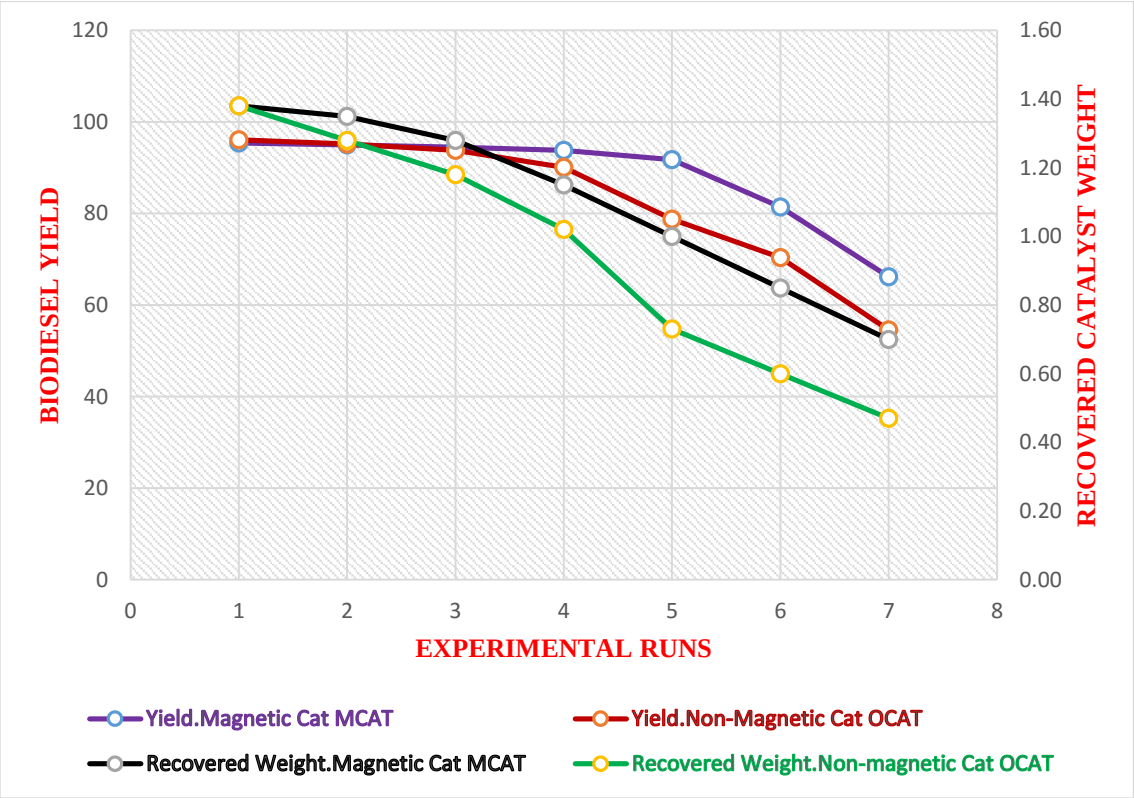

Figure 4.18: Comparative reusability studies

4.9 Eggshell and Commercial CaO Comparative Efficacy Studies

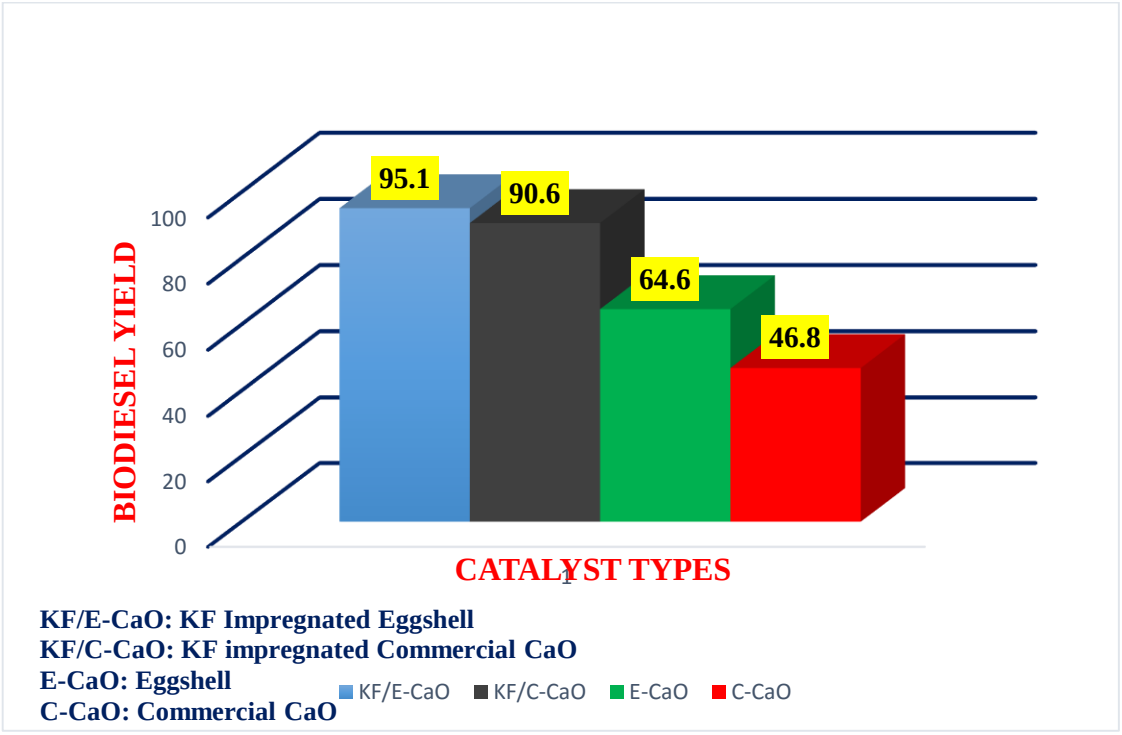

Figure 4.19: Comparative catalytic activity between eggshell and commercial CaO

The figure 4.19 presents the findings of the comparison between the OCAT and a similar catalyst synthesized using commercial CaO instead of eggshell. It was found that, the yield of biodiesel produced using the unmodified commercial CaO as a catalyst was 47%. Using unmodified eggshell for the same purpose resulted in the 65% yield of biodiesel. This huge difference may be attributed to synthesis method of the eggshell derived catalyst, this is believed to have enhanced its specific surface area. Also, eggshell contains other metallic oxide in various amounts as shown in the Table 4.7, they may possibly have positive effects on the yield of biodiesel, unlike a commercial CaO that is supposedly 100% CaO. Impregnation of KF undoubtedly improved the activity of both catalysts, nevertheless, KF/eggshell catalyst showed a tremendous activity compared to KF/CaO. This may be as a result of the stated inferred reasons which include high surface area and additional chemical constituents of eggshell.

CHAPTER FIVE

CONCLUSION AND RECOMMENDATION

5.1 Conclusions

Based on the results presented and discussed in chapter four, the following conclusions are made;

1. A solid base KF/Eggshell catalyst was successfully synthesized from spent eggshell and potassium fluoride, it was used for a single stage production of biodiesel from neem oil. The spent chicken eggshell was calcined at 900^{o}C.
2. The catalyst synthesis process factors were optimized, the optimal conditions were found to be 2 h eggshell calcination time, 29 wt.% KF dosage, 600^{o}C catalyst calcination temperature for 2 h.
3. Impregnation of KF on the calcined eggshell resulted in the formation of $KCaF_3$ crystals. The most significant synthesis factors that affect the performance of KF/Eggshell catalyst are the amount of the KF impregnated and the temperature of calcination of the KF/Eggshell catalyst.
4. Using the optimally synthesized KF/Eggshell catalyst, the transesterification process factors were also optimized, the optimal conditions were found to be 6 wt.% catalyst dosage, 1:15 oil-methanol ratio and 60^{o}C reaction temperature for 2h.
5. The catalyst and the produced biodiesel were characterized, modification of the eggshell with potassium fluoride enhanced its performance. The catalyst was able to transesterify neem oil having FFA content of 4.2% to produce 95% yield of biodiesel under optimal conditions without the occurrence of saponification as confirmed by GCMS and FTIR analyses.

6. The analyzed physicochemical properties of produced biodiesel meet the ASTM B100 standard for applications in diesel engine.
7. The magnetic and non-magnetic catalysts were utilized in a reusability studies. The magnetic KF/Eggshell-Fe_3O_4 catalyst produced 92% yield of the biodiesel after the fifth run, whereas the non-magnetic KF/Eggshell catalyst produced 79% yield for the same run. This significant difference confirmed that, the magnetism enhanced the recovery and reusability of the catalyst

5.2 Recommendations

1. Temperature-programmed desorption (TPD) analysis and X-ray Photoelectron Spectroscopy (XPS) should be carried out on the catalyst synthesized at the optimal conditions to fully understand its surface basicity and reactivity profile.
2. The magnetic property of the KF/Eggshell-Fe_3O_4 catalyst should be studied by vibrating sample magnetometer (VSM).
3. Full characterization should be carried out on the used catalyst to establish how much of its properties changed during the course of catalysis.
4. Quantitative GCMS analysis using internal calibration with analytical grade FAME Mix should be carried out on the biodiesel sample produced at optimal conditions.
5. The kinetics and reaction mechanism of the catalyzed transesterification reaction should be explored.

REFERENCES

Adene, D. F., & Oguntade, A. E. (2006). The structure and importance of the commercial and village based poultry industry in Nigeria. *Rome: FAO*.

Aharon, G., Piker, A., Tabah, B., Perkas, N., (2016). A green and low-cost room temperature biodiesel production method from waste oil using egg shells as catalyst. *Fuel*, *182*, 34-41.

Al-awwal, N. & Ali, U. (2015). Proximate Analyses of Different Samples of Egg Shells Obtained from Sokoto Market in Nigeria. *International Journal of Science And Research (IJSR)*, *4*(3), 564.

Ali, A., & Kaur, M., (2011). Lithium ion impregnated calcium oxide as nano catalyst for the biodiesel production from karanja and jatropha oils.*Renewable Energy*, *36*(11), 2866-2871.

Ali A., & Kaur, M., (2014). Potassium fluoride impregnated CaO/NiO: An efficient heterogeneous catalyst for transesterification of waste cottonseed oil. *European Journal of Lipid Science and Technology*, *116*(1), 80-88.

Ali, A., Mutreja, V., & Singh, S., (2011). Biodiesel from mutton fat using KOH impregnated MgO as heterogeneous catalysts. *Renewable Energy*, *36*(8), 2253-2258.

Al-Zuhair, S. (2007). Production of biodiesel: possibilities and challenges.*Biofuels, Bioproducts and Biorefining*, *1*(1), 57-66.

Amaral, N. G. D., Rezende, M. L. R. D., Hirata, F., Rodrigues, M. G. S., Sant'Ana, A. C. P., Greghi, S. L. A., & Passanezi, E. (2011). Comparison among four commonly used demineralizing agents for root conditioning: a scanning electron microscopy. *Journal of Applied Oral Science*, *19*(5), 469-475.

Arbeláez, A, M. & Rivera, M, P. (2007). *Diseño conceptual de un proceso para la obtención de biodiesel a partir de algunos aceites vegetales colombianos* (Master of Science dissertation, Universidad Eafit Medellín), Retrieved from https://repository.eafit.edu.co/bitstream/handle/10784/365/AngelaMaria_ArbelaezMarin_2007.pdf;jsessionid=2179DDEA7F951ADC19D0E2288FAA7A9B?sequence=1. (Accessed May 27, 2016)

Bancquart, S., Vanhove, C., Pouilloux, Y., & Barrault, J. (2001). Glycerol transesterification with methyl stearate over solid basic catalysts: I. Relationship between activity and basicity. *Applied Catalysis A: General*, *218*(1), 1-11.

Beckhoff, B., Kanngießer, B., Langhoff, N., Wedell, R., & Wolff, H. (2006). *Handbook of practical X-ray fluorescence analysis*. doi: 10.1007/978-3-540-36722-2

Berchmans, H. J., & Hirata, S. (2008). Biodiesel production from crude Jatropha curcas L. seed oil with a high content of free fatty acids. *Bioresource Technology*, *99*(6), 1716-1721.

Boey, P. L., Maniam, G. P., & Hamid, S. A. (2009). Biodiesel production via transesterification of palm olein using waste mud crab (Scylla serrata) shell as a heterogeneous catalyst. *Bioresource Technology*, *100*(24), 6362-6368.

Bonelli, B., Cozzolino, M., Tesser, R., Di Serio, M., Piumetti, M., Garrone, E., & Santacesaria, E. (2007). Study of the surface acidity of TiO_2/SiO_2 catalysts by means of FTIR measurements of CO and NH_3 adsorption. *Journal of Catalysis*, *246*(2), 293-300.

Borsato, D., Maia, E. C. R., Dall'Antonia, L. H., Silva, H. C. D., & Pereira, J. L. (2012). Kinetics of oxidation of biodiesel from soybean oil mixed with TBHQ: determination of storage time. *Química Nova*, *35*(4), 733-737.

Bournay, L., Casanave, D., Delfort, B., Hillion, G., & Chodorge, J. A. (2005). New heterogeneous process for biodiesel production: A way to improve the quality and the value of the crude glycerin produced by biodiesel plants. *Catalysis Today*, *106*(1), 190-192.

Box, G. E., Hunter, W. G., & Hunter, J. S. (1978). Statistics for experimenters.

Buasri, A., Chaiyut, N., Loryuenyong, V., Wongweang, C., & Khamsrisuk, S. (2013). Application of eggshell wastes as a heterogeneous catalyst for biodiesel production. *Sustainable Energy*, *1*(2), 7-13.

Canakci, M., & Van Gerpen, J. H. (2003). Comparison of engine performance and emissions for petroleum diesel fuel, yellow grease biodiesel, and soybean oil biodiesel. *Transactions of the ASAE*, *46*(4), 937.

Carlo, P., & Villa, P. (1997). Catalyst preparation methods. *Catalysis Today*, *34*(3), 281-305.

Carlos A., Guerrero F., Andrés G., and Fabio E. S. (2016). Biodiesel production from waste cooking oil. In Margarita S., and Gisela.M (Eds.), *Feedstocks and processing technologies* (pp.34 - 54) Rijeka, Croatia: Intech

Centi, G., Cavani, F., & Trifirò, F. (2001). *Selective Oxidation by Heterogeneous Catalysis*. Boston, MA: Springer US. (1st ed., pp. 141-201). Doi: 10.1007/978-1-4615-4175-2

Charter, W. F. (2008). Biodiesel guidelines. *Draft 1st ed., European Automobile Association*. http://www.acea.be/uploads/publications/20090423_B100_Guideline.pdf (Accessed June 5, 2016)

Chen, H., Peng, B., Wang, D., & Wang, J. (2007). Biodiesel production by the transesterification of cottonseed oil by solid acid catalysts. *Frontiers of Chemical Engineering in China*, *1*(1), 11-15.

Cho, Y. B., & Seo, G. (2010). High activity of acid-treated quail eggshell catalysts in the transesterification of palm oil with methanol. *Bioresource Technology*, *101*(22), 8515-8519.

Chouhan, A. S., & Sarma, A. K. (2011). Modern heterogeneous catalysts for biodiesel production: a comprehensive review. *Renewable and Sustainable Energy Reviews*, *15*(9), 4378-4399.

Cujia, G., & Bula, A. (2010). Potencial obtención de gas de síntesis para la producción de metanol a partir de la gasificación de residuos de palma africana. *Interciencia*, *35*(2), 106-112.

Danlin, Z., Zhang, Q., Chen, S., Liu, S., Chen, Y., Tian, Y., & Wang, G. (2015). Preparation and characterization of a strong solid base from waste eggshell for biodiesel production. *Journal of Environmental Chemical Engineering*, *3*(1), 560-564.

Demirbaş, A. (2003). Biodiesel fuels from vegetable oils via catalytic and non-catalytic supercritical alcohol transesterifications and other methods: a survey. *Energy Conversion and Management*, *44*(13), 2093-2109.

Demirbas, A. (2008). Comparison of transesterification methods for production of biodiesel from vegetable oils and fats. *Energy Conversion and Management*, *49*(1), 125-130.

Djibril, D., Mamadou, F., Gérard, V., Codou Geuye, M., Oumar, S., & Luc, R. (2015). Physical characteristics, Chemical composition and Distribution of constituents of the Neem seeds (Azadirachta indica A. Juss) collected in Senegal. *Research Journal Of Chemical Sciences*, *Vol. 5(7), 52-58,*(2231-606X).

Dong, J., Wang, X., Xu, H., Zhao, Q., & Li, J. (2007). Hydrogen storage in several microporous zeolites. *International Journal of Hydrogen Energy*, *32*(18), 4998-5004.

Eletta, O. A. A., Ajayi, O. A., Ogunleye, O. O., & Akpan, I. C. (2016). Adsorption of cyanide from aqueous solution using calcinated eggshells: Equilibrium and optimisation studies. *Journal of Environmental Chemical Engineering*, *4*(1), 1367-1375.

El-Gendy, N. S., Deriase, S. F., Hamdy, A., & Abdallah, R. I. (2015). Statistical optimization of biodiesel production from sunflower waste cooking oil using basic heterogeneous biocatalyst prepared from eggshells. *Egyptian Journal of Petroleum*, *24*(1), 37-48.

Encinar, J. M., Gonzalez, J. F., Rodriguez, J. J., & Tejedor, A. (2002). Biodiesel fuels from vegetable oils: transesterification of Cynara c ardunculus L. oils with ethanol. *Energy & fuels*, *16*(2), 443-450.

European Committee for Standardization, (2003) EN 14111. Fat and Oil Derivatives - Fatty Acid Methyl Esters (FAME) - Determination of Iodine Value, Berlin.

Faungnawakij, K., Luadthong, C., Nualpaeng, W., Changsuwan, P., Tongprem, P., Viriya-Empikul, N., & Khemthong, P., (2012). Industrial eggshell wastes as the heterogeneous catalysts for microwave-assisted biodiesel production. *Catalysis Today*, *190*(1), 112-116.

Feng, G., & Fang, Z. (2011). Biodiesel production with solid catalysts. *Biodiesel-Feedstock and Processing Technology.* InTech, Croatia, 339-358.

Freedman, B., Butterfield, R. O., & Pryde, E. H. (1986). Transesterification kinetics of soybean oil 1. *Journal of the American Oil Chemists' Society*, *63*(10), 1375-1380.

Freedman, B., Schwab, A. W., & Bagby, M. O., (1987). Preparation and properties of diesel fuels from vegetable oils. *Fuel*, *66*(10), 1372-1378.

Fukuda, H., Kondo, A., & Noda, H. (2001). Biodiesel fuel production by transesterification of oils. *Journal of Bioscience and Bioengineering*, *92*(5), 405-416.

Furuta, S., Matsuhashi, H., & Arata, K. (2004). Biodiesel fuel production with solid superacid catalysis in fixed bed reactor under atmospheric pressure. *Catalysis Communications*, *5*(12), 721-723.

Gao, L., Teng, G., Xiao, G., & Wei, R. (2010). Biodiesel from palm oil via loading KF/Ca–Al hydrotalcite catalyst. *Biomass and Bioenergy*, *34*(9), 1283-1288.

GCMS (2016). The Linde Group. Retrieved from http://hiq.lindegas.com/en/analytical methods/gas chromatography/index.html., Retrieved on (21 May, 2016).

Girón Gallego, E., & Torres Castañeda, H. G. (2010). Variables de operación en el proceso de transesterificación de aceites vegetales: una revisión-catálisis enzimática. *Ingeniería e Investigación*, *30*(1), 17-21.

Granados, M. L., Poves, M. Z., Alonso, D. M., Mariscal, R., Galisteo, F. C., Moreno-Tost, R., & Fierro, J. L. G. (2007). Biodiesel from sunflower oil by using activated calcium oxide. *Applied Catalysis B: Environmental*, *73*(3), 317-326.

Griffiths, P. R., & De Haseth, J. A. (Eds.) (2007). *Fourier Transform Infrared Spectrometry* (Vol. 171). John Wiley & Sons.

Guan, G., Kusakabe, K., Sakurai, N., & Moriyama, K. (2009). Transesterification of vegetable oil to biodiesel fuel using acid catalysts in the presence of dimethyl ether. *Fuel*, *88*(1), 81-86.

Hanna, M. A., Ma, F., & Clements, L. D., (1998). Biodiesel fuel from animal fat. Ancillary studies on transesterification of beef tallow. *Industrial & Engineering Chemistry Research*, *37*(9), 3768-3771.

Hannu J. (2009). Biodiesel Standards and Properties. Retrieved from https://www.dieselnet.com/tech/fuel_biodiesel_std.php. Retrieved on (August 12, 2016).

Heise, H., Crisan, A., & Theuvsen, L. (2015). The poultry market in Nigeria: Market structures and potential for investment in the market. *International Food and Agribusiness Management Review*, *18*(A).

Helwani, Z., Othman, M. R., Aziz, N., Kim, J., & Fernando, W. J. N. (2009). Solid heterogeneous catalysts for transesterification of triglycerides with methanol: a review. *Applied Catalysis A: General*, *363*(1), 1-10.

Hu, S., Guan, Y., Wang, Y., & Han, H. (2011). Nano-magnetic catalyst KF/CaO–Fe_3O_4 for biodiesel production. *Applied Energy* 88 (8), 2685–2690.

Hull, A. W. (1919). A new method of chemical analysis. *Journal of the American Chemical Society*, *41*(8), 1168-1175.

Hunton, P. (2005). Research on eggshell structure and quality: an historical overview. *Revista Brasileira de Ciência Avícola*, *7*(2), 67-71.

Ichihara, K. I., & Fukubayashi, Y. (2010). Preparation of fatty acid methyl esters for gas-liquid chromatography. *Journal of Lipid Research*, *51*(3), 635-640.

Joglekar, A. M., & May, A. T. (1987). Product excellence through design of experiments. *Cereal Foods World*, *32*(12), 857.

Jutika, B., Konwar, L. J., & Deka, D. (2014). Transesterification of non-edible feedstock with lithium incorporated egg shell derived CaO for biodiesel production. *Fuel Processing Technology*, *122*, 72-78.

Krasae, P., Yoosuk, B., Viriya-Empikul, N., Puttasawat, B., Chollacoop, N., & Faungnawakij, K. (2010). Waste shells of mollusk and egg as biodiesel production catalysts. *Bioresource Technology*, *101*(10), 3765-3767.

Leung, D. Y. C., & Guo, Y. (2006). Transesterification of neat and used frying oil: optimization for biodiesel production. *Fuel Processing Technology*,*87*(10), 883-890.

Leung, D. Y., Wu, X., & Leung, M. K. H. (2010). A review on biodiesel production using catalyzed transesterification. *Applied Energy*, *87*(4), 1083-1095.

Lotero, E., Goodwin Jr, J. G., Bruce, D. A., Suwannakarn, K., Liu, Y., & Lopez, D. E. (2006). The catalysis of biodiesel synthesis. *Catalysis*, *19*(1), 41-83.

MacLeod, C. S., Harvey, A. P., Lee, A. F., & Wilson, K. (2008). Evaluation of the activity and stability of alkali-doped metal oxide catalysts for application to an intensified method of biodiesel production. *Chemical Engineering Journal*, *135*(1), 63-70.

Manop, C., & Juthagate, T., (2011). Statistical optimization for biodiesel production from waste frying oil through two-step catalyzed process. *Fuel Processing Technology*, *92*(1), 112-118.

Masato, K., Kasuno, T., Tajika, M., Sugimoto, Y., Yamanaka, S., & Hidaka, J. (2008). Calcium oxide as a solid base catalyst for transesterification of soybean oil and its application to biodiesel production. *Fuel*, *87*(12), 2798-2806.

Masoud, Z., Daud, W. M. A. W., & Aroua, M. K. (2009). Activity of solid catalysts for biodiesel production: a review. *Fuel Processing Technology*, *90*(6), 770-777.

Meera, K. M., Niju, S., Begum, S., & Anantharaman, N. (2014). Modification of egg shell and its application in biodiesel production. *Journal of Saudi Chemical Society*, *18*(5), 702-706.

Meher, L. C., Kulkarni, M. G., Dalai, A. K., & Naik, S. N. (2006). Transesterification of karanja (Pongamia pinnata) oil by solid basic catalysts. *European Journal of Lipid Science and Technology*, *108*(5), 389-397.

Meng, L. (2011). *Identification and Partial Characterization of Locally Isolated Lipolytic Bacteria* (Doctoral dissertation, Universiti Malaysia Pahang).

Mittelbach, M., & Trathnigg, B. (1990). Kinetics of alkaline catalyzed methanolysis of sunflower oil. *Lipid/Fett*, *92*(4), 145-148.

Montgomery, C., & Rupp, A. A. (2005). A meta-analysis for exploring the diverse causes and effects of stress in teachers. *Canadian Journal of Education/Revue canadienne de l'éducation*, 458-486.

Montgomery, D. C., Keats, J. B., Runger, G. C., & Messina, W. S. (1994). Integrating statistical process control and engineering process control. *Journal of Quality Technology*, *26*(2), 79-87.

Mouloungui, Z., Poulenat, G., & Sentenac, S., (2003). Fourier-transform infrared spectra of fatty acid salts—Kinetics of high-oleic sunflower oil saponification. *Journal of Surfactants And Detergents*, 6(4), 305-310.

Muthu, K., & Viruthagiri, T. (2015). Study on Solid Base Calcium Oxide as a Heterogeneous Catalyst for the Production of Biodiesel. *Journal of Advanced Chemical Sciences*, 160-163.

Nakatani, N., Takamori, H., Takeda, K., & Sakugawa, H. (2009). Transesterification of soybean oil using combusted oyster shell waste as a catalyst. *Bioresource Technology*, *100*(3), 1510-1513.

Pragas, G. M., Boey, P. L., & Hamid, S. A. (2011). Performance of calcium oxide as a heterogeneous catalyst in biodiesel production: a review. *Chemical Engineering Journal*, *168*(1), 15-22.

Raissi, S., & Eslami, R. F. (2009). Statistical process optimization through multi-response surface methodology. *World Academy of Science, Engineering and Technology*, *51*(46), 267-271.

Ramesh, K., Reddy, K. S., Rashmi, I., & Biswas, A. K. (2014). Porosity distribution, surface area, and morphology of synthetic potassium zeolites: A SEM and N2 adsorption study. *Communications in Soil Science and Plant Analysis*, *45*(16), 2171-2181.

Rashid, U., Anwar, F., Moser, B. R., & Ashraf, S. (2008). Production of sunflower oil methyl esters by optimized alkali-catalyzed methanolysis. *Biomass and Bioenergy*, *32*(12), 1202-1205.

Reddy, V., C. R., Oshel, R., & Verkade, J. G. (2006). Room-temperature conversion of soybean oil and poultry fat to biodiesel catalyzed by nanocrystalline calcium oxides. *Energy & Fuels*, *20*(3), 1310-1314.

Rodrigo A. A., Fernandes D.M., Santos D.Q., Tatielli G. G., and Raquel M. F. (2016). Biodiesel: Production, characterization, metallic corrosion and analytical methods for contaminants. In Zhen F. (Eds.), *Feedstocks, Production and Application.* Rijeka, Croatia: Intech, (pp.131 - 165).

Rohman, A., & Man, Y. B. C. (2011). Determination of sodium fatty acid in soap formulation using Fourier Transform Infrared (FTIR) spectroscopy and multivariate calibrations. *Journal of Surfactants and Detergents*, *14*(1), 9-14.

Sani, Y.M., Daud W.M. and Abdul Aziz, A.R., (2016). Biodiesel: Production, characterization, metallic corrosion and analytical methods for contaminants. In Zhen F. (Eds.), *Feedstocks, Production and Application*. Rijeka, Croatia: Intech, (pp.78 - 94)

Santacesaria, E., Vicente, G. M., Di Serio, M., & Tesser, R. (2012). Main technologies in biodiesel production: State of the art and future challenges. *Catalysis Today*, *195*(1), 2-13.

Sardar, N., Ahmad, M., Khan, M. A., Ali, S., Zafar, M., Khalid, N., & Sultana, S. (2011). Prospects and potential of non-edible neem oil biodiesel based on physico-chemical characterization. *Energy Sources, Part A: Recovery, Utilization, and Environmental Effects*, *33*(15), 1422-1430.

Sarin, R., Sharma, M., Sinharay, S., & Malhotra, R. K. (2007). Jatropha–palm biodiesel blends: an optimum mix for Asia. *Fuel*, *86*(10), 1365-1371.

Satterfield, C. N. (1980). *Heterogeneous catalysis in practice*. McGraw-Hill Companies.

Shiyi., O.U, Wang, Y., Liu, P., Xue, F., & Tang, S. (2006). Comparison of two different processes to synthesize biodiesel by waste cooking oil. *Journal of Molecular Catalysis A: Chemical*, *252*(1), 107-112.

Sing, K. S. (1985). Reporting physisorption data for gas/solid systems with special reference to the determination of surface area and porosity (Recommendations 1984). *Pure and Applied Chemistry*, *57*(4), 603-619.

Sirivat, A., Phudkrachang, P., Kasemsumran, S., Kunanuruksapong, R., & Tangboriboon, N., (2012). An Innovative Measurement of Extractable Proteins from Concentrated Latex Containing Eggshell Calcium Oxide Compounds by Near-Infrared Spectroscopy. *Spectroscopy Letters*, *45*(1), 29-39.

Song, B. A., Xue, W., Zhou, Y. C., Shi, X., Wang, J., Yin, S. T., ... & Yang, S. (2009). Synthesis of biodiesel from Jatropha curcas L. seed oil using artificial zeolites loaded with CH_3COOK as a heterogeneous catalyst. *Natural Science*, *1*(01), 55.

Stadelman, W. J. (2000). Eggs and egg products. *Encyclopedia of Food Science and Technology*, *2*.

Standard, A. S. T. M. (1995). D5558. Standard Test Method for Determination of the Saponification Value of Fats and Oils. *Annual Book of ASTM Standards, ASTM International, West Conshohocken, PA*.

Standard, A. S. T. M. (2002). D6751-12. Standard Specification for Biodiesel Fuel (B100) Blend Stock for Distillate Fuels. *Annual Book of ASTM Standards, ASTM International, West Conshohocken, PA*.

Standard, A. S. T. M. (2011). D5555. Standard Test Method for Determination of Free Fatty Acids Contained in Animal, Marine, and Vegetable Fats and Oils Used in Fat Liquors and Stuffing Compounds. *Annual Book of ASTM Standards, ASTM International, West Conshohocken, PA*.

Standard, A. S. T. M. (2011). D5556. Standard Test Method for Determination of the Moisture and Other Volatile Matter Contained in Fats and Oils Used in Fat Liquors and Softening Compounds. *Annual Book of ASTM Standards, ASTM International, West Conshohocken, PA*.

Standard, A. S. T. M. (2011). D664-11ae1. Standard Test Method for Acid Number of Petroleum Products by Potentiometric Titration. *Annual Book of ASTM Standards, ASTM International, West Conshohocken, PA*.

Standard, A. S. T. M. (2012). D1298-12b. Standard Test Method for Density, Relative Density, or API Gravity of Crude Petroleum and Liquid Petroleum Products by Hydrometer Method. *Annual Book of ASTM Standards, ASTM International, West Conshohocken, PA*.

Suppes, G. J., Bockwinkel, K., Lucas, S., Botts, J. B., Mason, M. H., & Heppert, J. A. (2001). Calcium carbonate catalyzed alcoholysis of fats and oils. *Journal of the American Oil Chemists' Society*, *78*(2), 139-146.

Tanabe, K., & Yamaguchi, T. (1963). Basicity and acidity of solid surfaces. In *13th Discussion Meeting on Catalysis, Sapporo*.

Tanwar, D., Ajayta, D., Mathur, Y., & Sharma, D. (2013). Production and Characterization of Neem Oil Methyl Ester. *International Journal of Engineering Research and Technology. 2*(5), 1896 -1902.

Tsai, W. T., Hsien, K. J., Hsu, H. C., Lin, C. M., Lin, K. Y., & Chiu, C. H. (2008). Utilization of ground eggshell waste as an adsorbent for the removal of dyes from aqueous solution. *Bioresource Technology*, *99*(6), 1623-1629.

Tureli, M. C. M., Barbosa, T. S., & Gavião, M. B. D. (2009). Validity and reliability of the Child Perceptions Questionnaires applied in Brazilian children. *BMC Oral Health*, *9*(1), 1.

United States Department of Agriculture (USDA). (2013). International Egg and Poultry Report,http://www.thefarmsite.com/reports/contents/IntlPoultryandEgg19Feb2013.pdf. Retrieved on March 25, 2016.

Vargas, R. M., Schuchardt, U., & Sercheli, R., (1998). Transesterification of vegetable oils: a review. *Journal of the Brazilian Chemical Society*, *9*(3), 199-210.

Vargha, V., & Truter, P. (2005). Biodegradable polymers by reactive blending trans-esterification of thermoplastic starch with poly (vinyl acetate) and poly (vinyl acetate-co-butyl acrylate). *European Polymer Journal*, *41*(4), 715-726.

Verhe, R., Echim, C., De Greyt, W., and Stevens, C., (2011). Production of biodiesel via chemical catalytic conversion. In R.Luque. J. Campelo, J. Clark (Eds.), *Handbook of Biofuels Production: Processes and Technologies* (pp.97- 127). Sawston, Cambridge: Woodhead

Vinatoru, M., Stavarache, C., Nishimura, R., & Maeda, Y. (2005). Fatty acids methyl esters from vegetable oil by means of ultrasonic energy. *Ultrasonics Sonochemistry*, *12*(5), 367-372.

Vyas, A. P., Subrahmanyam, N., & Patel, P. A. (2009). Production of biodiesel through transesterification of Jatropha oil using KNO 3/Al 2 O 3 solid catalyst. *Fuel*, *88*(4), 625-628.

Wachs, I.E., in: Fierro, J. L. G. (Ed.). (2005). *Metal Oxides: Chemistry and Applications*. CRC press.

Watkins, R. S., Lee, A. F., & Wilson, K. (2004). Li–CaO catalyzed tri-glyceride transesterification for biodiesel applications. *Green Chemistry*, *6*(7), 335-340.

Wei, Z., Xu, C., & Li, B. (2009). Application of waste eggshell as low-cost solid catalyst for biodiesel production. *Bioresource Technology*, *100*(11), 2883-2885.

Wen, L., Wang, Y., Lu, D., Hu, S., & Han, H. (2010). Preparation of KF/CaO nanocatalyst and its application in biodiesel production from Chinese tallow seed oil. *Fuel*, *89*(9), 2267-2271.

Xu, H., Li, X., & Wu, Q. (2007). Large-scale biodiesel production from microalga Chlorella protothecoides through heterotrophic cultivation in bioreactors. *Biotechnology and Bioengineering*, *98*(4), 764-771.

Yoosuk, B., Udomsap, P., Puttasawat, B., & Krasae, P. (2010). Improving transesterification activity of CaO with hydration technique. *Bioresource Technology*, *101*(10), 3784-3786.

APPENDICES

Appendix A: Synthesis of Catalyst

Table A.1: Central composite design matrix of catalyst synthesis variables with responses

	Variables				Responses	
Run No.	A-Eggshell Calcination time (Hr)	B-KF dosage (Wt. %)	C-Catalyst calcination temp (^{0}C)	D- Catalyst calcination time (Hr)	Observed Biodiesel Yield (%)	Predicted Biodiesel Yield (%)
1	4	15	300	2	69	68
2	2	15	300	2	68	67
3	3	25	450	3	80	80
4	4	15	600	2	80	78
5	4	15	600	4	81	79
6	3	25	450	1	80	81
7	2	35	300	4	72	72
8	3	45	450	3	71	70
9	2	35	600	2	88	89
10	1	25	450	3	82	82
11	5	25	450	3	83	86
12	4	15	300	4	71	69
13	3	5	450	3	48	52
14	2	15	600	4	79	78
15	3	25	450	5	82	84
16	3	25	450	3	80	80
17	4	35	300	2	73	73
18	2	35	600	4	91	91
19	3	25	750	3	94	96
20	4	35	600	2	93	92
21	2	35	300	2	71	71
22	3	25	450	3	79	80
23	2	15	300	4	68	68
24	2	15	600	2	77	76
25	3	25	150	3	67	68
26	3	25	450	3	81	80
27	4	35	300	4	74	74
28	4	35	600	4	93	93

Table A.2: ANOVA data for catalyst synthesis

Response					Transform:	None	
		Biodiesel Yield			Internally	Externally	
Run	Actual	Predicted			Studentized	Studentized	Cook's
	Value	Value	Residual	Leverage	Residual	Residual	Distance
1	69.00	68.04	0.96	0.583	0.721	0.707	0.049
2	68.00	66.71	1.29	0.583	0.972	0.970	0.088
3	80.00	80.00	0.000	0.250	0.000	0.000	0.000
4	80.00	78.21	1.79	0.583	1.348	1.397	0.170
5	81.00	79.38	1.62	0.583	1.223	1.249	0.140
6	80.00	81.25	-1.25	0.583	-0.941	-0.936	0.083
7	72.00	72.38	-0.38	0.583	-0.282	-0.272	0.007
8	71.00	69.92	1.08	0.583	0.815	0.804	0.062
9	88.00	88.88	-0.88	0.583	-0.659	-0.644	0.040
10	82.00	82.08	-0.083	0.583	-0.063	-0.060	0.000
11	83.00	85.75	-2.75	0.583	-2.070	-2.428	0.400
12	71.00	68.71	2.29	0.583	1.725	1.887	0.278
13	48.00	51.92	-3.92	0.583	-2.948	-4.918[2]	0.811
14	79.00	77.54	1.46	0.583	1.098	1.107	0.112
15	82.00	83.58	-1.58	0.583	-1.192	-1.213	0.133
16	80.00	80.00	0.000	0.250	0.000	0.000	0.000
17	73.00	73.04	-0.042	0.583	-0.031	-0.030	0.000
18	91.00	90.54	0.46	0.583	0.345	0.333	0.011
19	94.00	96.08	-2.08	0.583	-1.568	-1.673	0.229
20	93.00	91.71	1.29	0.583	0.972	0.970	0.088
21	71.00	71.21	-0.21	0.583	-0.157	-0.151	0.002
22	79.00	80.00	-1.00	0.250	-0.561	-0.546	0.007
23	68.00	67.88	0.12	0.583	0.094	0.090	0.001
24	77.00	75.88	1.12	0.583	0.847	0.837	0.067
25	67.00	67.75	-0.75	0.583	-0.564	-0.549	0.030
26	81.00	80.00	1.00	0.250	0.561	0.546	0.007
27	74.00	73.71	0.29	0.583	0.220	0.211	0.004
28	93.00	92.88	0.12	0.583	0.094	0.090	0.001

APPENDIX B: Transesterification process

Table B.1: Design of experiments and responses for transesterification process

Std	Run	Factor 1 A:Weight of catalyst Wt%	Factor 2 B:Methanol-Oil Ratio	Factor 3 C:Reaction time Hr	Factor 4 D:Reaction temperature deg C	Response Actual Biodiesel Yield %	Response Predicted Biodiesel Yield %
10	1	5	9	1.5	65	80	79.00
28	2	4	12	2.25	60	78	78.25
9	3	3	9	1.5	65	74	73.08
1	4	3	9	1.5	55	65	65.79
17	5	2	12	2.25	60	76	77.46
8	6	5	15	3	55	92	92.42
26	7	4	12	2.25	60	77	78.25
7	8	3	15	3	55	87	86.50
27	9	4	12	2.25	60	79	78.25
23	10	4	12	2.25	50	77	77.46
22	11	4	12	3.75	60	88	88.46
5	12	3	9	3	55	75	74.50
20	13	4	18	2.25	60	94	96.63
11	14	3	15	1.5	65	88	86.58
3	15	3	15	1.5	55	85	83.04
21	16	4	12	0.75	60	75	76.29
4	17	5	15	1.5	55	90	88.96
25	18	4	12	2.25	60	79	78.25
12	19	5	15	1.5	65	92	92.50
19	20	4	6	2.25	60	72	71.13
15	21	3	15	3	65	91	90.04
6	22	5	9	3	55	81	80.42
18	23	6	12	2.25	60	89	89.29
24	24	4	12	2.25	70	87	88.29
13	25	3	9	3	65	81	81.79
14	26	5	9	3	65	87	87.71
2	27	5	9	1.5	55	71	71.71
16	28	5	15	3	65	98	95.96

Legends:

Reaction time: 0.25h implies 15 minutes, 0.5h: 30 minutes and 0.75h: 45 minutes

Weight of catalyst: 4 wt. % implies (4/100 × weight of oil)

Oil-methanol ratio: 9 implies (1:9)

Table B.2: ANOVA of transesterification process

ANOVA for Response Surface Quadratic model						
Analysis of variance table [Partial sum of squares - Type III]						
Source	Sum of Squares	df	Mean Square	F Value	p-value Prob > F	
Model	1710.36	14	122.17	48.87	< 0.0001	significant
A-Weight of catalyst	*210.04*	*1*	*210.04*	*84.02*	*< 0.0001*	
B-Methanol-Oil	*975.37*	*1*	*975.37*	*390.15*	*< 0.0001*	
C-Reaction time	*222.04*	*1*	*222.04*	*88.82*	*< 0.0001*	
D-Reaction temperature	*176.04*	*1*	*176.04*	*70.42*	*< 0.0001*	
AB	*0.56*	*1*	*0.56*	*0.23*	*0.6431*	
AC	*0.56*	*1*	*0.56*	*0.23*	*0.6431*	
AD	*0.063*	*1*	*0.063*	*0.025*	*0.8768*	
BC	*27.56*	*1*	*27.56*	*11.02*	*0.0055*	
BD	*14.06*	*1*	*14.06*	*5.62*	*0.0338*	
CD	*0.063*	*1*	*0.063*	*0.025*	*0.8768*	
A^2	*39.40*	*1*	*39.40*	*15.76*	*0.0016*	
B^2	*47.46*	*1*	*47.46*	*18.98*	*0.0008*	
C^2	*25.52*	*1*	*25.52*	*10.21*	*0.0070*	
D^2	*32.09*	*1*	*32.09*	*12.83*	*0.0033*	
Residual	32.50	13	2.50			
Lack of Fit	*29.75*	*10*	*2.97*	*3.25*	*0.1809*	*not significant*
Pure Error	*2.75*	*3*	*0.92*			
Cor Total	1742.86	27				

Table B.3: Correlation coefficient data of transesterification process.

Std. Dev.	1.58	R-Squared	0.9814
Mean	82.43	Adj R-Squared	0.9613
C.V. %	1.92	Pred R-Squared	0.8989
PRESS	176.25	Adeq Precision	26.643
-2 Log Likelihood	83.63	BIC	133.62
		AICc	153.63

Table B.4: ANOVA data for transesterification process

Response					Transform:	None	
	Biodiesel yield				Internally	Externally	
Run	Actual	Predicted			Studentized	Studentized	Cook's
	Value	Value	Residual	Leverage	Residual	Residual	Distance
1	80.00	79.00	1.00	0.333	0.869	0.863	0.034
2	78.00	78.25	-0.25	0.250	-0.205	-0.199	0.001
3	74.00	73.08	0.92	0.333	0.797	0.788	0.029
4	65.00	65.79	-0.79	0.333	-0.688	-0.677	0.022
5	76.00	77.46	-1.46	0.583	-1.603	-1.688	0.327
6	92.00	92.42	-0.42	0.333	-0.362	-0.353	0.006
7	77.00	78.25	-1.25	0.250	-1.024	-1.026	0.032
8	87.00	86.50	0.50	0.333	0.435	0.424	0.009
9	79.00	78.25	0.75	0.250	0.615	0.603	0.011
10	77.00	77.46	-0.46	0.583	-0.504	-0.493	0.032
11	88.00	88.46	-0.46	0.583	-0.504	-0.493	0.032
12	75.00	74.50	0.50	0.333	0.435	0.424	0.009
13	94.00	96.63	-2.63	0.583	-2.886	-3.921[2]	1.060[1]
14	88.00	86.58	1.42	0.333	1.231	1.252	0.069
15	85.00	83.04	1.96	0.333	1.702	1.813	0.132
16	75.00	76.29	-1.29	0.583	-1.420	-1.468	0.257
17	90.00	88.96	1.04	0.333	0.905	0.900	0.037
18	79.00	78.25	0.75	0.250	0.615	0.603	0.011
19	92.00	92.50	-0.50	0.333	-0.435	-0.424	0.009
20	72.00	71.13	0.87	0.583	0.962	0.960	0.118
21	91.00	90.04	0.96	0.333	0.833	0.825	0.032
22	81.00	80.42	0.58	0.333	0.507	0.496	0.012
23	89.00	89.29	-0.29	0.583	-0.321	-0.312	0.013
24	87.00	88.29	-1.29	0.583	-1.420	-1.468	0.257
25	81.00	81.79	-0.79	0.333	-0.688	-0.677	0.022
26	87.00	87.71	-0.71	0.333	-0.616	-0.604	0.017
27	71.00	71.71	-0.71	0.333	-0.616	-0.604	0.017
28	98.00	95.96	2.04	0.333	1.775	1.907	0.143

Table B.5: Reusability table

Run No.	Yield. Magnetic Cat MCAT	Yield. Non-Magnetic Cat OCAT	Recovered Weight. Magnetic Cat MCAT	Recovered Weight. Non-magnetic Cat OCAT
1	95.4	96.1	1.38	1.38
2	95	95.2	1.35	1.28
3	94.5	93.8	1.28	1.18
4	93.8	90.1	1.15	1.02
5	91.8	78.8	1.00	0.73
6	81.4	70.4	0.85	0.60
7	66.2	54.6	0.70	0.47

Plate B.1: Mr.Oladipo S.A carrying out laboratory exercise for this research